

THE UNIVERSITY OF CHICAGO

DEVELOPMENT AND VALIDATION OF A PRIMARY MOUSE HEPATOCYTE SYSTEM
IN THE EVALUATION OF DIOXIN-LIKE PCB EXPOSURE

A DISSERTATION SUBMITTED TO
THE FACULTY OF THE DIVISION OF THE BIOLOGICAL SCIENCES
AND THE PRITZKER SCHOOL OF MEDICINE
IN CANDIDACY FOR THE DEGREE OF
DOCTOR OF PHILOSOPHY

COMMITTEE ON MOLECULAR METABOLISM AND NUTRITION

BY

WENSHUO ZHANG

CHICAGO, ILLINOIS

JUNE 2011

TABLE OF CONTENTS

List of figures	iii
List of abbreviations	iv
Acknowledgements	vii
Abstract	ix
CHAPTER	
I. Dioxins, dioxin-like PCBs, and the liver: an overview	1
A. Overview, definitions, and nomenclature	1
B. The liver as a central target of dioxin-like compounds	3
C. Primary mouse hepatocytes as a tool for mechanistic DLC studies	6
D. A brief history of DLCs	9
E. Evaluating the toxicity of dioxin-like compounds: the TEF and TEQ	11
F. The aryl hydrocarbon receptor as a mediator of DLC toxicity	14
G. Summary	21
II. Development and validation of a primary mouse hepatocyte system	22
A. Introduction	22
B. Materials and methods	23
C. Results	34
D. Discussion	54
III. PCB 126 and other dioxin-like PCBs specifically suppress hepatic PEPCK expression by AhR-dependent and-independent mechanisms	64
A. Introduction	64
B. Materials and methods	66
C. Results	70
D. Discussion	89
IV. Additional studies and future directions for application of primary mouse hepatocytes in mechanistic studies of DLCs	97
A. Introduction	97
B. Long-term maintenance of hepatocyte phenotype and function	98
C. Addressing the physiological significance of dioxin-like PCB suppression of cytosolic PEPCK	101
D. Confirmation of AhR involvement in dioxin-like PCB suppression of hepatocyte PEPCK through isolation of hepatocytes from hepatocyte-specific AhR and ARNT knockout mice	107
E. Conclusion	109
Reference List	110

LIST OF FIGURES

CHAPTER I

1-1: Generic structures of PCDDs, PCDFs, and PCBs.....	2
1-2: Overview of known DLC effects on metabolic pathways in the liver	4
1-3: Model of AhR signaling following binding of agonist.....	15

CHAPTER II

2-1: Descriptive characterization of isolated primary hepatocytes.....	35
2-2: Glycogen synthesis and insulin signaling and action in primary hepatocytes	39
2-3: Glycogenolysis in primary mouse hepatocytes	44
2-4: GNG in primary mouse hepatocytes	46
2-5: Beta oxidation in primary mouse hepatocytes.....	49
2-6: Lipogenesis in primary mouse hepatocytes.....	51
2-7: First-phase xenobiotic metabolizing enzyme induction and function in primary mouse hepatocytes.....	53
2-8: Adenovirus infection competence of primary mouse hepatocytes	55

CHAPTER III

3-1: Summary tables	68
3-2: PCB 126 suppresses glycogen storage in primary murine hepatocytes	71
3-3: PCB 126 treatment does not modulate glucose incorporation into glycogen, glycogen metabolizing enzymes, or glycogenolysis in primary hepatocytes	74
3-4: Suppression of forskolin-induced GNG from lactate but not glycerol following PCB 126 treatment	76
3-5: PCB 126 specifically suppresses forskolin-induced expression of PEPCK.....	79
3-6: A partial AhR antagonist does not affect the suppression of forskolin- stimulated PEPCK gene expression by PCB 126	82
3-7: Other non-ortho-substituted dioxin-like PCBs, but not all AhR agonists are able to suppress forskolin-stimulated PEPCK	84
3-8: Standard least squares analysis of CYP1A1 gene induction by compound vs. fold PEPCK gene induction by forskolin.....	88
3-9: Overview of PCB 126 effects on hepatic glucose metabolism	95

CHAPTER IV

4-1: Effect of various plating strata on primary mouse hepatocyte glycogen synthesis.....	100
4-2: Visualization of hepatocyte phenotype after 24 h of culture on various 2-D strata.....	102
4-3: Overview of hepatic GNG and integration with NADH production and the TCA cycle.....	104

LIST OF ABBREVIATIONS

7-ER.....	7- ethoxyresorufin
ABTS.....	2,2'-azino-bis(3-ethylbenzthiazoline-6-sulphonic acid)
ACC.....	Acetyl-CoA carboxylase
ADP.....	Adenosine diphosphate
AGC2.....	Aspartate/glutamate carrier isoform 2
AhR.....	Aryl hydrocarbon receptor
AICAR.....	Aminoimidazole carboxamide ribonucleotide
AIP.....	AhR-interacting protein/ARA9
α -KG.....	Alpha-ketoglutarate
ALT.....	Alanine aminotransferase
AMPK.....	AMP-activated protein kinase
ANOVA.....	Analysis of variance
APQ9.....	Aquaporin 9
ARA9.....	AhR-associated protein 9/AIP
ARNT.....	AhR nuclear translocator
AST.....	Aspartate aminotransferase
ATP.....	Adenosine triphosphate
BNF.....	Beta-naphthoflavone
BSA.....	Bovine serum albumin
cAMP.....	Cyclic adenosine monophosphate
c/EBP α	CCAAT/enhancer-binding protein alpha
ChREBP.....	Carbohydrate response element binding protein
CIC.....	Citrate carrier
CYP.....	Cytochrome P450
DHA.....	Dihydroxyacetone
DHAP.....	Dihydroxyacetone phosphate
DIC.....	Dicarboxylate carrier
DLC.....	Dioxin-like compound
DMEM.....	Dulbecco's modification of Eagle's medium
DMSO.....	Dimethylsulfoxide
DNL.....	De novo lipogenesis
DRE.....	Dioxin response element
ECOD.....	Ethoxycoumarin-o-deethylase
EGTA.....	Ethylene glycol tetraacetic acid
EROD.....	Ethoxyresorufin-o-deethylase
F-1,6-P ₂	Fructose-1,6-bisphosphate
Fbp1.....	Fructose bisphosphatase 1
FBS.....	Fetal bovine serum
FFA.....	Free fatty acid
G6Pc.....	Glucose 6-phosphatase
GAPDH.....	Glyceraldehyde 3-phosphate dehydrogenase
GDP.....	Guanine diphosphate
GK.....	Glycerol Kinase

Glucose 6P	Glucose 6-phosphate
GNG.....	Gluconeogenesis
GOD.....	Glucose oxidase
GP.....	Glycogen phosphorylase
GPDH.....	Glycerol 3-phosphate dehydrogenase
GPI.....	Glucose phosphate isomerase
GSK.....	Glycogen synthase kinase
GTP	Guanine triphosphate
h.....	Hour
HBSS.....	Hank's buffered salt solution
HEPES	(4-(2-hydroxyethyl)-1-piperazineethanesulfonic acid)
HGO.....	Hepatic glucose output
hsp.....	Heat shock protein
IP.....	Intraperitoneal
IRS	Insulin receptor substrate
IVC.....	Inferior vena cava
LDH	Lactate dehydrogenase
LXR.....	Liver X receptor
MCT.....	Monocarboxylate transporter
MDH	Malate dehydrogenase
MOI.....	Multiplicity of infection
MPC.....	Mitochondrial pyruvate carrier
mTOR	Mammalian target of rapamycin
NADH.....	Nicotinamide adenine dinucleotide, reduced
NADPH.....	Nicotinamide adenine dinucleotide phosphate, reduced
NEFA.....	Nonesterified fatty acid
OAA.....	Oxaloacetate
OGC.....	Oxyglutarate carrier
PAS.....	Per-Arnt-Sim
PBS	Phosphate buffered saline
PCB.....	Polychlorinated biphenyl
PCDD.....	Polychlorinated dibenzodioxin
PCDF.....	Polychlorinated dibenzofuran
Pcx.....	Pyruvate carboxylase
PDE	Phosphodiesterase
PEP.....	Phosphoenolpyruvate
PEPCK.....	Phosphoenolpyruvate carboxykinase
PERID	Peroxidase
PGK.....	Phosphoglycerate kinase
PGM.....	Phosphoglycerate mutase
PKC.....	Protein kinase C
PPP.....	Pentose phosphate pathway
qRT-PCR	Quantitative real-time polymerase chain reaction
REP	Relative potency
SREBP-1	Sterol regulatory element binding protein 1

TCA.....	Tricarboxylic acid cycle OR Trichloroacetic acid
TCDD.....	2,3,7,8-Tetrachlorodibenzodioxin
TEF	Toxic equivalent factor
TEQ.....	Toxic equivalent
TNF	Tumor necrosis factor
TG	Triglyceride
TPI.....	Triose phosphate isomerase
VLDL.....	Very low density lipoprotein
WHO.....	World Health Organization
XRE.....	Xenobiotic response element

ACKNOWLEDGEMENTS

First and foremost, I would like to thank Matthew Brady for his support, guidance, and unending willingness to take the time out to help out in experiments, proofreading, and all aspects of graduate school life. The CMMN has progressed far beyond its state just six years ago, and we are all deeply indebted to Matthew's efforts to recruit high-caliber students and continually promote and expand the program.

I would like to extend my gratitude to my committee members, who so graciously agreed to mentor me during my career at the University of Chicago. Dr. Christopher Rhodes has been a most effective Chair for the CMMN, and his strong leadership has been a cornerstone of the growth and progress of the committee. Dr. Ronald Cohen is easily the finest neighbor one could ask for, and has been a continuing source of support throughout my years in graduate school. Dr. Catherine Reardon graciously agreed to fill an opening on the committee on very short notice, and her skill and patience as a teacher during my first years as a graduate student has left lasting impressions.

Scientific progress cannot occur without the assistance of others, and in this respect, I am grateful for the support and companionship of my fellow graduate students. In particular, I would like to thank Paul Volden, Katie Markan, and Christopher Carmean; as labmates, Paul, Katie, and Chris have always been willing to set aside time to discuss results and ideas. Paul especially has been a valued colleague, but more importantly, a friend, from whom I have learned much in regards to alternative approaches to experimental procedures. I would be remiss if I did not also mention Dr. Robert Sargis, who was the driving force behind my thesis project, and has offered much guidance since I joined the Brady lab.

Collaboration has been a key aspect to my development as a scientist, and for this I thank the Bell lab as well as the MacLeod lab. Dr. Graeme Bell has continuously offered invaluable insight, and his generosity in allowing use of his lab resources are much appreciated. I would especially like to thank Honggang Ye in the Bell lab, as without his assistance in troubleshooting the primary hepatocyte isolation, I would have been lost. I would like to thank Kay MacLeod for having faith in my hepatocytes, and Danielle Glick for her support- the opportunity to collaborate on the BNip project has been a unique and valuable learning experience.

I would like to give a special thanks to Dr. Xiao Jian Sun, my principal mentor during my first five years of graduate school. Dr. Sun took me in fresh out of college with 10 weeks of laboratory experience, and patiently guided my development as a scientist- and much guidance was required. I am eternally grateful to have been able to train under such a fine scientist.

Finally, but certainly not least of all, I would like to thank my family, and in particular, my wife, Amanda, for her support. Amanda's skill and efforts allowed the details surrounding the isolation and culture of primary mouse hepatocytes to be published online for the benefit of the scientific community. Were it not for Amanda constantly challenging me to grow as a scientist and as a person, I would not possess the technical prowess, nor the interpersonal skills that I have today- and for this I will always be indebted to her.

Abstract

A host of critical metabolic and biosynthetic processes are mediated hepatocytes, the dominant cell type found in the liver. Despite decades of literature documenting the isolation and characterization of isolated hepatocytes, the overwhelming majority of investigations center on either the metabolic or xenobiotic arm of hepatic function. While regulation of metabolic substrates and detoxification of xenobiotic compounds are independently crucial, these functions are invariably interrelated. For most investigations, metabolic functions are arguably of greater interest due to their physiological relevance; even in drug metabolism studies, the overarching questions often center upon whether a compound affects key biosynthetic processes (i.e. glucose synthesis). Furthermore, extensive evidence suggests that metabolic functions (i.e. synthesis of glycogen and oxidation of fatty acids) are more sensitive markers for hepatocyte integrity than xenobiotic processes (i.e. induction of cytochrome P450-1-A1 activity). However, isolation of high-quality hepatocytes suitable for metabolic investigations is challenging; this issue has been compounded by a lack of standard reference ranges for comparison purposes. In this dissertation, a means for isolation of fully competent primary mouse hepatocytes is detailed, along with an array of metabolic and xenobiotic assays designed to validate their performance. Key biosynthetic rates are provided relative to published literature, and proof of concept is provided by application of these tools towards fundamental questions concerning the specific versus nonspecific impact of dioxin-like polychlorinated biphenyls on hepatic glucose metabolism. Together, these investigations provide the framework for future mechanistic studies that integrate multiple aspects of liver function in a reproducible, high-throughput manner.

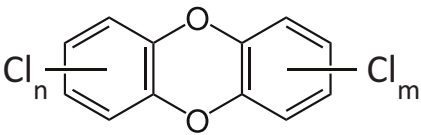
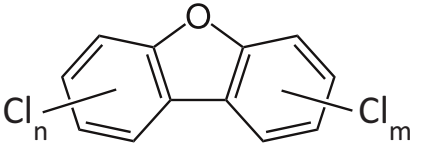
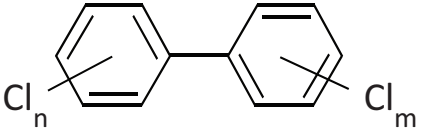
CHAPTER I

Dioxins, dioxin-like PCBs, and the liver: an overview

1.A. Overview, definitions, and nomenclature

Dioxins and dioxin-like compounds are persistent environmental pollutants produced by both natural and synthetic means. The term *dioxin* technically refers to the heterocyclic organic compound 1,4-dioxin; however, in the context of environmental toxins, *dioxin* more commonly refers to a group of structurally and chemically related polycyclic, polychlorinated molecules that contain the 1,4-dioxin backbone. More specifically, the term is used in reference to certain highly toxic members of the two principle classes of dioxins, the polychlorinated dibenzodioxins (PCDDs) and the polychlorinated dibenzofurans (PCDFs) (White and Birnbaum, 2009). This is an important distinction to make, as there are 75 possible chlorine-substituted PCDDs and 135 possible chlorine-substituted PCDFs, but the World Health Organization (WHO) only classifies 7 PCDDs and 10 PCDFs as dioxins on the basis of their toxicological profiles (White and Birnbaum, 2009; Poland and Knutson, 1982). Polychlorinated biphenyls (PCBs) comprise a separate family of polycyclic, polychlorinated environmental pollutants that are structurally related to PCDDs and PCDFs, but do not possess a dioxin backbone (**Fig. 1-1**). However, 12 out of the 209 possible PCB congeners have sufficient structural, chemical, and biochemical congruence to dioxins to be classified as dioxin-like by the WHO (White and Birnbaum, 2009).

Dioxin-like PCBs, and PCDDs and PCDFs which are classified as dioxins, are collectively referred to as dioxin-like compounds (DLCs) on the basis of their similar physical, chemical, and biological properties as well as their analogous toxicological effects and molecular mechanisms of action. All dioxins and PCBs share certain characteristics, including resistance to

Compound Class	General structure	Highest in-class TEF*
PCDD (polychlorinated dibenzodioxin)		1.0 2,3,7,8-TCDD & 1,2,3,7,8-PeCDD
PCDF (polychlorinated dibenzofuran)		0.3 2,3,4,7,8-PeCDF
PCB (polychlorinated biphenyl)		0.1 3,3',4,4',5-PCB (PCB 126)

* WHO 2005

Figure 1-1: Generic structures of PCDDs, PCDFs, and PCBs. TEF rankings are based on WHO 2005 values. Subscripts *n* and *m* denote variable numbers of chlorine substituents.

thermal, physical, and enzymatic breakdown, lipophilicity, and a tendency to bioaccumulate; however, only the DLCs are known to pathologically activate the aryl hydrocarbon receptor (AhR), a widely-expressed and highly conserved transcription factor that controls the expression of a number of first and second-phase drug metabolizing enzymes (van den Berg et al., 2006). The consequences of exposure to PCDDs/PCDFs/PCBs classified as DLCs versus those considered non-DLCs are therefore highly disparate, with the former inciting a host of system-wide anomalies including chloracne, hepatotoxicity, impaired immune function, lowered reproductive success, developmental abnormalities, and endocrine and metabolic disruption (Birnbaum and Tuomisto, 2000; Poland and Knutson, 1982; Guo et al., 2004). PCDDs/PCDFs/PCBs that are not classified as DLCs are also toxic, but adverse outcomes require significantly higher doses and tend to be far more diffuse with respect to physiological manifestation (Giesy and Kannan, 1998).

1.B. The liver as a central target of dioxin-like compounds

In addition to its role in maintenance of plasma glucose levels, lipoprotein synthesis and processing, bile synthesis, and albumin production, the liver is also the principal site of endo- and xenobiotic metabolism owing to its extensive expression of phase I, II, and III drug metabolizing enzymes. The inducibility of several of these enzyme systems, particularly with respect to the AhR, in conjunction with preferential sequestration of DLCs (likely secondary to CYP1A2 upregulation) makes the liver a logical focal point for investigation of DLC effects. Evaluation of DLCs on general toxicity often centers upon histological changes in liver ultrastructure (i.e. fatty acid infiltration, fibrosis, and necrosis) along with release of hepatic enzymes as biochemical markers of hepatocyte insult. However, DLCs have also been shown to impact hepatic glucose and lipid metabolism (**Fig. 1-2**), and this may play a role in the often-

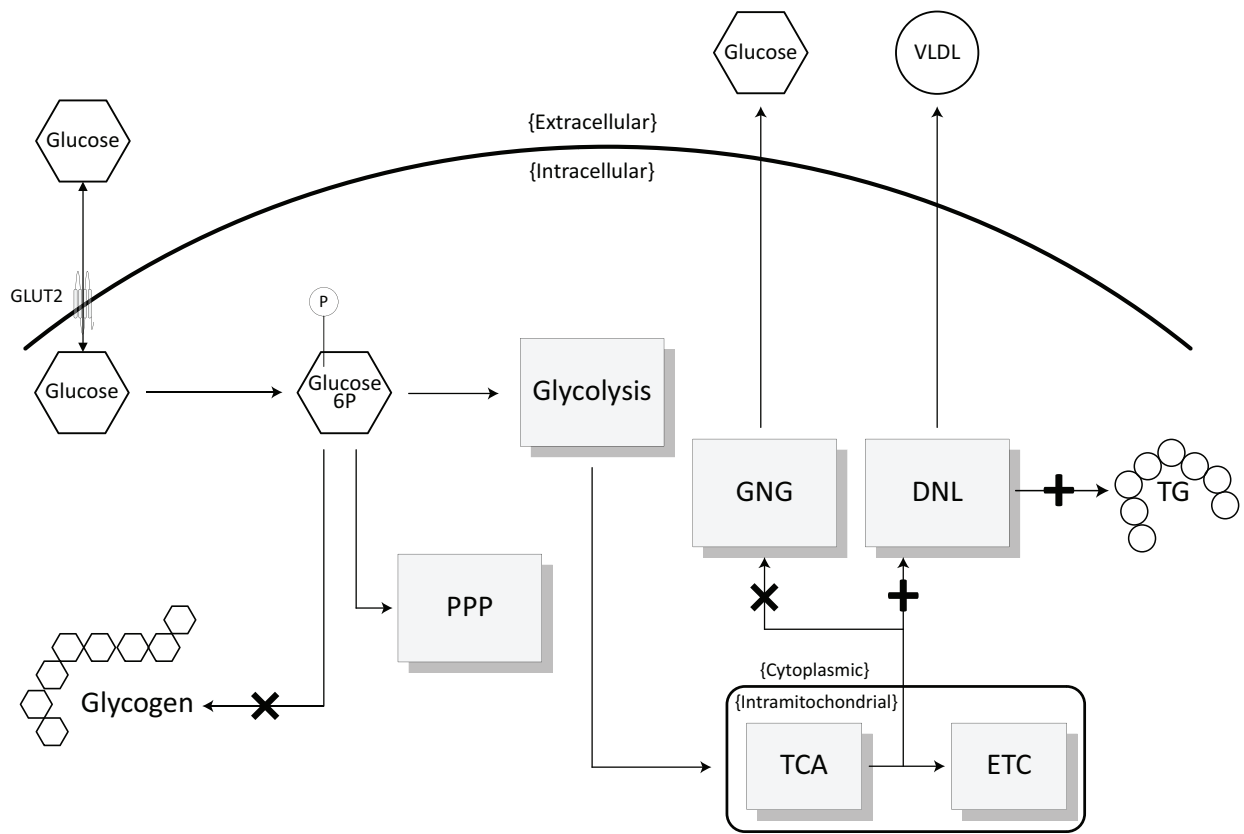


Figure 1-2: Overview of known DLC effects on metabolic pathways in the liver. Inhibitory effects are denoted by (x) and stimulatory effects by (+).

lethal wasting syndrome frequently observed during *in vivo* TCDD exposure experiments (Weber et al., 1991b; Viluksela et al., 1995). Furthermore, many metabolic perturbations occur before the onset of actual liver injury; therefore, DLC-incited metabolic abnormalities may provide a more sensitive means to investigate the mechanism of DLC effects in the liver in the absence of secondary factors introduced by cellular damage.

The liver maintains tight control of blood glucose levels both acutely and chronically, under fed and fasted states, through integration of nutrients and hormones at the level of glycogen synthesis and release, as well as the synthesis of glucose from non-glucose precursors via gluconeogenesis (GNG); the latter pathway is specifically (i.e. independent of histological or biochemical toxicity) affected by DLC treatment both *in vivo* and *in vitro*, implying that DLCs directly impact liver glucose metabolism (Stahl, 1995; Viluksela et al., 1995). Regulation of hepatic GNG is the principal means by which glycemia is maintained, and appears to be a constitutive process whose rate is controlled by both hormones and substrate availability, although the relative contribution of each is highly variable depending on physiological state and experimental parameters (Landau et al., 1996; Petersen et al., 1996). Glycogen, on the other hand, is primarily a short-term buffer for glycemic regulation during overnight fasting, where it contributes approximately 50% of the total glucose required for maintenance of euglycemia (Corssmit et al., 2001). The proportion of glucose derived from glycogenolysis versus GNG decreases as the length of fasting increases, and GNG accounts for almost all hepatic glucose output after 40-48 hours of fasting (Corssmit et al., 2001; Landau et al., 1996). Given the importance of hepatic GNG with respect to plasma glucose concentrations, the impact of DLCs on the critical gluconeogenic enzymes has been extensively investigated as a mechanism for DLC-induced wasting.

The specific mechanisms that mediate DLC-induced wasting remain unknown, as the severity and reversibility of wasting depend on the species and strain of animal used, as well as the chosen DLC and dosing parameters. A rapid and significant decrease in the activity and expression of the gluconeogenic enzyme phosphoenolpyruvate carboxykinase (PEPCK) is readily observed in livers and hepatocytes of DLC-treated rodents, while the decrease in another gluconeogenic enzyme, glucose-6-phosphatase (G6pc) is less marked and often coincides with general toxicity (Stahl et al., 1993; Weber et al., 1991b; Hsia and Kreamer, 1985). PEPCK and G6pc are key enzymes in the gluconeogenic pathway, catalyzing the conversion of oxaloacetate (OAA) to phosphoenolpyruvate (PEP) and glucose-6-phosphate to glucose, respectively. The specificity and rapidity of PEPCK suppression by DLCs has been proposed to be a mechanism for DLC-induced wasting. However, the magnitude of suppression of PEPCK (by DLCs) is often far greater than the observed decrease in plasma glucose (Viluksela et al., 1998; Boll et al., 1998), and the importance of PEPCK as a central determinant of hepatic GNG has been brought into question by the liver-specific PEPCK knockout mouse, which is able to maintain normal glucose levels during fasting by shifting its gluconeogenic fuel source (Burgess et al., 2004; Burgess et al., 2007). Nonetheless, DLCs suppress PEPCK expression and activity rapidly (within 8 hours of exposure) and in dose-dependent manner, with generally tight correspondence to the magnitude of CYP1A1 induction (Viluksela et al., 1999; Stahl et al., 1993; 2006a), implying that the suppression of PEPCK may be useful as a sensitive, metabolically relevant marker for DLC exposure.

1.C. Primary mouse hepatocytes as a tool for mechanistic DLC studies

Treatment of rats and mice with DLCs has shown that the liver is a principal target, likely due to its ability to sequester DLCs, abundant expression of xenobiotic metabolizing enzymes, and

central role in metabolic processes which, if interrupted, may contribute to physiological wasting. The list of liver-specific effects caused by DLC exposure is extensive, but to date, little is known about the steps leading from overactivation of AhR to any toxic or abnormal endpoint. Elucidation of the mechanisms that mediate physiological effects may be most readily performed using a well-controlled, thoroughly validated *in vitro* system. The liver is overwhelmingly composed of a single cell type –the hepatocyte- and hepatocyte-specific knockout studies have confirmed that in the context of hepatotoxicity, excessive activation of the AhR in hepatocytes is the overarching mechanism (Nukaya et al., 2010b; Nukaya et al., 2010a). Furthermore, numerous studies have confirmed the utility of primary hepatocytes in evaluating the relative potencies of DLCs within and between species (Carlson et al., 2009; Boess et al., 2003; Zeiger et al., 2001). While there are obvious limitations with *in vitro* primary cell culture versus *in vivo* studies, including alterations in gene expression due to culture conditions and loss of cross-tissue interactions, *in vitro* systems offer flexibility, control, and scalability that make them invaluable tools for mechanistic investigations.

Primary hepatocytes have traditionally been difficult to isolate, have short useful culture times (24-72 hours on average), are demanding in terms of technical skill and resources required, and are subject to the same inter-animal variance associated with *in vivo* studies. However, despite these challenges and limitations, primary hepatocytes remain the closest and most readily manipulable *in vitro* model of the liver (Boess et al., 2003). Cell lines are a readily available, convenient, and highly consistent tool for *in vitro* investigations; however, in the context of liver metabolism, a substitute for properly isolated primary cells currently does not exist. Numerous hepatoma cell lines have been used as surrogates or as reference points for comparison to primary hepatocytes, including the commonly used HepG2 (human hepatoma), HepaRG (human

hepatoma), and H4IIE (rat hepatoma) line. However, comparative studies evaluating glucose and lipid metabolism have demonstrated significantly reduced uptake of glucose and fatty acids, as well as drastically lower rates and hormonal responsiveness of gluconeogenesis in hepatoma cells versus primary hepatocytes (Hansson et al., 2004; Okamoto et al., 2009). Toxicological studies have revealed that although hepatoma cells generally respond to DLCs, as determined by CYP1A1 gene expression and activity, they require DLC concentrations several orders of magnitude higher than primary hepatocytes from the same species (Boess et al., 2003; Zeiger et al., 2001; Silkworth et al., 2005). Thus, while the use of human cell lines may be understandable given the difficulties associated with procurement of primary human hepatocytes, rodent hepatoma lines have severely limited applicability for metabolic or toxicological studies involving the liver.

Extensive studies employing primary mouse, rat, pig, monkey, and human hepatocytes have confirmed their utility in toxicological studies. Inter-species sensitivities to DLCs are reproducible in their respective primary hepatocyte systems, and the WHO has recognized the applicability of primary hepatocyte findings by allowing data generated from such cells to be used in revising DLC toxicity rankings (provided the study design meets the required criteria for inclusion) (Carlson et al., 2009; van den Berg et al., 2006; Van der Burght et al., 2000). However, *in vivo* studies are still the benchmark by which DLC potency is categorized, as the liver is a main target organ for DLCs but is hardly the only organ affected. A more appropriate role for primary hepatocytes may be in the evaluation of targeted genetic models of the AhR and associated signaling molecules to elucidate the contribution of AhR signaling to DLC effects.

The majority of *in vitro* studies on DLCs have utilized primary rat hepatocytes for practical reasons (i.e. ease of cannulation and high cell yield); however, almost all genetically

altered animal models, including the AhR global knockout and the ARNT hepatocyte-specific knockout, are based on the mouse. Isolation of hepatocytes from mice, though, is more challenging due to their smaller physical size (relative to rats), which also limits total cell yield per liver. A single rat liver may yield hundreds of millions of hepatocytes, potentially enough cells to seed over 100 plates, while an average mouse may only provide 30-60 million cells; pooling of cells from multiple mice may overcome this limitation, but would require additional operators isolating in tandem. Still, even tens of millions of hepatocytes provide sufficient material for mechanistic investigations and may be more suitable for smaller-scale experiments. Mice also possess the advantages of easier handling, less expensive housing, and generally faster responses to environmental manipulations (i.e. diet) compared to rats. Finally, mouse hepatocytes are no less competent than hepatocytes from other species with respect to physiologically relevant functions (i.e. glycogen synthesis, lipogenesis, beta oxidation, and gluconeogenesis) as well as toxicological responses (i.e. induction of CYP expression and activity), making them an ideal tool for investigating the mechanism of DLC-induced alterations in hepatic metabolism.

1.D. A brief history of DLCs

Of the three primary constituents of the DLCs, only PCBs have been produced for industrial and commercial purposes; PCDDs and PCDFs have no known use outside of scientific research and are solely unintentional byproducts, mainly resulting from improper/unregulated incineration. PCBs, on the other hand, were extensively used worldwide until their production was internationally banned in 2001. PCB production was halted in the United States in 1979, but total U.S. production until the ban has been estimated at over one billion pounds (Poland and Knutson, 1982). Leakage of PCBs from electrical capacitors, residual PCB contamination from

industrial spills and accidents, and improper disposal of old PCB-containing machinery account for the majority of present-day PCB contamination; PCDDs/PCDFs continue to be generated by both natural and human-mediated incineration events, but increased regulatory pressures have also contributed to significant decreases in new PCDD/PCDF synthesis (Liem et al., 2000).

Despite the trend towards reduced dietary intake of DLCs as a result of increased awareness of their toxicity, the long half-life of many DLCs and their resistance to breakdown has allowed them to become a semi-permanent part of the global environment, including the food supply. There are detectable levels of DLCs in all human populations (Safe, 1998; Wickizer et al., 1981; Wittsiepe et al., 2007), and the average daily intake of DLCs is approximately equal across the globe, although the actual source of DLC contamination varies according to country (Safe, 1998). Furthermore, industrial accidents have exposed large groups of people to high levels of DLCs, with short-term (skin and nerve), intermediate (neurological and immunological), and long-term (reproductive and developmental) ramifications – the latter of which may span generations due to the particular sensitivity of developing fetuses to DLCs (Guo et al., 2004; McHale et al., 2007; Birnbaum and Tuomisto, 2000). However, with respect to *background* exposure- that is, humans with no history of being exposed to abnormally high levels of DLCs- establishing clear cause-effect relationships (in humans) between DLC exposure and actual disease states has been challenging, and in many cases, questionable, due to obvious ethical and practical limitations in experimental methodology. Therefore, current detailed knowledge of DLC toxicity and the relative potencies of the various DLCs in terms of their effect on mammalian health are derived from non-human primate and rodent studies. It is critical to keep the species in mind when attempting to extrapolate findings from one species to another due to a wide range of sensitivities that spans several orders of magnitude with respect to dose

(Poland and Knutson, 1982), so that implications for average human populations are neither underestimated nor overestimated.

Studies of industrial tragedies, including the 1968 Yusho contamination in Japan, the similar 1979 Yucheng incident in Taiwan, the 1976 exposure in Seveso, Italy, and even the recent 1994 poisoning of Victor Yushchenko have unequivocally shown that high-level exposure to DLCs is toxic to humans and wildlife alike (White and Birnbaum, 2009). It is less clear how much of a threat the low levels of DLCs in almost all meat, fish, and dairy products pose to the general human population, as detectable levels of DLCs do not necessarily implicate their role in any pathological condition(s). This does not, however, undermine the value of studying the mechanism of action of DLCs, as (a) wildlife have been shown to be susceptible to DLC poisoning, particularly in sites where concentrated PCDD/PCDF and PCB waste have been generated, (b) human cases of high-level DLC poisoning have not entirely disappeared even though production has been halted (Geusau et al., 2001; Heres et al., 2010), and (c) the molecular mechanism(s) of DLC toxicity is (are) still unknown. Therefore, DLCs are invaluable tools for advancing current knowledge concerning the function and role of their principal molecular target, the AhR, which has clear implications for facilitating drug design.

1.E. Evaluating the toxicity of dioxin-like compounds: The TEF and TEQ

Since the mid-1980s, a relative ranking system, the toxic equivalency factor (TEF) has been used to categorize the various DLCs on the basis of their potency in reference to a PCDD, 2,3,7,8-tetrachloro-p-dioxin (TCDD), the most potent known DLC (van den Berg et al., 1998; WHO, 2003). The TEF is an order-of-magnitude (on a logarithmic scale) ranking of the currently recognized DLCs, with TCDD being assigned the highest value, 1.0; the most recent update to

the TEF values makes the important assumption that each TEF has a degree of uncertainty $\pm 0.5 \log$ (± 3 fold) to reflect experimental variance and gaps in the available literature (WHO, 2003). The TEF initially included only the PCDDs and PCDFs, and was updated to include the dioxin-like PCBs during the first WHO meeting in 1993, where an extensive review of the existing literature was performed to establish the first WHO database for DLCs. The WHO TEF list has since been updated twice, once in 1997 and most recently in 2005 to integrate more up-to-date information into the TEF rankings (Haws et al., 2006; van den Berg et al., 2006).

There are several criteria that a compound must fulfill to be assigned a TEF: (1) the compound must be structurally similar to PCDDs/PCDFs, (2) the compound must bind to the AhR, (3) the compound must exert toxicity following AhR binding, and (4) the compound must be environmentally and biologically cumulative (van den Berg et al., 2006). The TEF applies only to single, pure compounds, and assumes that in a mixture of compounds, the individual TEFs of applicable DLCs is additive. This latter point is critical, as DLCs rarely occur independent of one another; all industrially manufactured PCBs were mixtures of congeners, and PCDDs/PCDFs are often simultaneously generated by incineration and may be found as trace contaminants in industrial PCB mixtures. A derivative of the TEF, the toxic equivalent (TEQ), is therefore used to quantify the toxicity (*toxicity* as defined by the TEF) of a mixture of DLCs; the TEQ is simply the sum of the individual concentrations of single DLCs (in a mixture) multiplied by said DLC's TEF (Safe, 1998). The TEQ is especially useful for identifying highly relevant DLCs for study. For example, PCB 126 is not only the most toxic dioxin-like PCB (TEF = 0.1), it also can account for as much as 90% of the total TEQ contributed by the dioxin-like PCBs, and over 60% of the total TEQ when PCDDs/PCDFs are also taken into account (Bhavsar et al.,

2008). As a derivative value, however, it is important to keep in mind that TEQs change in accordance to updates to TEF rankings and are species-specific.

Though useful as a relative reference, the TEF has weaknesses that affect its use as an absolute means for ranking dioxin and PCB *toxicity*. First, the fact that a PCDD, PCDF, or PCB has not been assigned a TEF does not imply that it is not toxic- it simply implies that the mechanism for toxicity is not directly mediated by the AhR. Along the same line of reasoning, a compound without a TEF may still bioaccumulate as well as bind the AhR, albeit in a nonproductive fashion. Second, it has been shown that in mixtures, compounds without a TEF (i.e. non dioxin-like PCBs) may compete with DLCs for AhR binding, lowering the overall toxicity of the mix; since studies with AhR knockout mice have demonstrated that the DLCs appear to exert almost all of their toxic effects through the AhR, it can be assumed that *toxicity* in this context can be taken literally (Schmidt et al., 1996; Fernandez-Salguero et al., 1995). Third, the TEF must be used in a species-specific manner, as the TEF values for many DLCs vary between mammals, fish, and birds – although the TEF value for TCDD and, in most studies, PCB 126, may be globally applicable (van den Berg et al., 1998). Finally, the TEF does not currently take into account species-specific metabolism and sequestration of certain DLCs, which may cause preferential accumulation in adipose versus skin or liver, resulting in divergent toxicological outcomes (Rifkind, 2006; Diliberto et al., 1997; Devito et al., 1998).

Despite these flaws, the TEF is the standard and most widely-used means for assessing DLC toxicity, and the data used to establish and revise TEFs is based on stringent criteria, with heavy reliance upon relative potency (REP) databases (with their own stringent criteria for data inclusion) that are constantly updated as new literature is generated. The REP is simply a means to compare the relative potency of AhR activation (and therefore, presumably, toxicity) of

different DLCs within a single study, provided either TCDD or PCB 126 is used as a reference (van den Berg et al., 2006; Haws et al., 2006). The ranking of compounds with respect to TEF generally has an excellent correlation with actual experimental data (within a species) for both AhR activation and toxicological outcomes. Ultimately, the utility of the TEF as a means to quickly and accurately predict relative DLC toxicity depends on the quality of future research.

1.F. The aryl hydrocarbon receptor as a mediator of DLC toxicity

The AhR is a member of the basic helix-loop-helix, Per-ARNT-Sim (PAS) family of transcription factors that mediates almost all of the toxic effects of DLCs. (Gu et al., 2000). Unliganded AhR resides in the cytosol in a complex with several proteins including chaperones (two molecules of hsp90) and co-chaperones (p23 and AIP, also known as ARA9/XAP-2) (Petrulis and Perdew, 2002). The role of these associated proteins is thought to include localization, stabilization, and maintenance of ligand binding capacity, and perturbation of any of the associated proteins results in a reduction, but not complete ablation of AhR signaling (Nukaya et al., 2010a; Flaveny et al., 2009; Wiseman and Vijayan, 2007). Upon ligand binding, a nuclear localization sequence within the AhR is exposed, allowing translocation of the AhR complex into the nucleus, where it dissociates from its chaperones and co-chaperones. This dissociation exposes a binding site on the PAS region which allows for heterodimerization with the AhR nuclear translocator protein (ARNT). Heterodimerization with ARNT is a critical step in activation of target gene expression, as the AhR is thought to bind to one half of the nucleotides comprising the dioxin response element (TNGCGTG; DRE, also known as XRE, or xenobiotic response element) of target genes, while the ARNT binds to the other half (Gu et al., 2000) (**Fig. 1-3**). The crucial role of the ARNT in mediating AhR-related toxicity, as well as target gene regulation was recently demonstrated by the hepatocyte-specific ARNT knockout

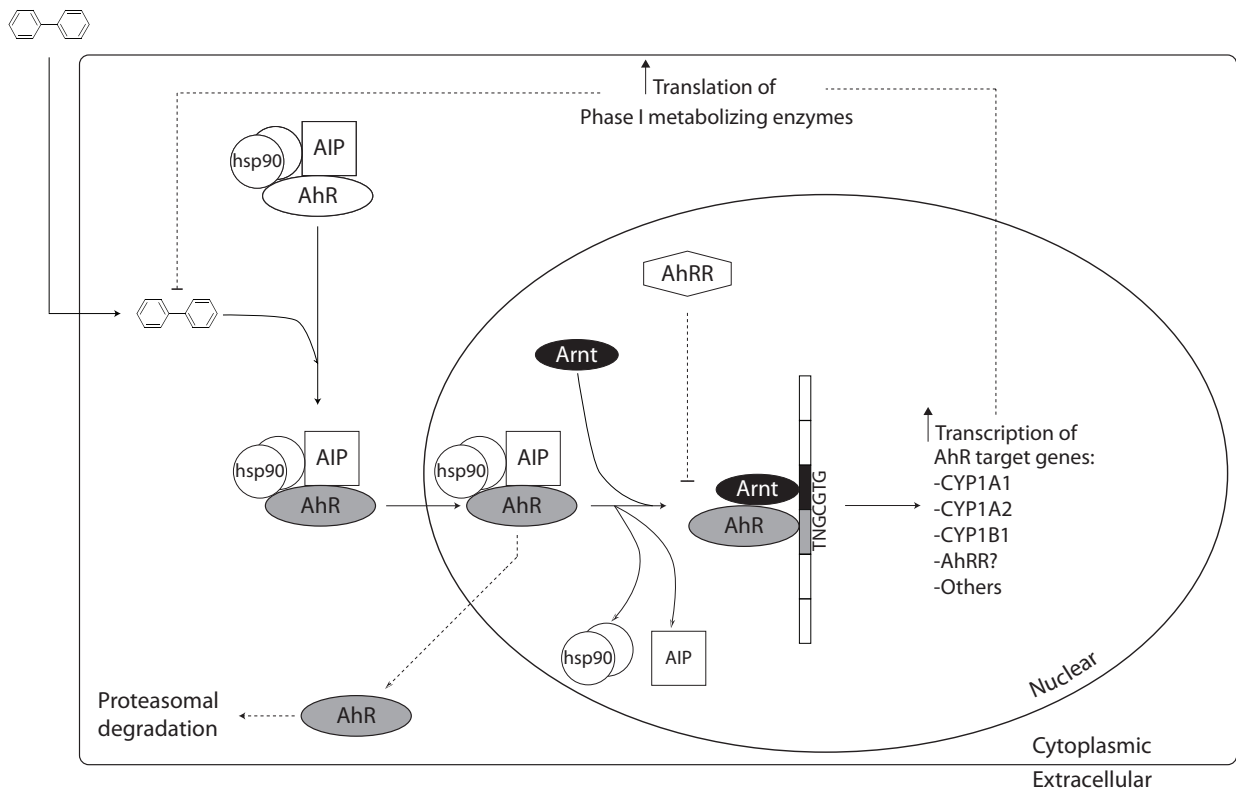


Figure 1-3: Model of AhR signaling following binding of agonist. Agonist is depicted by bicyclic compound. Dotted lines indicate potential counter-regulatory mechanisms for AhR signaling. AhR = aryl hydrocarbon receptor, AhRR = AhR repressor, AIP = AhR-interacting protein, Arnt = AhR nuclear translocator, hsp90 = heat-shock protein 90.

mouse; much like the global AhR knockout mouse (Schmidt et al., 1996) and the hepatocyte-specific AhR knockout (Walisser et al., 2005), the ARNT hepatocyte knockout was completely resistant to TCDD-induced upregulation of AhR target genes as well as TCDD-incited hepatotoxicity (Nukaya et al., 2010b).

The role of the AhR in mediating the toxic effects of DLCs has been demonstrated in several global and tissue-specific mouse models. The most recent evidence comes from the aforementioned findings using the hepatocyte-specific ARNT knockout mouse (Nukaya et al., 2010b); however, the first conclusive studies revealing the central role of the AhR in DLC toxicity emerged during the mid-1990s from two independent laboratories, both reporting similar results: global loss of AhR prevented TCDD-induced AhR target gene upregulation, abrogated thymic atrophy, and protected against hepatotoxicity and hepatomegaly (Fernandez-Salguero et al., 1995; Schmidt et al., 1996). These observations were seen even with 10 x higher doses of TCDD (2000 ug/kg, single IP injection) than that required to maximally induce AhR target genes and affect organ physiology in wild-type mice (Fernandez-Salguero et al., 1996); at such a dose, survival could be considered proof enough for the necessity of AhR in mediating TCDD toxicity (the LD50 for IP TCDD in the C57 strain is estimated to be 200 ug/kg). In addition to establishing the role of the AhR in mediating DLC toxicity, the global AhR knockout model revealed a critical role for AhR signaling during development, evidenced by smaller livers, liver portal tract fibrosis, fatty infiltration in livers of young mice, and splenic abnormalities in early and late stages in life (Fernandez-Salguero et al., 1995; Schmidt et al., 1996). The normal liver phenotype of the hepatocyte-specific ARNT knockout implies that the role of AhR signaling on liver development is likely extrahepatic (Nukaya et al., 2010b), and this is supported by the hepatocyte-specific AhR knockout model (Walisser et al., 2005).

The mechanism by which DLCs induce toxicity through the AhR is currently a subject of extensive investigation. The logical expectation is that abnormal and excessive upregulation of AhR target genes plays a role; however, the actual target genes of AhR have not been completely elucidated, an issue complicated by the fact that the physiological ligand(s) of AhR is (are) currently unknown. To date, the downstream targets of ligand-activated AhR may be roughly categorized into two classes: genes controlling first and second-phase drug/xenobiotic metabolism, and genes that control cell proliferation/cell cycle progression and inflammation (Bock and Kohle, 2009). The former class appears to be entirely mediated by classical nuclear signaling, while the latter may involve both genomic and non-genomic (i.e. protein phosphorylation) pathways (Blankenship and Matsumura, 1997; Tanno and Aoki, 1996). The induction of first-phase drug metabolizing enzymes, and specifically that of cytochrome P450 (CYP), family 1, member A1 (CYP1A1), has been extensively investigated as a potential means by which overactivation of AhR might result in toxicity.

The most potent and consistently observed effect of DLC exposure is the induction of CYP1A1, a member of the CYP1 family, which in turn is a constituent of the superfamily of cytochrome P450 enzymes of first-phase drug metabolism. CYP1A1 is the best-characterized member of the CYP1 family (CYP1A2 and CYP1B1 are the other members), and is expressed in a number of tissues, including liver, lung, skin, adipose, and intestine (Androutsopoulos et al., 2009); induction of CYP1A1 in response to DLCs, though, is highest in liver and endothelium (Rifkind, 2006). As is the case with most P450 enzymes, CYP1A1 is primarily localized to the endoplasmic reticulum, where it catalyzes the first step of the oxidative metabolism of substrates (Nebert et al., 2004). Basal levels of CYP1A1 mRNA and protein are often undetectable, but increase dramatically upon treatment with AhR agonists. Therefore, the extent to which most

AhR agonists can effectively signal is limited due to agonist-induced augmentation of first-phase drug metabolizing enzyme synthesis, particularly that of CYP1A1; the poor first-phase metabolizability of most DLCs likely plays a role in their toxicity. Furthermore, the potency, dose-responsiveness, and specificity of CYP1A1 induction following treatment with AhR agonists (particularly TCDD) has established CYP1A1 expression (mRNA and protein) and activity as readouts for AhR activation (Rifkind, 2006). The other CYP1 genes are also specifically induced following AhR activation, but the lower basal expression and higher inducibility of CYP1A1 results in a higher (and therefore, generally more experimentally useful) signal-to-noise ratio.

As a result of its high inducibility following DLC exposure, CYP1A1 upregulation has been suggested as a mechanism by which persistent AhR activation leads to toxicity. Several pieces of evidence support this view, including the ability of CYP1A1 to bioactivate certain substrates into toxic/more toxic intermediates, the excessive generation of reactive oxygen species by poorly metabolizable CYP1A1 substrates (Park et al., 1996), and the finding that the CYP1A1 knockout mouse is partially protected from TCDD-induced wasting and hepatotoxicity (Uno et al., 2004). However, there is equally compelling evidence that CYP1A1 induction may be protective, as shown by a recent study where TCDD-incited hepatotoxicity was actually increased in either the CYP1A1 or CYP1A2 knockout, or in a dual CYP1A1/A2 partial knockout mouse compared to wild-type control (Nukaya et al., 2009). Additional support for a protective effect of CYP1A1/A2 may be found in a study where the hepatotoxic effect of bile duct ligation in conjunction with TCDD treatment was augmented by an order of magnitude in the CYP1A1/A2 double knockout mouse (Ozeki et al., 2011). Despite these seemingly opposing views, it is important to consider that complete or extensive loss of a gene, normal

activation/expression of a gene, and pathological activation/expression of a gene may be viewed as physiologically disparate states. Studies using rats with AhR polymorphisms that result in several hundred-fold differences in LD 50 values for TCDD indicate that at the very least, CYP1 gene upregulation does not determine sensitivity to TCDD-induced lethality; dioxin-sensitive and -resistant rat strains show equal induction of all three CYP1 genes following TCDD treatment; however, despite equivalent CYP1 upregulation, resistant strains exhibit considerable tolerance to TCDD-induced hepatic insult and death (Franc et al., 2008; Tuomisto et al., 1999).

In contrast to CYP1A1, less research has been conducted on the impact of CYP1A2 or CYP1B1 induction by DLCs, and even less on the phase II metabolizing enzymes. CYP1A2 has been shown to sequester DLCs, but not structurally related non-DLCs in the liver, evidenced by drastic shifts in the liver:adipose ratios following administration of DLCs versus non-DLCs (Devito et al., 1998; Diliberto et al., 1997). This pattern of preferential hepatic sequestration was not seen in the livers of CYP1A2 knockout mice (Devito et al., 1998). The implications of sequestration are currently unknown, although a reasonable expectation would be a shift in toxicity away from other DLC target organs (i.e. the thymus) at the expense of the liver. The role of CYP1B1 in AhR-mediated toxicity is currently unclear, possibly due to limited inducibility in most organs, including those which demonstrate robust CYP1A1 induction in response to DLC treatment, such as the liver and kidney (Buters et al., 1999). The role of the phase II metabolizing enzymes, if any, is even less clear. The DLCs are generally poor substrates for phase I enzymes, and therefore may not undergo significant phase II metabolism. A detailed study of TCDD metabolism and clearance in Victor Yushchenko revealed that more than 60% of total TCDD was eliminated through feces, urine, and sweat in unmetabolized form, with an estimated half-life of approximately 15 months. The remaining 40% was eliminated in the form of hydroxylated

TCDD metabolites, consistent with phase I and not phase II metabolism (Sorg et al., 2009). Similarly, in rats injected with a dioxin-like PCB, 40% of the total administered dose was excreted in the feces as hydroxylated metabolites within 5 days (Yoshimura et al., 1987), and in germ-free rats, similar rates and pathways of elimination have been observed following dioxin-like PCB exposure, implicating first-phase metabolism followed by fecal excretion as the dominant route for DLC clearance (Wehler et al., 1989; Morck et al., 2002).

Non-genomic signaling by the AhR has been demonstrated in several studies, with activation of the protein tyrosine kinase c-src as the most widely observed effect (Matsumura, 2009). However, the majority of studies concerning non-genomic AhR signaling have focused on inflammatory responses in cell lines, yielding only sparse data pertaining to DLC toxicity. While c-src has been proposed to be a mediator of TCDD-induced toxicity, studies using the c-src homozygous knockout mouse have not yielded convincing evidence pertaining to the importance of c-src as a mediator of AhR (TCDD)-driven toxicity (Dunlap et al., 2002; Matsumura et al., 1997). Additionally, recent findings from the hepatocyte-specific ARNT knockout mouse suggest that at least in the context of hepatotoxicity, genomic signaling through the AhR is required, as heterodimerization of activated AhR and ARNT occurs after nuclear translocation of the liganded AhR (Nukaya et al., 2010b). Therefore, the role of non-genomic AhR signaling in DLC toxicity remains unclear.

Data from *in vivo* dose-response studies, global and tissue-specific knockout mouse models, and microarray studies have shown that the AhR-ARNT pathway of signaling is required to mediate the toxic effects of pathological AhR activation by DLCs. Given the extensive inducibility of the CYP1 enzymes, particularly that of CYP1A1, as well as the correlation between DLC target organs and the responsiveness of said organs to CYP1 induction

(i.e. the liver and endothelium), it is plausible that excessive activation of the CYP1 genes may play a partial role in the tissue injury often observed following DLC treatment. However, the validity of this and other proposed and potential mechanisms, including the role of the AhR-repressor and proteasomal degradation of activated AhR remain to be determined, as the specific pathway(s) connecting AhR-ARNT and toxicity is (are) currently unknown (**Fig. 1-3**).

1.G. Summary

Having established the impact of DLCs on the liver, the principal role of the liver in mediating DLC toxicity, and the utility of primary hepatocytes derived from mice, the remainder of this paper focuses on the value of a well-characterized two-dimensional (2-D) primary hepatocyte system for the mechanistic investigation of dioxin-like PCB effects on hepatic glucose metabolism using a variety of metabolic, biochemical, and molecular assays. The following three chapters will outline the process for isolating and validating the quality and function of primary mouse hepatocytes, present data on the application of primary mouse hepatocytes for studying the toxicological and metabolic effects of dioxin-like PCBs, and postulate additional experiments utilizing primary mouse hepatocytes to further elucidate the molecular mechanism connecting overactivation of the AhR to disrupted liver function.

CHAPTER II

Development and validation of a primary mouse hepatocyte system

2.A. Introduction

Properly isolated and cultured primary murine hepatocytes are invaluable tools for metabolic and toxicological studies. Although the useful lifespan of primary hepatocytes in standard two-dimensional culture is restricted to 2-3 days, the range of functional, physiologically relevant assays that may be performed in hepatocytes largely compensates for this limitation. Much of the progress in the past few decades in the field of primary hepatocyte isolation and culture is a direct result of the pioneering work of Berry and Friend, who introduced the scientific community to the collagenase-mediated perfusion-driven method of rat liver cell isolation (1974). Prior to perfusion-assisted digestion, most hepatocyte isolations involved mechanical manipulation (i.e. mincing or slicing) in conjunction with enzymatic digestion of liver pieces, resulting in a higher percentage of damaged cells and lower yields compared to the method published by Berry and Friend (Howard et al., 1967).

The highly vascularized nature of the liver is well-suited to perfusion-assisted digestion, as this method exposes the majority of the liver cell population to digestive enzymes and allows for their rapid and efficient release, thereby minimizing isolation time and mechanical stress. However, even with perfusion-mediated, collagenase-catalyzed primary hepatocyte isolation, validation of hepatocyte function is critical to ensure that data generated from isolated cells is consistent, and that observed trends are as closely reflective of *in vivo* conditions as possible. The importance of high-quality hepatocyte preparations is underlined by the fact that the majority of published papers note that only batches of cells demonstrating > 90% initial viability

(via trypan blue staining) are used. The specific reasons for utilizing only high-viability cell batches are generally not elaborated upon, but experience has confirmed that both yield and viability are reflective of the appropriateness of the isolation technique and degree of care implemented during handling of cells. Fundamental flaws in seemingly minor details, including cannulation efficiency, flow rate and pressure of perfusion, chelating agent concentration in the wash buffer, batch of collagenase used, and filtration and wash method generally manifest in sub-optimal yield and/or viability; more insidious are issues that lead to high yield and viability but compromised function (i.e. cell surface receptor cleavage leading to reduced peptide hormone responsiveness). It is therefore essential to compare yield, viability, and function with established values in the literature.

2.B. Materials and methods

Isolation of primary mouse hepatocytes - A modification of the non-recirculating two-step perfusion method was used (Klaunig et al., 1981a). Chow-fed (*ad libitum*) 8 to 12 week-old male C57BL/6 mice were anesthetized with isoflurane and the portal vein was cannulated with a twenty-three gauge needle. Cannulation was performed with a slow (1 mL/min) drip of Hank's Balanced Salt Solution (HBSS, containing 5 mM glucose supplemented with 0.5 mM EGTA and 25 mM HEPES (pH 7.4 at 37 °C) to prevent injection of air into the portal vein. Successful cannulation was defined as observation of a near-instantaneous blanching effect within the entire liver immediately upon insertion of the cannula into the portal vein. Upon confirmation of successful cannulation, the inferior vena cava (IVC) was immediately cut to allow fluid to drain and the flow rate increased from 1 mL/min to 8-10 mL/min over the course of 5 s; the increase in flow rate combined with drainage through the IVC caused the liver to finish blanching within seconds. HBSS was perfused at 8-10 mL/min for 6 min with periodic clamping (5 s clamp every

20 s) of the IVC to accelerate the process. DMEM containing 5 mM glucose (Mediatech) supplemented with 100 U/mL Penicillin and 0.1 mg/mL Streptomycin (Pen/Strep), 15 mM HEPES, and 100 U/mL collagenase (Type IV, Worthington) was then perfused at 8-10 mL/min for an additional 6 to 8 min to digest the liver. Intermittent clamping of the IVC was also performed during this step of the process to augment total cell yield, as reported by Klaunig et al. (1981). After sufficient digestion, the gall bladder was removed and the liver was excised and transferred to a 9.5-cm Media-Miser dish (Fisher) containing 15 mL of the same medium used for digestion. Cells were liberated by tearing and shaking of the liver with forceps. Cells were then gently triturated, filtered through a 74 μ m stainless steel strainer (Dual Manufacturing), and washed 3 times by spinning at 50 x g for 2 minutes at 4 °C followed by resuspension in isolation medium (DMEM with 25 mM glucose supplemented with Pen/Strep, 15 mM HEPES, 100nM dexamethasone and 10% FBS). Viability and yield were assessed by removing an aliquot of cells and mixing in a 4:1 ratio with 0.4% trypan blue for 1 min at room temperature followed by counting cells that excluded trypan blue using a hemocytometer. Since trypan blue tends to overestimate viability, only cells that both excluded trypan blue and appeared small, clear, and bright under a standard light microscope were considered to be viable; hepatocytes from steatotic livers were not subject to the latter criteria, since freshly isolated steatotic hepatocytes are larger due to lipid infiltration, and therefore do not appear as small/bright spheres, but nonetheless attach and recover normally. Viability was > 90% for all preparations, with an average viable yield of 4×10^7 cells per animal. For consistency, all isolation procedures were performed in the morning.

Plating of primary mouse hepatocytes - Hepatocytes were plated on collagen-coated (5 μ g/cm² Type I collagen; BD) 12 or 24-well plates (Corning); consistent results with 24-well plates

required the use of non tissue culture-treated plates to ensure even distribution of cells (i.e. avoidance of a *bullseye* effect of excessive concentration of cells in the center and around the outer perimeter of the well), due to the reduced meniscus effect as a result of the more hydrophobic nature of non tissue culture-treated plastic. Collagen coating was performed by diluting concentrated collagen in 0.02 N acetic acid to a volume sufficient to cover the bottom of a well with shaking (50-75 μL /well for a 24-well plate and 100-125 μL /well for a 12-well plate). For consistency and efficiency, coating of all wells was performed using a repeater pipette followed by brief shaking and tapping to ensure even distribution of collagen; overnight exposure to UV under a hood allowed collagen to dry and the plates to sterilize. All plates were washed with sterile PBS prior to use. Freshly isolated hepatocytes were maintained in isolation medium at 4 °C until plating (generally less than 30 min, but no adverse effects were seen up to 3 h). Cells were diluted to 3×10^5 cells/mL in isolation medium for plating, with 12-well plates receiving between 700-800 μL /well and 24-well plates receiving between 380-450 μL /well. Visual examination of a single well was performed prior to mass plating to ensure that an initial density of 65-70% was achieved to allow for a confluent monolayer the following day. All cell quantitation and density estimates were based on viable cells only. Immediately after plating, cells were evenly distributed by careful but very thorough shaking in the X-Y axis. Cells were allowed to attach for 1 h at 37 °C in a humidified 5% CO₂ incubator, washed once with DMEM (5 mM glucose), and the media then changed to culture medium (DMEM with 5 mM glucose supplemented with Pen/Strep, 5 mM HEPES, 10 nM dexamethasone, and 10% FBS) for a 3-4 h recovery period. Media was then switched to the required overnight culture medium, which varied based on experimental parameters, but always contained 2-4 mM L-glutamine, Pen/Strep, 5-10 mM HEPES, 10 nM dexamethasone, and 44 mM NaHCO₃. A more detailed description,

images, videos, and additional information concerning the isolation and culture of primary mouse hepatocytes may be found at www.mouselivercells.com.

Isolation and plating of primary rat hepatocytes – Hepatocytes were isolated from a 16 week-old male lean Zucker rat using the same basic process as described for mouse hepatocyte with the following modifications: a 19 gauge needle was utilized for portal vein cannulation, flow rate for HBSS and collagenase solutions were increased to 25 mL/min, the digested liver was torn apart in a 20-cm dish to accommodate the larger liver size, and the viable cell concentration for plating was increased from 3×10^5 cells/mL to 4×10^5 cells/mL to compensate for the smaller physical size of rat versus mouse hepatocytes. Total yield was $> 2 \times 10^8$ viable cells, with viability $> 90\%$ by trypan blue staining. All other isolation, plating, and culture conditions were identical.

Visual assessment of phenotype – Hepatocyte phenotype was assessed at regular intervals on a standard inverted light microscope to evaluate cell quality and health. Images were taken directly through the eyepiece at 400x magnification to document the progression of cells from plating through the following day (Canon SX20IS).

Measurement of glycogen - Total intracellular glycogen was measured by a combination and modification of the methods outlined in Roe and Dailey (1966) and Lingohr et al. (2002). Following treatment(s), media was removed and cells were washed twice with cold PBS. Cells were lysed with 0.75% SDS (200 μ L/well for 12-well plates and 100 μ L/well for 24-well plates) and lysates transferred into 1.7 mL microfuge tubes. Unless radiolabel had been added to cells, samples were briefly sonicated (1 s at low power) to facilitate pipetting, and a small aliquot was removed for protein determination (Pierce). Protein was precipitated from the remaining lysate for 1 h at 4 °C by addition of 100% TCA to a final concentration of 5-10%. TCA precipitates

were spun at 4 °C at 14,000 x g for 10 min to pellet protein and the entire volume of supernatant was transferred to a new set of tubes. To precipitate glycogen, 2.5 supernatant volumes of 95% EtOH were added to the supernatant. Glycogen was allowed to precipitate at -80 °C for > 1 h, pelleted by spinning at 14,000 x g for 15-20 min at 4 °C, washed once with 1 mL of 70% EtOH, re-spun, and dried using a SpeedVac. Glycogen was redissolved in 350 µL of 0.2 N NaAc and sonicated briefly (unless radiolabel had been added) to minimize the interference of residual protein in the digestion process (2-5 s at medium power). Tubes were briefly spun following sonication and an excess of glucoamylase (700 µU activity based on glucose liberation from starch/µL digest) was added to digest glycogen. Glycogen was digested using glucoamylase in 0.2 N sodium acetate (pH 4.4-4.6 at room temperature) in the dark with shaking at 37-45 °C for 90 min. High glycogen standards and no- glucoamylase blanks were included to ensure completeness and specificity of digestion, respectively. Liberated glucose was measured following neutralization of the digest to pH 6.5-7.0 with NaOH. Total glucose was assayed via the glucose oxidase-peroxidase (GOD-PERID) method by measuring the oxidation of 2,2'-azino-bis(3-ethylbenzthiazoline-6-sulphonic acid) (ABTS) at 405 nm using a 96-well plate reader (Thermo Multiskan MCC) and quantitation was performed using a glucose-based standard curve after confirming that both glucose and glycogen-based standard curves were equivalent.

Measurement of glucose - Glucose was assayed using the ABTS-linked glucose oxidase-peroxidase method. 50x solutions of glucose oxidase (GOD; 2000-5000 β-D-glucose oxidizing units/mL) and horseradish peroxidase (PERID; 5000 ABTS units/mL) were made in 50% glycerol/0.2 M sodium phosphate (pH 6.4 at room temperature) and stored at -20 °C. A 33x solution of ABTS was made in 0.2 M sodium phosphate and stored at -20 °C. The assay reaction mix consisted of 1x GOD, 1x PERID, and 1x ABTS with 0.2 M sodium phosphate to reach a

final volume of 100 μ L, and standard curves were made using glucose in H₂O. Due to the speed of the reaction, the standard curve was often situated in the middle of the plate, and for larger experiments, each plate contained its own standard curve for calibration. A repeater pipette was used for all assay reactions to facilitate expediency and consistency; for some reactions where glucose concentrations spanned wide ranges, the reaction mix was scaled into a 10 μ L volume to further facilitate pipetting speed. All incubations were performed at room temperature and oxidized ABTS was measured via spectrophotometry at 405 nm on a 96-well plate reader (Thermo Multiskan MCC).

Glycogen synthesis - Treatment of cells for assessment of basal, acute, and insulin-stimulated glycogen synthesis were as follows: basal glycogen was determined by washing and lysis of cells after overnight incubation with the desired treatment conditions. Acute glycogen synthesis was performed by washing cells and adding the desired treatment conditions for specified periods of time (1 – 5 h); to control for overnight glycogen accumulation, a set of wells was lysed immediately before acute treatment began, both before and after washing, to obtain a baseline reading. Insulin, if used, was added at the beginning of the acute synthesis period. At the end of incubation, all media was removed, wells were washed twice with cold PBS, and cells were processed for glycogen measurement.

Glycogenolysis - Cells were incubated overnight in the specified glucose condition. Glycogenolysis was initiated by direct addition of glucagon/forskolin or an equal volume of DMSO to cells. Insulin, if used, was added immediately before glucagon/forskolin. For larger-scale experiments, two repeater pipettes loaded with glucagon/forskolin and insulin at the appropriate concentrations were used to minimize time differences, and volume and vehicle controls were performed first. Hormone incubations persisted for at least 15 min, but for no

longer than 60 min, depending on the experiment. At the end of treatment, all media was removed, wells were washed twice with cold PBS, and cells were processed for glycogen measurement.

Gluconeogenesis (GNG) - Glucose synthesis from 3-carbon intermediates was assessed using glucose-free, phenol red-free media and measuring the release of glucose into the media at specified time points. Pilot experiments were performed to determine the contribution of glycogen to total glucose output, and if need be, cells were depleted of glycogen by a 30 – 60 min preincubation with glucose free media. Gluconeogenesis was most commonly performed with overnight glucose concentrations between 5 – 10 mM to prevent excessively high glycogen accumulation, which would necessitate a several hour-long depletion period. Stimulated GNG was performed by continuous incubation with glucagon or forskolin. For insulin suppression of GNG, insulin was added on its own, and was also co-incubated with glucagon or forskolin. All GNG assays were performed in glucose-free, phenol red-free media supplemented with 44 mM NaHCO₃, 2 mM L-glutamine, Pen/Strep, 10 mM HEPES (pH 7.4), 10 nM dexamethasone, and 10 mM of the specified substrate. At specified intervals, an aliquot of media was removed for analysis of glucose by the GOD-PERID assay. The remainder of the media was then removed and fresh media added for the next time point. At the termination of the assay, cells were lysed in 0.75% SDS for protein determination.

Beta oxidation – Fatty acid oxidation was assessed by measurement of tritiated H₂O released during beta oxidation of [9, 10-³H]-palmitic acid, based on a modification of the method outlined by Moon and Rhead (1987). A concentrated solution of BSA-coupled palmitate was made by dissolving sodium palmitate in 0.01 N NaOH and adding [9, 10-³H]-palmitic acid (Perkin-Elmer, 5 μCi/μL) in a 70 °C water bath. The labeled mixture was coupled to 2 mM BSA (Jackson

ImmunoResearch) in HBSS to reach a final BSA:palmitate molar ratio of 3:1; for experiments specifically designed test BSA:palmitate molar ratios, labeled mixture was added to BSA to attain the desired ratio. Immediately before addition of the BSA-palmitate concentrate, media was removed from wells and replaced with HBSS. The BSA-palmitate concentrate was then diluted into HBSS present in wells to attain the desired palmitate concentration; the final quantity of radioactivity per well for a 12-well plate was approximately 0.15 μCi . The reaction was allowed to proceed for the specified length of time, after which media was collected, protein precipitated with TCA, and the clarified supernatant alkalinized with 6 N NaOH; replicate aliquots of media (non-specific blanks) that had never been applied to cells were processed in the same manner to account for radioactivity not attributable to cellular beta oxidation. Alkalinized samples were applied to 1 mL columns containing Dowex 1x2-400 ion-exchange resin, eluted with water, and the flow-through counted after addition of scintillation fluid (Beckman Coulter LS6500); non-specific blanks were subtracted from total counts, and counts per minute were converted to μg palmitate oxidized through the use of ^3H media standards. Total cellular uptake of palmitate was measured by washing cells with cold PBS three times and lysing in 0.75% SDS. Lysates were directly added to scintillation vials and counted and quantitated using ^3H standards (media plus 0.75% SDS). When used, L-carnitine was added concurrently with the substrate, while etomoxir was pre-incubated for 30 min prior to the start of beta oxidation and was also present during beta oxidation.

Lipogenesis - Lipogenesis from glucose was determined by measuring the incorporation of [$^{14}\text{C}(\text{U})$]-glucose (American Radiolabeled Chemicals) into the lipid extractable fraction of cell lysates. Cells were incubated with at least 1.5 μCi of ^{14}C glucose per well containing the indicated concentration of glucose, and the assay was allowed to proceed for the specified time;

if used, insulin was added in conjunction with radiolabel. The reaction was terminated by removal of all media followed by three washes with cold PBS. Cells were hypotonically lysed using H₂O (300 µL/well in a 12-well plate) with gentle rocking at room temperature and then scraped into 6 mL plastic scintillation vials (PerkinElmer). One additional volume of H₂O was added to wells to facilitate transfer of residual lysate. Separation of lipid soluble radioactivity was performed by addition of the maximum volume of organic scintillation fluid (Betafluor) that still allowed for enough air space to permit shaking (~4.5 mL). Samples were vigorously shaken and allowed to sit for > 4 h; media ¹⁴C standards were processed in the same manner to ensure specificity of partitioning, and partitioning blanks were made for ¹⁴C standard counting. After partitioning, the organic phase was carefully transferred to new scintillation vials and counted (Beckman Coulter LS6500). ¹⁴C media standards were added to partitioning blanks for conversion of counts per minute into µg of glucose incorporated. Due to the limited ability of even small volumes of aqueous liquids to remain dispersed in the organic scintillation fluid, standards were shaken well and counted immediately in replicate.

Oil Red O staining - Cells were washed with cold PBS twice followed by 1 h fixation in formalin; For quantitation, wells in a separate plate were treated in the same manner to assess background. A 0.35% Oil Red O concentrated stock was made in 60% triethylphosphate and stored at 4 °C. Prior to use, the solution was diluted in a 3:2 ratio with H₂O and filtered through a 0.22 µm membrane (Millipore). Before staining, all formalin was removed and wells were washed once with 75% isopropanol and allowed to dry. A minimal volume of filtered Oil Red O solution was added to wells (200 µL/well for a 12-well plate) and cells were allowed to stain for 10 min. Oil Red O stain was immediately removed by siphoning off the excess stain and rapidly washing wells with 1 mL H₂O 3 times. Images were taken through the eyepiece of a standard

inverted light microscope. For quantification, stain was eluted with a minimal volume of 100% isopropanol and immediately transferred to a clear-bottomed 96-well plate. Absorbance was measured at 490 nm using a 96-well plate reader (Molecular Devices Versamax).

Ethoxyresorufin-O-deethylase (EROD) - The conversion of 7-ethoxyresorufin (7-ER) to resorufin was performed by a modification of Kennedy et al. (1993). Cells were washed twice in cold PBS and disrupted by a single round of freezing/thawing (-80 °C/37 °C). Thawed plates were placed on ice and the EROD assay mixture was added (150 µL/well for a 24-well plate; 1 mg/mL BSA, 5 µM 7-ER, and 0.5 mM NADPH in 50 mM Tris (pH 7.4 at 37 °C)). The reaction was initiated by placing plates on a shaker at 37 °C in the dark. Total incubation time was 15 min, and the assay was terminated by addition of 0.8 volumes of 2 M glycine (pH 10.4 at room temperature). The terminated reaction mix was transferred into microfuge tubes, spun for 1 min at 14,000 x g at room temperature, and an aliquot of the supernatant was transferred to a solid black fluorescence microwell plate. Fluorescence of resorufin was assessed on a spectrofluorimeter (Beckman Coulter DTX 880) at 535 nm excitation/595 nm emission. A resorufin standard curve was used for quantitation.

Insulin signaling and immunoblotting – Cells were treated with the specified doses of insulin for 10 min, media was removed, and cells were lysed in 2x Laemmli sample buffer containing 0.1 M DTT. Lysates were transferred to microcentrifuge tubes, sonicated for 5 s at medium power, heated to 80-90 °C for 5 min, and stored at -20 °C. Proteins were separated by SDS-PAGE using 7.5% or 10% gels and transferred to nitrocellulose or PVDF membranes. Membranes were blocked overnight at 4 °C in 5% milk-TBST (w/v) and sodium azide. Anti-phospho Akt (Ser⁴⁷³), anti-phospho-ERK 1/2 (Thr²⁰²/Tyr²⁰⁴), or total ERK2 (Cell Signaling) were incubated for 3 h at

room temperature (1:3000 - 1:5000 antibody concentration) in TBST containing 5% BSA. Membranes were then thoroughly washed with TBST and probed with an HRP-linked secondary antibody (Santa-Cruz) at 1:3000 dilution in 5% milk-TBST for 1 h. After incubation, membranes were washed with TBST and TBS and developed following application of SuperSignal substrate (Pierce) for 5 min. Signal was captured by exposing membranes to BioMax MR film (Kodak). For PKC α adenovirus experiments, activity of overexpressed WT-PKC α was verified as described above, except primary antibody incubation was performed using phospho-PKC α / β II (Thr^{638/641}) (Cell Signaling) at 1:2000.

Treatment of cells for mRNA analysis – For validation of cellular responses to forskolin and insulin, cells were cultured overnight in the specified condition and treated with 5 or 25 μ M forskolin (DMSO), 10 nM insulin, or forskolin + insulin for the final 3 h of culture via direct addition to the medium. For determination of cellular responses to AhR agonists, cells were treated overnight (16 h) with the specified congener and concentration of PCB.

Quantitative real-time PCR (qRT-PCR) – RNA was isolated using the Qiagen RNEasy kit. Briefly, all media was removed and cells were washed twice with cold PBS. Buffer RLT containing 10 μ L/mL beta-mercaptoethanol was added to all wells, and plates were stored immediately at -80 °C for later processing. The purity and concentration of RNA was assessed via spectrophotometry (NanoDrop 2000); 260/230 ratios were consistently >2.0. Synthesis of cDNA was performed with 0.5 μ g of RNA using the Bio-Rad iScript kit, and was stored at -20 °C. Quantitative RT-PCR was performed using Sybr Green (Bio-Rad) on a Bio-Rad MyiQ real-time PCR detection system. Primers were from IDT and were designed using PerlPrimer v1.1.18; when possible, primer pairs spanned introns. Primer specificity was assessed by melt curve analysis and agarose gel evaluation. Gene expression levels were evaluated by the delta-delta Ct

method after confirmation that amplification efficiency was between 90% - 110% for all primer pairs. Both 18S and beta-actin were validated as suitable reference genes, and 18S was chosen for subsequent runs.

Adenovirus infection – Cells were infected with adenovirus or an empty adenovirus control at identical multiplicities of infection (MOI; average 200-300 MOI/well). After plating, cells were allowed to recover for 3-4 h before infection. For infection, media was changed to culture medium containing 2% FBS. Virus was then added for 2-3 h, after which virus was removed by 2-3 washes with low-glucose DMEM. Cells were then placed in the desired overnight culture conditions for at least 12-14 h to allow for protein expression. Adenoviruses were a kind gift from Dr. Christopher Rhodes; details of virus construction may be found in Wrede et al. (2002) and Dickinson et al. (2001).

Statistical analysis - Comparisons between two treatments or conditions were performed with two-tailed Student's *t*-tests. Comparisons between > 2 treatments or conditions were made using 1-way ANOVA with post-hoc Tukey-Kramer analysis. JMP 7.0 was used for all analysis, and significance was set at $p < 0.05$.

2.C. Results

Isolated mouse hepatocytes attach, recover, and develop as described in the literature – Mouse hepatocytes in standard 2-D culture have been reported to initially present a rounded appearance followed by gradual spreading into an epithelial-like monolayer, assuming sufficient cellular density (Klaunig et al., 1981b). As seen in the time course in **Fig. 2-1 A**, freshly isolated cells were small, bright, and clear at time 0. Cells rapidly attached and started to flatten 2 h post-plating, with the most notable changes being the ability to clearly observe nuclei under low-

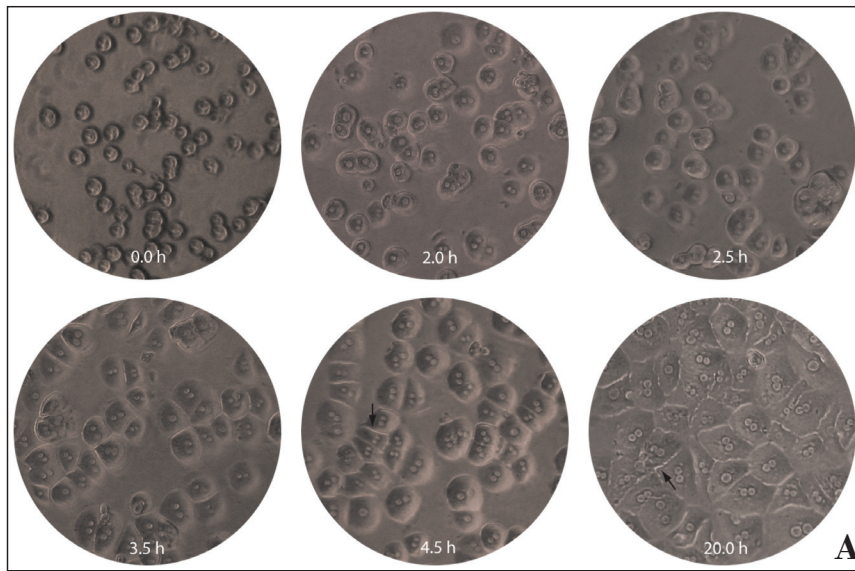
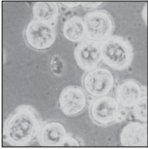
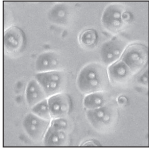
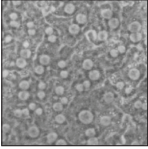
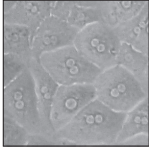


Figure 2-1: Descriptive characterization of isolated primary hepatocytes. A) Time-course of primary mouse hepatocyte development following plating onto thin-layer collagen-coated plates. Black arrows depict bile-canaliculi-like structures. Images taken at 400x magnification through the eyepiece of an inverted light microscope. B) Comparison of isolation and plating parameters of primary mouse hepatocytes as performed by Klaunig et al. (1981) and the current, adapted system (2011).

	Klaunig et al., 1981	Zhang et al., 2011
Mouse strain	BALB/c (male)	C57BL/6 (male)
Mouse body weight, g (avg)	30-35	20-25
Perfusion method	Portal vein nonrecirculating	Portal vein nonrecirculating
Perfusion flow rate, mL/min	10	9
Viability, %	> 90	> 90
Viable cells/g body weight ($\times 10^6$)	2.2	1.8
Collagenase concentration, U/mL	100 (Type I)	100 (Type IV)
Plating density, cells/cm ² ($\times 10^4$)*	4.0	4.3
Post-plating, 2 h		
Post-plating, 20-24 h		

B

power magnification and a tendency for cells in close contact to attach; these results paralleled those documented by Klaunig et al (1981b) (**Fig. 2-1 B**). The majority of cells were binucleated, consistent with the report that over 80% of mouse hepatocytes have two nuclei (Klaunig et al., 1981b). By 3.5 h post-plating, hepatocytes had mostly transformed from a rounded to a more cuboidal shape, with most cells having 4-6 clearly defined sides and readily observable cell-cell junctions. Bright, sharply defined cell-cell junctions were visible by 4.5 h post-plating, consistent with establishment of bile canaliculi-like structures (Tuschl and Mueller, 2006; Gallin, 1997). These structures were much more prominent after overnight recovery, as seen in the 20 h post-plating time point, where the majority of cell-cell junctions were bright, well-defined, and continuous across several cells.

A particularly important observation was that in healthy preparations, the cytoplasm had a uniformly granular appearance, but was clear of vacuolization, which occurs in response to stressors and often precedes cell death (unpublished observations). Consistent with the literature, cell morphology continued to change after the first 24 h of culture, with most cells taking on a fibroblastic appearance characterized by cytoplasmic projections, degeneration of cuboidal shape, and a general blurring of cell-cell junctions (Klaunig et al., 1981b); by 48 h, the monolayer resembled a mesh of cells rather than a network of well-defined hepatocytes (data not shown). The presence of 10% FBS accelerated this progression by approximately 6-8 h after overnight culture, again consistent with reported findings (Tuschl and Mueller, 2006; Gallin, 1997); because serum has been reported to aid in the initial attachment of cells (Klaunig et al., 1981b), hepatocytes were initially cultured in the presence of serum (first 4-5 h), but were maintained in serum-free media after that time.

Steatotic livers were chosen to assess the suitability of the isolation and culture methods under suboptimal conditions. Steatosis has been linked to increased incidence of adverse surgical outcomes in animal models (Vetelainen et al., 2007), as well in human transplantations studies (Selzner and Clavien, 2001), possibly due to reduced resistance to ATP stress and/or inflammation. Initial studies were performed using *ob/ob* mice with pale, grossly enlarged livers. Total cell yield was slightly but not significantly lower in *ob/ob* mice versus lean heterozygous littermates, but cell viability, attachment, and overall performance was not significantly impaired aside from the expected alterations in various metabolic functions secondary to the phenotype (data shown in later sections). Furthermore, gross steatosis was maintained immediately after isolation and did not diminish even after 24 h of culture. The most notable observation was the foamy appearance of freshly isolated cells from *ob/ob* and other highly steatotic livers, which, in a normal liver would be indicative of damaged or dying cells; however, in fatty livers, this visual indicator did not apply, as the swollen, bubbly appearance was due to lipid droplets and not vacuolization and/or swelling secondary to cell membrane damage. Additional validation was performed using fatty livers from high fat-fed mice as well as other genetically steatotic mouse models (data not shown).

Finally, the isolation procedure was evaluated for scalability in a lean Zucker rat. The much larger size of the rat compared to a mouse necessitated a higher flow rate and volume; however, enzyme concentration and total length of perfusion were kept constant to reduce the number of variables. Total cell yield was comparable to reported values (Berry, 1974), and viability was >90 %. As expected, rat hepatocytes were approximately 30% smaller than mouse hepatocytes, with significantly less binucleation (<30% of cells). There were no other notable differences in attachment, overall phenotype, survival, or function (data shown later).

Hepatocytes synthesize glycogen and are responsive to glucose, 3-carbon intermediates, and insulin – A defining characteristic of hepatocytes is the ability to synthesize and store glycogen from both glucose and 3-carbon gluconeogenic intermediates. Glucose may be stored as glycogen by the direct pathway, where glucose-6-phosphate is converted to glucose-1-phosphate and then incorporated into glycogen, or via the indirect pathway, where glucose first undergoes glycolysis and cycles through the gluconeogenic pathway and then converted back to glucose-6-phosphate→glucose-1-phosphate→glycogen (Moore et al., 1991; Newgard et al., 1984). Whether direct or indirect, total hepatocyte glycogen increases in a nearly linear fashion with respect to glucose concentration *in vitro* (Salhanick et al., 1989; Fleig et al., 1987), and this effect was confirmed in the current system, as seen in **Fig. 2-2 A**; total glycogen levels/mg protein also corresponded with reported values for hepatocytes (isolated from fed rats) cultured under similar conditions (Salhanick et al., 1989).

Glycogen synthesis is responsive to insulin due to the hormone's ability to increase the activity of enzymes that synthesize glycogen (Miller, Jr. et al., 1984), antagonize the activity of enzymes that induce glycogenolysis (Hartmann et al., 1987), and possibly through nonspecific effects, including augmentation of cell volume (Peak et al., 1992). However, unlike skeletal muscle or adipose tissue, the actual influx of glucose into the liver is not directly controlled by insulin, and therefore, the majority of investigators have found that the robustness of glycogen augmentation in response to insulin is lower (30-65% increase) in the liver versus GLUT4-containing tissues (Menuelle and Plas, 1991; Salhanick et al., 1989), although some studies have reported potent (several fold) insulin responses, possibly due to differences in basal glycogen synthesis rates (Fleig et al., 1987). Insulin responsiveness of hepatocytes was first evaluated by Akt and ERK signaling. Cells were incubated with increasing doses of insulin for 10 min, and

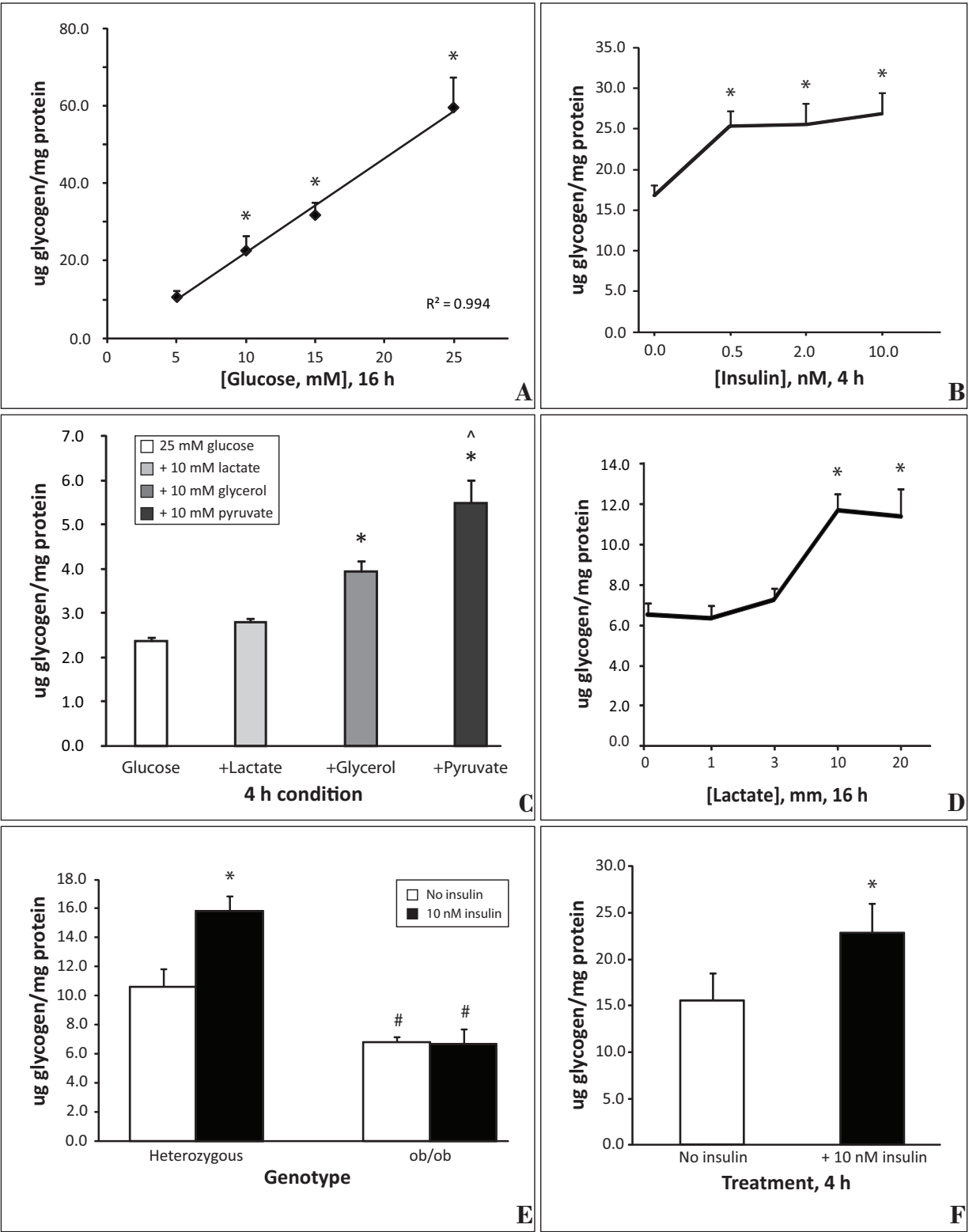
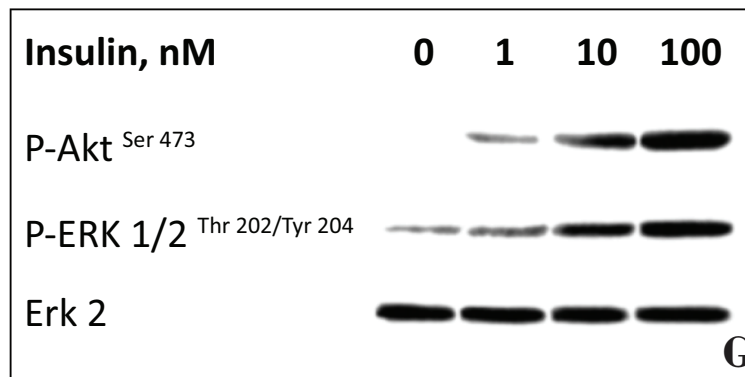


Figure 2-2: Glycogen synthesis and insulin signaling and action in primary hepatocytes (continued on next page)



(Figure 2-2 continued from previous page)

A) Dose-response relationship between overnight glucose concentration and total glycogen synthesized. * = $p < 0.05$ versus previous glucose concentration, $n = 4$ experiments performed in triplicate. B) Insulin dose-response for short-term glycogen synthesis; cells were incubated in 5 mM glucose overnight and treated for 4 h with specified concentration of insulin. * = $p < 0.05$ for insulin versus no insulin, single experiment performed in triplicate. C) Effect of 3-carbon substrates on total glycogen; cells were incubated overnight in 10 mM glucose followed by addition of 10 mM of specified substrate for 4 h. * = $p < 0.05$ versus glucose alone, $n = 2$ experiments performed in triplicate. D) Dose-response of overnight incubation with lactate on total glycogen; cells were incubated in 5 mM glucose with the specified concentration of lactate. * = $p < 0.05$ versus no lactate, $n = 2$ experiments performed in triplicate. E) Total and insulin-stimulated glycogen synthesis in *ob/ob* versus heterozygous controls; cells were incubated in 5 mM glucose overnight followed by 4 h treatment with 25 mM glucose +/- 10 nM insulin. * = $p < 0.05$ for insulin effect within genotype, # = $p < 0.05$ for total glycogen within respective +/- insulin condition across genotypes, $n = 2$ experiments performed in triplicate. F) Insulin-stimulated glycogen synthesis in primary hepatocytes from a lean Zucker rat; cells were incubated overnight in 5 mM glucose followed by 4 h treatment with 25 mM glucose +/- insulin. * = $p < 0.05$ for insulin effect, $n =$ single experiment performed in triplicate. G) Insulin signaling dose-response in primary mouse hepatocytes. Note: The upper band of P-ERK 1/2 was unusually weak in this blot and was lost during digital conversion. Cells were incubated in 5 mM glucose overnight and stimulated with the specified dose of insulin for 10 min. Blot is representative of at least two separate experiments; figure adapted from primary data published in Zhande et al., 2006. All error bars are +/- SD.

maximal stimulation during this acute treatment was seen with 10-100 nM insulin (**Fig. 2-2 G**); in the majority of studies, 10 min of 3-10 nM insulin was maximally effective for all insulin signals tested, including phospho- Akt, ERK, GSK-3 β , p70S6K, and FoxO-1 (data not shown). For insulin-stimulated glycogen synthesis, a longer treatment period was utilized to allow time for insulin signaling to manifest as glycogen accrual. On average, insulin increased total glycogen by ~50% with maximal efficacy at 1-10 nM (**Fig. 2-2 B**).

In addition to synthesizing glycogen from glucose via the indirect pathway, the liver can also incorporate 3-carbon gluconeogenic precursors of extrahepatic origin into glycogen (Agius et al., 1990; Tosh et al., 1994). In cells incubated with 5 mM glucose overnight in the absence of 3-carbon gluconeogenic intermediates, short-term treatment with high glucose plus 10 mM glycerol or pyruvate induced significant glycogen synthesis compared to glucose alone. Lactate did not appreciably augment total glycogen during this treatment period versus 25 mM glucose alone (**Fig. 2-2 C**), but dose-dependently increased total glycogen following overnight treatment in the presence of 5 mM glucose (**Fig 2-2 D**). The trend and magnitude of these observations are in line with those of Tosh et al., (1994) who reported that in rat hepatocytes, addition of 5 mM lactate or glycerol doubled total glycogen during 3 h incubation in 10 mM glucose, while pyruvate quadrupled total glycogen versus glucose alone. The principal mechanism by which lactate, glycerol, and pyruvate augment total cellular glycogen is likely through conversion into glucose (via GNG) followed by incorporation into glycogen (i.e. the indirect pathway) as opposed to secondary effects on the direct pathway, as the efficacy with which lactate, glycerol, and pyruvate were able to augment total glycogen paralleled the responsiveness of gluconeogenesis to the three substrates (data not shown).

Due to the sensitivity of cellular glycogen to stressors (decreases drastically- unpublished observations), glycogen was assayed in hepatocytes isolated from grossly steatotic livers of *ob/ob* mice, and was also used to evaluate the health of rat hepatocytes. Rat hepatocytes were comparable to mouse liver cells with respect to both basal and insulin-stimulated glycogen synthesis (**Fig 2-2 F**). Consistent with a phenotype of insulin resistance, glycogen synthesis in *ob/ob* hepatocytes was unresponsive to insulin (**Fig. 2-2 E**). However, total cellular glycogen was also significantly reduced in *ob/ob* hepatocytes, while total liver glycogen in *ob/ob* mice has been reported to be identical to, or higher than that of lean controls (van de Werve et al., 1983), likely due to chronic hyperglycemia/hyperinsulinemia. Thus, in the standard low-glucose, insulin-free overnight culture conditions, it is probable that the *ob/ob* liver glycogen levels seen *in vivo* could not be sustained. It is unlikely that the reduced glycogen was an artifact of general cell damage or stress, as hepatocytes from *ob/ob* mice were similarly competent compared to heterozygous hepatocytes with respect to beta oxidation (data not shown) and produced far more glucose from lactate (**Fig 2-4 E**).

Isolated mouse hepatocytes respond acutely to cAMP agonists, and this effect is suppressible by insulin – Glycogenolysis provides approximately 50% of the glucose needed to maintain glycemia during short-term fasting (Petersen et al., 1996; Nascimento et al., 2008) and is normally stimulated by a shift in the insulin:glucagon ratio, which decreases during fasting, leading to a dominance of glucagon signaling. The resulting increase in cAMP activates PKA, ultimately enhancing the activity of glycogen phosphorylase and leading to breakdown of glycogen. Other cAMP agonists, including nonmetabolizable cAMP analogs and adenylate cyclase activators, have similar effects on glycogenolysis and possess the advantage of being more stable in solution than a peptide hormone such as glucagon. Therefore, forskolin, an

agonist of adenylate cyclase, was used to induce glycogenolysis in primary hepatocytes. For glycogenolysis, cells were incubated overnight in 25 mM glucose to maximize glycogen content (**Fig. 2-3 A**), although similar trends were observed for the assay with lower overnight glucose concentrations (data not shown). Forskolin rapidly and potently reduced glycogen stores, with maximal efficacy at 1 μ M. A 10-fold increase in forskolin dose did not augment the rate of glycogenolysis versus 1 μ M, but prevented insulin from suppressing the glycogenolytic effect; at 1 μ M forskolin, insulin suppressed glycogenolysis by > 70%, in line with reported findings (Gabbay and Lardy, 1984; Beebe et al., 1985). Insulin suppression of cAMP signaling is primarily mediated by activation of phosphodiesterase (PDE), which in turn hydrolyzes cAMP (Beebe et al., 1985). The loss of insulin suppression of forskolin-induced glycogenolysis at 10 μ M forskolin was likely due to increased activation of adenylate cyclase (compared to 1 μ M forskolin), leading to cAMP levels beyond that which could be hydrolyzed by insulin-stimulated PDE; this is supported by the observation that cAMP agonists, such as glucagon, augment cAMP to levels in excess that needed to maximally induce glycogenolysis (Yamatani et al., 1987). To determine the effect of time on the hormone responsiveness of the assay, two time points, 20 and 40 min, were evaluated. As demonstrated by **Fig 2-3 B**, 40 min incubation with 1 μ M forskolin resulted in a more robust glycogenolytic effect compared to 20 min, with equally effective insulin suppression.

Isolated mouse hepatocytes respond chronically to cAMP agonists, and this effect is suppressible by insulin – While glycogen is able to supply half of the required glucose for glycemic maintenance during a short-term (i.e. overnight) fast, GNG is the principle means by which glucose is synthesized during longer periods of fasting (Corssmit et al., 2001; Landau et al., 1996). GNG is also a key measure of hepatocyte function, as it involves both cytosolic and

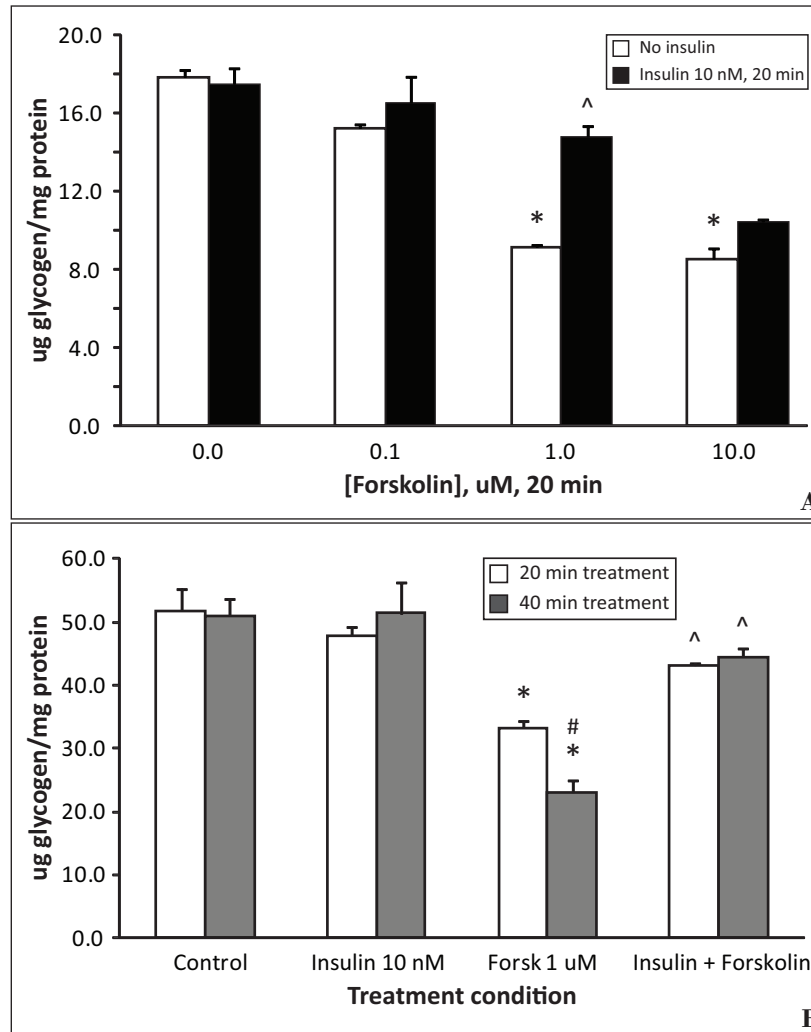


Figure 2-3: Glycogenolysis in primary mouse hepatocytes. A) Insulin suppression of a dose-response of forskolin-stimulated glycogenolysis. Cells were incubated overnight in 25 mM glucose and treated for 20 min with the specified concentration of forskolin +/- 10 nM insulin. * = $p < 0.05$ for forskolin effect, ^ = $p < 0.05$ for insulin attenuation of forskolin effect within respective forskolin dose, n = single experiment performed in triplicate. B) Glycogenolysis with 20 versus 40 min incubation with forskolin and forskolin/insulin. Cells were incubated overnight in 25 mM glucose and the specified treatments were applied for 20 or 40 min. * = $p < 0.05$ for forskolin effect within each time point, # = $p < 0.05$ forskolin effect at 20 versus 40 min, ^ = $p < 0.05$ for insulin attenuation of forskolin effect within each respective time point, n = single experiment performed in triplicate. All error bars are +/- SD.

mitochondrial reactions. The rate of GNG and its responsiveness to stimulation is largely determined by the energy state of the cell, and therefore these characteristics may be used as functional markers for general hepatocyte integrity (Hanson and Reshef, 1997; Foretz et al., 2010); intracellular glycogen, however, remains the most sensitive functional readout for hepatocyte health (unpublished observations). Hepatocytes incubated in glucose-free media containing 10 mM lactate responded both acutely (1 – 2 h) and over the course of 24 h to forskolin (**Fig. 2-4 A**) or glucagon (**Fig. 2-4 B**). Insulin was able to suppress agonist-induced GNG, but generally, suppression was not evident until approximately 8 - 12 h after co-incubation with forskolin or glucagon. The reason for this delay is not known, although it is likely that the dose of forskolin or glucagon needed to significantly induce GNG and/or GNG enzyme transcription (10 nM for glucagon and 25 μ M for forskolin; **Fig. 2-4 C** and **Fig. 2-4 D** respectively) far exceeds the capacity for insulin to acutely and sufficiently degrade cAMP via PDE, and therefore any inhibition may require a lag period where newly induced protein is degraded, allowing the suppressive effect of insulin on GNG gene expression to be observed. In support of this hypothesis, 3 h treatment with maximally but not submaximally effective doses of glucagon or forskolin robustly induced glucose output and G6Pc and PEPCCK gene expression (**Fig. 2-4C-D**); insulin strongly suppressed the induction of GNG genes by 25 μ M forskolin after 3 h (data presented in chapter 3), but was unable to suppress actual glucose output augmentation by agonist within this time frame (**Fig. 2-4 A**).

The GNG assay was used in *ob/ob* hepatocytes to verify function, as well as provide an additional readout for insulin resistance. However, while *ob/ob* liver cells were highly active with respect to GNG from lactate, they failed to respond to forskolin, and therefore insulin efficacy could not be evaluated (**Fig 2-4 D**). Reduced responsiveness of *ob/ob* mice to glucagon

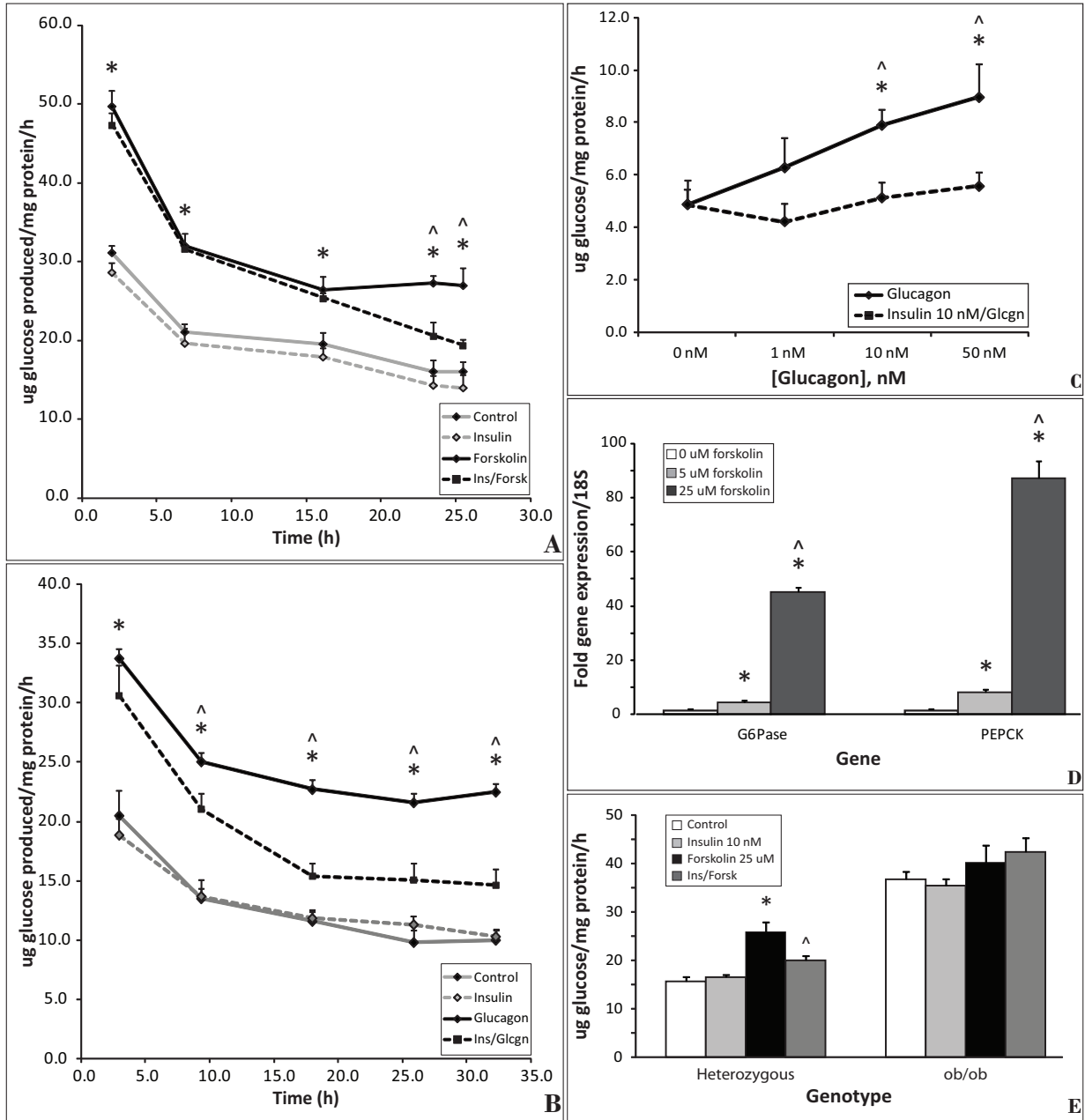


Figure 2-4: GNG in primary mouse hepatocytes (continued on next page)

(Figure 2-4 continued from previous page)

A) Time course of GNG using 25 μ M forskolin. Cells were incubated in 5 mM glucose overnight, washed with glucose-free media, and GNG initiated in glucose-free media with additions as specified. Complete media refreshes were performed at each time point. * = $p < 0.05$ for forskolin effect versus Control at specified time point, ^ = $p < 0.05$ for insulin attenuation of forskolin effect at specified time point, $n = 3$ experiments performed in triplicate. B) Time course of GNG using 1 nM glucagon, all other details as listed in (A), $n =$ single experiment performed in triplicate. C) GNG dose-response using glucagon, and insulin suppression of glucagon effect. Cells were treated as described in (A); glucose output values represent output after 20 h of GNG condition treatment. * = $p < 0.05$ for forskolin effect, and ^ = $p < 0.05$ for insulin attenuation of glucagon effect at specified glucagon concentration, $n =$ single experiment performed in triplicate. D) qRT-PCR determination of low versus high forskolin effect on expression of key gluconeogenic genes. Cells were incubated overnight in 5 mM glucose and treated with specified dose of forskolin for 3 h. * = $p < 0.05$ for forskolin versus no forskolin within each respective gene, ^ = $p < 0.05$ for 25 μ M versus 5 μ M effect on respective gene, $n = 2$ experiments performed in triplicate. E) GNG in *ob/ob* versus heterozygous controls. Cells were incubated in 5 mM glucose overnight and treated as described in (A). Data represent glucose values after 20 h of GNG condition treatment. * = $p < 0.05$ for forskolin effect within genotype versus Control, ^ = $p < 0.05$ for insulin attenuation of forskolin effect within genotype, $n = 2$ experiments performed in triplicate. All error bars are \pm SD.

has been reported, although the mechanism is unknown (Lahtela et al., 1990). The extraordinarily high basal level of GNG in *ob/ob* cells correlated well with *in vivo* findings (Turner et al., 2005), though, and also served as an indication that the cells, though grossly steatotic, were functionally sound.

Hepatocytes oxidize fatty acids – Beta oxidation of fatty acids provides the majority of ATP for cardiac and skeletal muscle as well as the liver under basal conditions (Burgess et al., 2006). Beta oxidation in the liver also produces ketones, which serve as critical fuels during starvation and when carbohydrate availability is limited. As seen in **Fig. 2-5 A**, hepatocytes were able to take up and oxidize palmitate, and there was an inverse relationship between palmitate taken up (lysate) and the fraction which was oxidized ($^3\text{H}_2\text{O}$). Carnitine slightly increased the rate of beta oxidation, while the CPT-I inhibitor etomoxir significantly suppressed it; the weak effect of carnitine was not entirely unexpected, as beta oxidation may be compromised when carnitine is rate-limiting, but providing an excess has minimal effect on further augmenting beta oxidation (Nakajima et al., 1997).

The rate of beta oxidation was linear over the course of several hours (**Fig. 2-5 B**), and was dependent upon the concentration of both BSA and palmitate (**Fig. 2-5 C-D**). *In vivo*, the majority of free fatty acids are coupled to albumin, and uncoupled NEFA is in the nanomolar range (Richieri and Kleinfeld, 1995). *In vitro*, it is necessary to manually couple free fatty acids to BSA to prevent excessive unbound FFA from forming cytotoxic micelles. A single molecule of (highly purified, fatty acid-free) BSA may be capable of binding up to seven molecules of free fatty acid, and in most studies, a molar ratio of 2-3:1 (palmitate to BSA) is used to provide a margin of safety (Spector, 1975). However, BSA has also been shown to inhibit the rate of beta oxidation, possibly by limiting uptake of FFA (Ontko, 1972). In an experiment designed to test

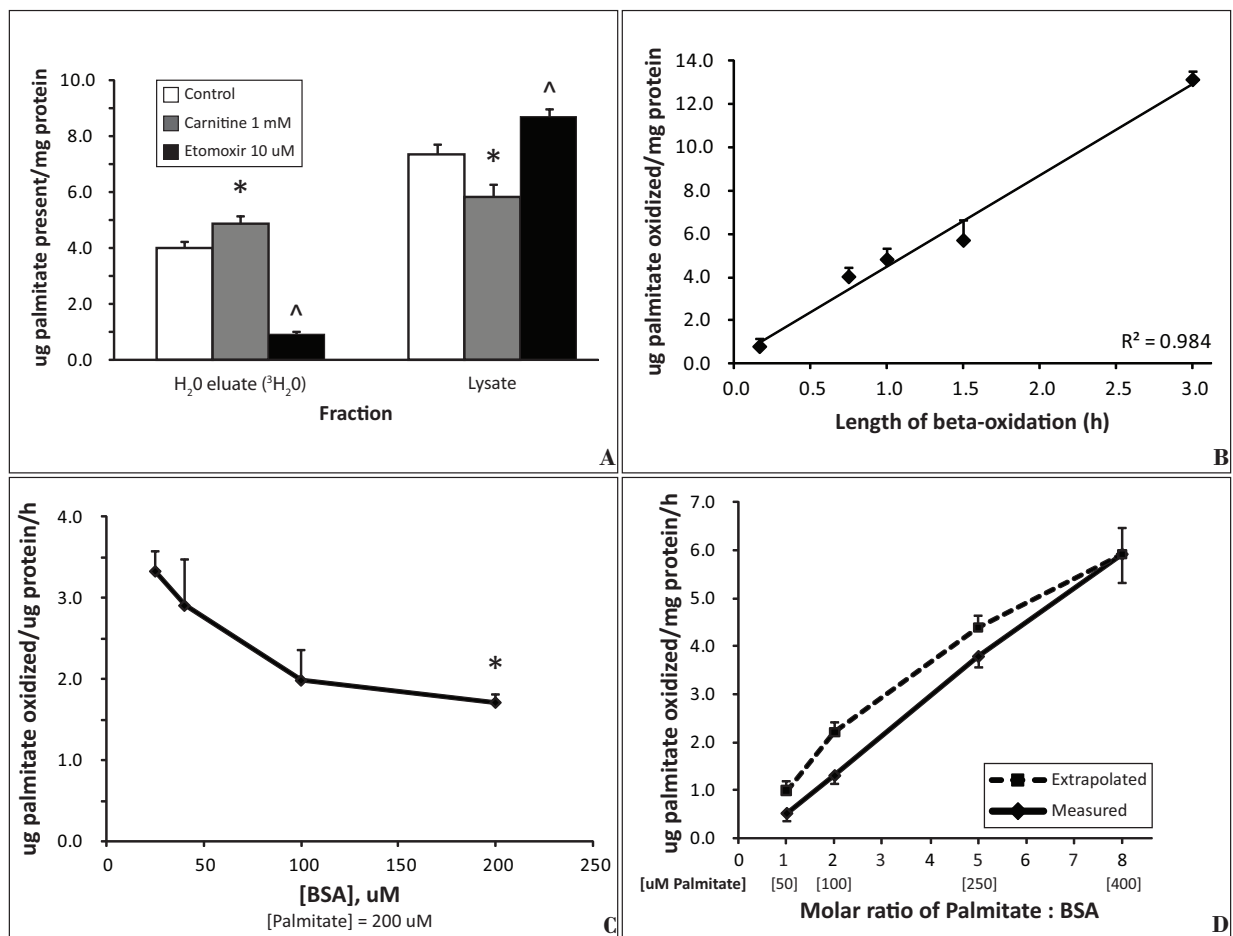


Figure 2-5: Beta oxidation in primary mouse hepatocytes. A) Comparison of total radioactivity in H₂O versus lysate fraction after 1 h treatment with ³H-palmitate. Cells were incubated overnight in 5 mM glucose, washed, and 200 μM ³H palmitate was added in 1x HBSS containing 5 mM glucose. Etomoxir was pre-incubated for 30 min and was also present during the 1 h beta-oxidation period, while carnitine was added at the start of beta-oxidation. H₂O eluate represents net beta-oxidation while Lysate represents net palmitate taken up. Palmitate:BSA ratio = 3:1. * = p < 0.05 for carnitine effect versus control within each respective fraction, ^ = p < 0.05 for Etomoxir effect versus control within each respective fraction, n = 3 experiments performed in triplicate. B) Time-course of beta-oxidation using 200 μM palmitate. Cells were incubated overnight with 5 mM glucose and ³H-labeled palmitate was added for the specified length of time. Palmitate:BSA ratio = 3:1; n = two experiments performed in triplicate. C) Dose-response of BSA effect on beta-oxidation. Cells treated as described in (A), except initiation of oxidation was performed with a fixed dose of palmitate and increasing doses of BSA. * = p < 0.05 for BSA effect on beta-oxidation versus lowest dose of BSA, n = single experiment performed in triplicate. D) Dose-response of palmitate at a fixed concentration of BSA on beta-oxidation. Cells were treated as described in (A); solid line represents actual beta-oxidation, and dotted line represents extrapolated beta-oxidation values taking into consideration the suppressive effect of BSA as seen in (C); n = single experiment performed in triplicate. All error bars are -/+ SD.

the effect of increasing BSA concentrations at a static concentration of palmitate, BSA suppressed beta oxidation in a dose-dependent but nonlinear fashion (**Fig 2-5 C**). In a parallel experiment using a fixed concentration of BSA and varying doses of palmitate, beta oxidation increased in a linear fashion with increasing palmitate concentration (**Fig 2-5 D**, solid line). The estimated rate of beta oxidation adjusted for the effect of BSA inhibition is represented by the (nonlinear) dashed line in **Fig 2-5 D**; in practice, though, most dose-response experiments utilize constant fatty acid to BSA ratios, and therefore, a more linear response would be expected.

De novo lipogenesis and lipid accumulation are responsive to glucose and insulin in primary hepatocytes - *De novo* lipogenesis from glucose occurs in response to elevated glucose and insulin in the liver. Acute mechanisms for insulin-induced lipogenesis include activation of acetyl-CoA-carboxylase (ACC) and suppression of AMP-activated protein kinase (AMPK); in the short term, glucose-induced changes in glycolytic flux and cellular energy state favor a lipogenic environment (Witters and Kemp, 1992; Ishii et al., 2004). Moderate and long-term effects of insulin and glucose include activation of transcription factors that affect lipogenic gene expression, including SREBP-1, ChREBP, and LXR (Uyeda and Repa, 2006). The acute responsiveness of lipogenesis to insulin was demonstrated in primary hepatocytes by addition of radiolabeled 5 mM glucose with 10 nM insulin (**Fig. 2-6 A**). There was minimal lipogenesis with 5 mM glucose in the absence of insulin, evidenced by the lack of significant lipid-extractable glucose at 30 versus 90 minutes (**Fig. 2-6 A** and **Fig. 2-6 B**, white bars). In the presence of insulin, or with 25 mM glucose, there was a robust and statistically significant accumulation of lipid-extractable glucose at 90 min; the effect of 25 mM glucose versus 5 mM glucose was evident even at 30 min (**Fig 2-6 B**). This effect was also seen after overnight incubation with 5mM versus 25 mM glucose by quantitation of Oil Red O staining of hepatocytes from a wild-

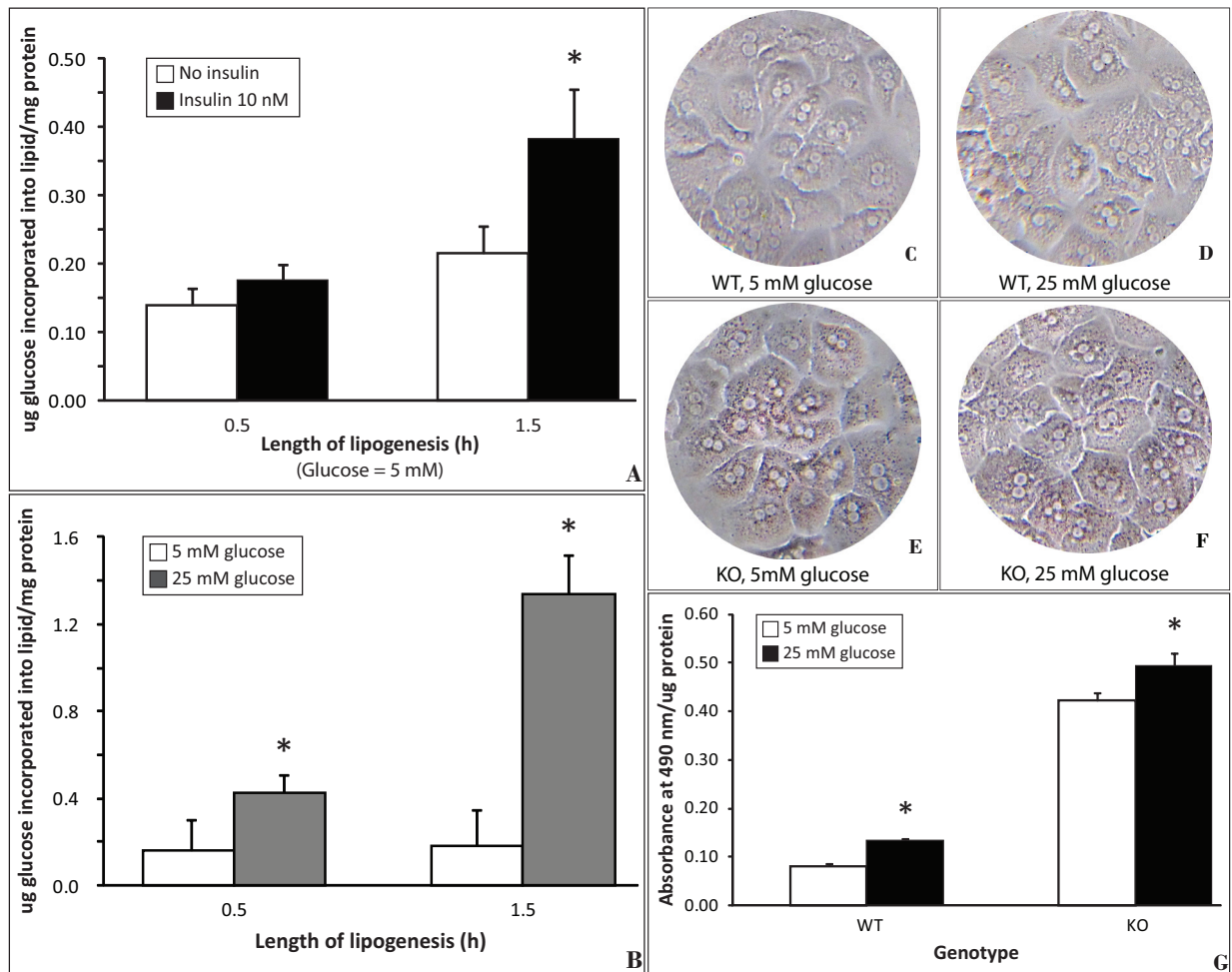


Figure 2-6: Lipogenesis in primary mouse hepatocytes. A) 30 versus 90 min lipogenesis with and without insulin. Cells were incubated in 5 mM glucose overnight, and lipogenesis was initiated by addition of radiolabeled glucose +/- insulin. * = $p < 0.05$ for insulin effect within respective time point, $n =$ single experiment performed in triplicate. B) 30 versus 90 min lipogenesis in 5mM versus 25 mM glucose. Cells were treated as described in (A). * = $p < 0.05$ for 25 mM glucose versus 5 mM glucose within each respective time point, $n = 2$ experiments performed in triplicate. C-F) Oil-Red O staining of wild-type versus BNip3 knockout mouse known to present with elevated lipogenesis, following overnight incubation with 5 mM versus 25 mM glucose. Stains are representative of 2 separate experiments, $n = 3$ per experiment. G) Quantitation of Oil-Red O staining as described in C-F. * = $p < 0.05$ for 25 mM versus 5 mM glucose within respective genotype. All error bars are +/- SD.

type mouse (**Fig. 2-6, panels C, D, and G**) and a transgenic (*Bnip3* ^{-/-}) littermate with a liver phenotype characterized by elevated basal lipogenesis (**Fig. 2-6, panels E, F, and G**).

Isolated hepatocytes are suitable for toxicological screening – Hepatocytes are the central site for endo- and- xenobiotic metabolism, which has made them valuable tools for drug screening and toxicological investigations. The majority of detoxification events are induced via activation of the AhR and subsequent upregulation of first-phase oxidative enzymes; the most commonly utilized readout for this effect is induction of CYP1A1 activity and gene expression due to its inducibility and specificity as a downstream AhR target gene (Rifkind, 2006). To gauge the potency of an unknown compound, standard inducing agents are commonly used as calibrators and/or positive controls, with TCDD and PCB 126 being the primary reference standards owing to their potency and specificity towards the AhR (van den Berg et al., 2006). To evaluate the utility of primary mouse hepatocytes for toxicology screening, cells were incubated with varying doses of PCB 126, PCB 77, or PCB 153; these three PCBs represent a highly potent AhR agonist (PCB 126), a less potent AhR agonist (PCB 77), and a structurally similar PCB incapable of activating the AhR (PCB 153), which served as a negative control. Both PCB 126 and 77 potently activated CYP1A1 activity (**Fig 2-7 A**) and induced CYP1A1 gene expression (**Fig. 2-7 B**) after 16 h treatment, with PCB 77 demonstrating a dose-response; PCB 126 was maximally effective even at the lowest tested dose, consistent with its 30 - 100-fold greater potency with respect to AhR activation compared to PCB 77 (van den Berg et al., 2006). As expected, PCB 153 was completely without effect on CYP1A1 activity or expression at all tested doses.

Primary mouse hepatocytes are competent for adenoviral infection and functional protein overexpression – Injection of adenoviruses into the tail vein of rodents is a common technique to modify gene expression in the liver, and cultured rodent hepatocytes are known to be highly

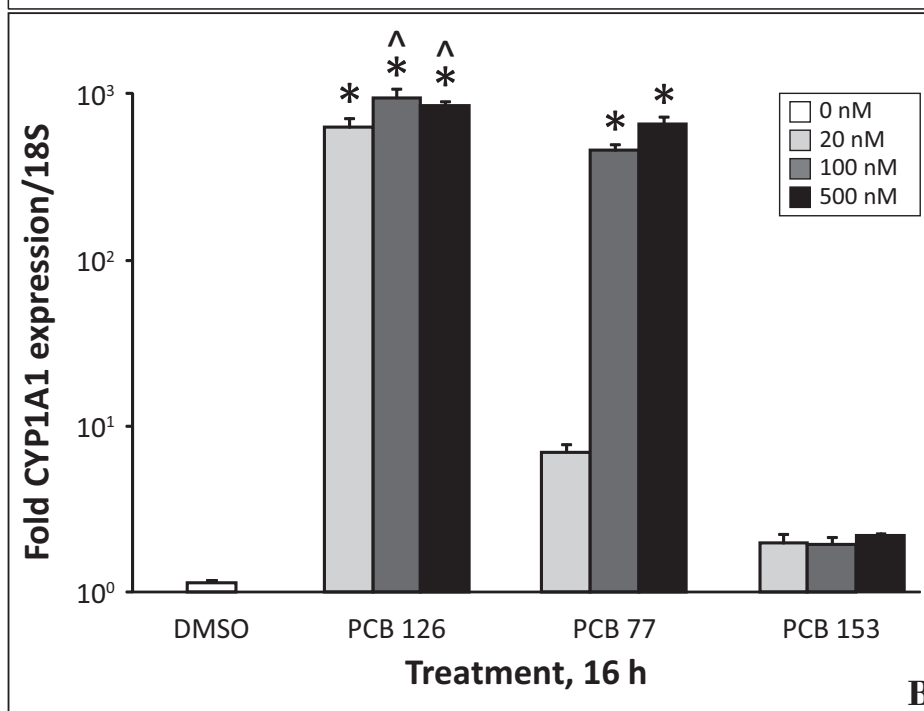
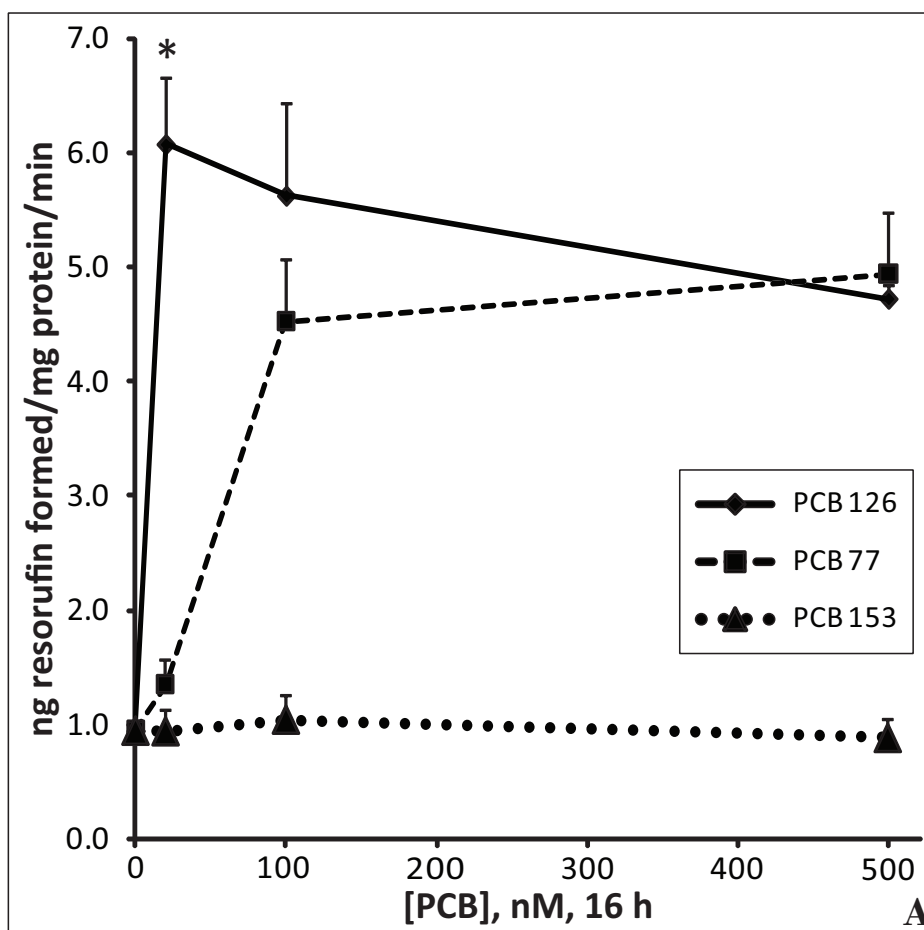


Figure 2-7: First-phase xenobiotic metabolizing enzyme induction and function in primary mouse hepatocytes. A) EROD following 16 h incubation with specified PCB at listed concentration. Cells were incubated with 5 mM glucose overnight. * = $p < 0.05$ EROD activity at specified concentration versus 0 nM PCB within each individual PCB, $n = 2$ experiments performed in triplicate. B) qRT-PCR evaluation of CYP1A1 induction. Cells were incubated as described in (A). * = $p < 0.05$ for CYP1A1 effect versus DMSO within each respective PCB, ^ = $p < 0.05$ for dose-effect versus 20 nM within each respective PCB, $n = 3$ experiments performed in triplicate. All error bars are $-/+$ SD.

competent for adenoviral infection as well (Nguyen and Ferry, 2004; Jaffe et al., 1992). To demonstrate the ability of hepatocytes to overexpress protein via adenoviral infection, cells were treated with wild-type PCK α containing adenovirus. Expression was assessed by immunoblotting for active (phosphorylated) PCK α . As seen in **Fig. 2-8 A**, 2 h infection followed by overnight expression resulted in a significant increase in active (phosphorylated) PCK α ; additionally, it was observed that PCK α overexpression induced insulin resistance, both in terms of signaling (**Fig. 2-8 A**) and insulin suppression of forskolin-induced gluconeogenesis (**Fig. 2-8 B-C**), providing multiple readouts for determining expression competence. Infection with viruses coding for constitutively active GSK3 β , dominant-negative AMPK- α 2, and wild-type mTOR was successful as well, with no detectable visual or functional changes (data not shown) suggestive of cellular stress at maximally effective MOIs.

2.D. Discussion

Taking advantage of the detailed studies of Klaunig et al. (1981a), who adapted the rat hepatocyte isolation technique of Berry and Friend to mice, the current system was developed with adaptations where appropriate to reflect the availability of modern equipment and analytical techniques. The yield and viability of isolated cells were closely in line with reported values, including viability of 90-95% and an average total yield of ~2 million cells per gram of body weight (**Fig. 2-1 B**). Importantly, the appearance of cells shortly after plating and after overnight culture paralleled Klaunig et al.'s observations, including the appearance of extensive cell-cell junctions, binucleation in > 80% of cells (**Fig. 2-1 A-B**), and gradual progression towards a fibroblastic phenotype with extended culture time (data not shown) (1981b). The flattened epithelial-like monolayer of fully recovered cells with well-defined cell-cell boundaries

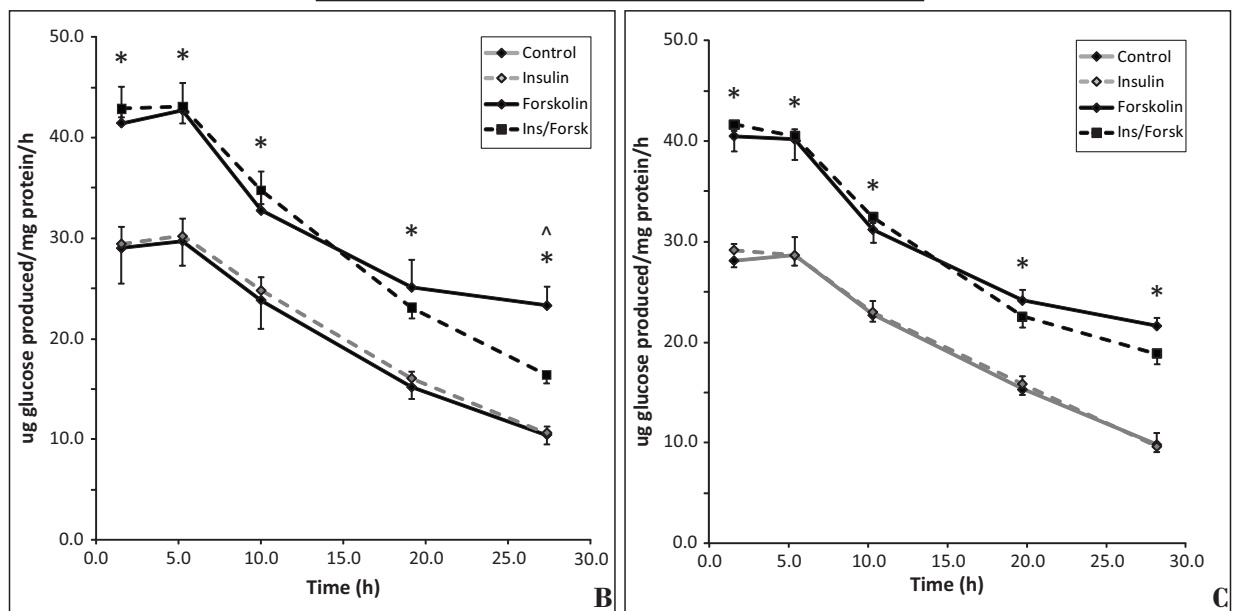
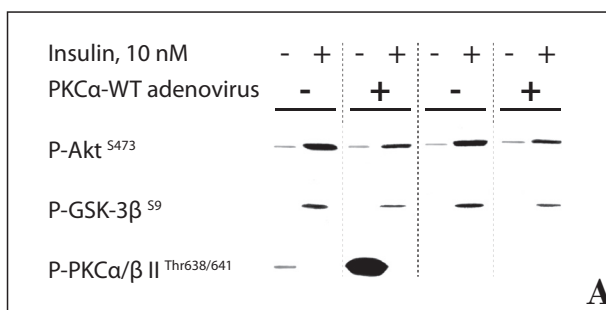


Figure 2-8: Adenovirus infection competence of primary mouse hepatocytes. A) Effect of PKC α -WT adenovirus on insulin signaling and phospho-PKC α expression. Cells were infected with 300 MOI virus for 2 h and protein expression was allowed to occur overnight. Cells were treated with 10 nM insulin for 10 min the following day. Blot is representative of 2 independent experiments. B-C) Effect of PKC α -WT adenovirus on forskolin-stimulated, and insulin suppression of forskolin-stimulated GNG. Panel B represents empty virus control, while Panel C represents PKC α -WT adenovirus. * = $p < 0.05$ for forskolin effect versus control at each time point, ^ = $p < 0.05$ for insulin attenuation of forskolin effect at each time point, n = single experiment performed in triplicate. All error bars \pm SD.

(consistent with descriptions of bile canaliculi *in vivo*) was also in line with published observations of mouse and rat hepatocytes (Gallin, 1997).

Functional tests were performed in isolated mouse hepatocytes to confirm that their metabolic and signaling processes were intact. The responsiveness of hepatocytes to insulin was a primary concern, not only because it would allow the cells to be utilized in a wider variety of studies, but also because improper selection of collagenase has been reported to induce cleavage of cell surface receptors, resulting in blunted downstream signaling in response to hormone treatment (Garrison and Haynes, Jr., 1973). Initial tests using grades of type I collagenase proved unsatisfactory, as cell viability was inconsistent and insulin responses weak, despite high total cell yields (data not shown); therefore, type IV collagenase was selected based on the 10x lower tryptic activity of Type IV versus Type I enzyme. As seen in **Fig. 2-2 G**, cells isolated using Type IV collagenase demonstrated a typical insulin dose-response with respect to signaling; more significantly, glycogen synthesis was increased by insulin (**Fig. 2-2 B**). Absolute glycogen levels as well as the responsiveness of glycogen to insulin were both considered to be critical indicators of cellular integrity, as glycogen synthesis is particularly sensitive (relative to other tested metabolic readouts) to suboptimal isolation or culture conditions, varying > 10 x between healthy and stressed batches of cells treated under identical conditions (unpublished observations). Using Type IV collagenase, glycogen levels following overnight incubation in 5mM – 25 mM glucose were consistent with values reported in the literature (Chen and Lardy, 1985; Salhanick et al., 1989; Agius et al., 1990; Tosh et al., 1994); 5 mM glucose was chosen to reflect physiologically relevant basal glucose levels in most mammalian species, and 25 mM, though supraphysiological, is within the range of commonly used experimental conditions (20 - 30 mM) for assessment of glucose-responsive hepatocyte functions (Agius et al., 1990; Fleig et

al., 1987). Finally, cells responded to glucose and 3-carbon gluconeogenic precursors, again, consistent with several published studies (Fleig et al., 1987; Tosh et al., 1994).

The principal role of insulin with respect to liver glucose metabolism is suppression of hepatic glucose output (HGO); therefore, it was critical to determine if insulin could suppress the effect of counterregulatory signals, i.e. cAMP, by using glucagon and forskolin. HGO is comprised of two components- *de novo* glucose synthesis from non-glucose precursors (GNG) and release of glycogen as glucose (glycogenolysis). However, the mechanism by which insulin suppresses HGO due to GNG versus glycogenolysis may vary, as glycogenolysis is an acute phenomenon due to the limited stores of glycogen in the liver, while GNG is critical for sustaining glycemia at almost all times, and is primarily subject to transcriptional-level control. The ability of insulin to counter cAMP signaling was evident in the glycogenolysis assay (**Fig. 2-3 A**); however, insulin was unable to acutely suppress glucagon or forskolin-induced GNG, nor could insulin suppress the basal (unstimulated) level of GNG at any tested time point (**Figs. 2-4 A-B**). It is unclear what factors account for the differential effect of insulin *in vitro* versus *in vivo* with respect to GNG, as it has been demonstrated *in vivo* that physiologic hyperinsulinemia rapidly and potently suppresses HGO from both GNG and glycogenolysis (Ramnanan et al., 2010). Responsiveness of GNG to cAMP agonists may be reduced under the current culture conditions, necessitating levels of cAMP that could not be acutely and/or sufficiently countered by insulin; the concentration of glucagon required to maximally induce GNG in isolated hepatocytes has been reported to be as high as 100 nM (Tosh et al., 1988), while maximal glycogenolysis has been observed with 1 nM glucagon (data not shown). It is also possible that optimal GNG requires the presence of glucose and/or fatty acids to maintain TCA flux (Burgess et al., 2006; Gonzalez-Manchon et al., 1992; Williamson et al., 1969). The failure of insulin to

suppress basal GNG may be explained by the fact that *in vivo*, there is never a complete lack of counterregulatory signal (i.e. glucagon, and adrenergic hormones). This, combined with the knowledge that GNG appears to be constitutive in the liver, (evidenced by significant contribution of the indirect pathway to glycogenesis even postprandially), implies that GNG always occurs at a set level that may be determined by the energy state of the cell, secondary to flux through glycolysis and/or the TCA cycle. Complete suppression of basal GNG was only seen when cells were treated with AMPK agonists (i.e. Metformin, AICAR, and berberine) known to reduce the intracellular energy charge (data not shown) (Foretz et al., 2010; Yin et al., 2008).

While HGO is an essential mechanism for short and long-term maintenance of glycemia, hepatic beta oxidation is equally important during long-term starvation and/or during limited carbohydrate availability; in the short term, efficient oxidation of circulating fatty acids is essential for preventing steatosis, particularly the microvesicular type (Grefhorst et al., 2005) . Hepatic beta oxidation provides the reducing equivalents needed to drive GNG under fasting conditions, and the derived acetyl groups serve as the carbon source for ketogenesis (Gonzalez-Manchon et al., 1989). The reliance of beta oxidation on mitochondrial integrity and cellular energy state also makes it a useful indicator of culture integrity. While ketogenesis was not measured in this system, hepatocytes oxidized palmitate at rates consistent with the literature (Spurway et al., 1997), and the ratio of total palmitate oxidized to palmitate taken up (~30%; **Fig. 2-5 A**) was also close to reported values (Gerondaes et al., 1988). As expected, beta oxidation was modestly responsive to carnitine and strongly responsive to etomoxir. The weak response of primary rodent hepatocytes to supplemental carnitine has been observed in other studies (Yeh, 1981; Schulze et al., 1986), and it is possible that carnitine may be limiting only under stimulated

beta oxidation, which may require long-term incubation with glucagon or other cAMP agonists (Gerondaes et al., 1988). In early preparations under suboptimal isolation conditions, carnitine had a profound effect (5-8x increase) on beta oxidation, although net oxidation of palmitate was significantly lower than in cells isolated under the optimized procedure outlined in this paper (data not shown); therefore, the lower carnitine responsiveness of healthy hepatocytes in conjunction with higher rates of overall beta oxidation may be indicative of reduced leakage of carnitine during isolation and/or culture (unpublished observations). Acutely, beta oxidation may be modestly increased by glucagon (Malewiak et al., 1983; Guzman and Castro, 1989) and slightly decreased by insulin (Guzman and Castro, 1989), although others have observed more robust glucagon responses but no direct insulin effect (Witters and Trasko, 1979); in general, ketogenesis demonstrates a more potent glucagon response than beta oxidation. Very modest (10-20%) increases and subtle (10%) decreases in beta oxidation of palmitate in response to 100 nM glucagon and insulin, respectively, have been observed in the current system (data not shown). It is unknown if the magnitude of response could be enhanced by varying culture/treatment conditions, as the mechanism(s) by which insulin or glucagon might significantly affect beta oxidation in low glucose within 1 h is (are) unclear.

Under fed conditions, particularly in the context of carbohydrate excess, hepatic *de novo* lipogenesis (DNL) assists in clearance of circulating glucose by converting glucose to fatty acids. Following synthesis, esterification of synthesized fatty acids leads to their storage in the liver as triglycerides or export in VLDL and long-term storage in adipocytes (Uyeda and Repa, 2006). Lipogenesis in hepatocytes is transcriptionally regulated in response to both glucose and insulin through SREBP-1c and ChREBP, respectively (Dentin et al., 2004), although both insulin and glucose acutely affect the activity of lipogenic enzymes as well (Witters and Kemp, 1992;

Morrall et al., 2007). Aside from the significance of DNL as a contributing factor to steatosis *in vivo*, DNL requires the integration of nonoxidative and oxidative pathways in both the cytosol and mitochondria and is therefore a useful substrate and hormonally-responsive means to assess the general metabolic competence of plated hepatocytes. Absolute levels of glucose incorporated into lipid and the responsiveness of lipogenesis to 5 mM versus 25 mM glucose were similar to reported values (Kinlaw et al., 1995; M'Zali et al., 1997). There was also a robust increase in lipogenesis upon insulin addition, even in the 5 mM glucose condition (**Fig. 2-6 A-B**). Lipogenesis may be significantly suppressed by glucagon (Guzman and Castro, 1989), but this effect remains to be evaluated in the current system. In the absence of insulin, low glucose was unable to stimulate net lipogenesis, evidenced by the lack of a time-response for lipogenesis in 5 mM glucose. This effect has also been observed in hepatocytes isolated from a transgenic mouse known to have increased lipogenesis, where little difference in lipogenesis was detected between transgenic and wild-type cells in 5 mM glucose, but a > 2x difference was elicited using 25 mM glucose (data not shown). This trend parallels that of ¹⁴C glucose experiments for glycogen partitioning, where no net glycogen synthesis from glucose occurred during a 1-3 h incubation with 5 mM glucose, but significant glycogen was synthesized in 25 mM glucose (data not shown), underlining the importance of substrate concentration for resolving metabolic effects in hepatocytes.

In addition to its involvement in numerous metabolic processes, the liver is also the site of endobiotic and xenobiotic metabolism. Toxicological studies have routinely employed primary hepatocytes due to the variety of uptake, metabolism, and pharmacokinetic studies that can be performed in these cells, as well as the persistence of drug-metabolizing function even after cryopreservation (Malewiak et al., 1983; Gomez-Lechon et al., 2006). The latter point is

particularly important due to the relative scarcity of primary hepatocytes from higher mammals, particularly humans. However, cryopreservation introduces significant changes to the viability, attachment efficiency, and general function of hepatocytes (Gomez-Lechon et al., 2006). While many drug-metabolizing functions are relatively well-maintained in cryopreserved versus freshly isolated cells (Gomez-Lechon et al., 2006), one must consider that many of these are activities are localized to microsomes, and assays such as EROD are commonly performed in isolated microsomal liver or hepatocyte fractions (Shinkyo et al., 2003; Craft et al., 2002). Thus, many drug metabolism-related assays may have limited utility as a means to validate the general health or quality of cultured primary hepatocytes. Nonetheless, determination of primary hepatocyte performance in standard drug metabolizing assays is necessary for toxicological studies. Baseline levels of AhR activation were determined by measuring CYP1A1 activity (EROD) as well as CYP1A1 gene expression (**Fig. 2-7 A-B**). EROD activity in the literature is highly variable depending on culture and assay conditions, and fold induction following maximally effective TCDD doses ranges from 10 - 1000x (Petrulis and Bunce, 1999; Silkworth et al., 2005); CYP1A1 gene expression has a similarly wide induction range. Therefore, the key factors evaluated in the current system were the dose of dioxin-like PCB required for maximal effect and absence of AhR induction with non dioxin-like PCBs. The absolute quantity of resorufin formed from the EROD assay was close to levels reported by Pertulis and Brunce (1999), but several-fold lower than that observed by Silkworth et al. (2005). However, the dose of PCB 126 and 77 required to maximally induce EROD and CYP1A1 gene expression was in line with reported concentrations (Silkworth et al., 2005; Petrulis and Bunce, 1999; French et al., 2004), and the non dioxin-like PCB, congener 153, had no effect on either EROD or CYP1A1 gene transcription. Furthermore, the induction of another AhR target gene, CYP1A2, was observed in

the expected pattern- that is, higher basal expression and lower inducibility by DLCs (data not shown).

Gene expression in the liver and in isolated hepatocytes is readily altered by infection with adenoviruses containing transcripts for native, constitutively active, or inactive variants of proteins. To demonstrate the infection competence of hepatocytes in the current system, cells were treated with adenoviruses containing wild-type mTOR, constitutively active and kinase-dead GSK-3 β , constitutively-active and kinase dead AMPK- α 2, and constitutively-active PKC α . Adenovirus treatment caused no observable cellular stress, either by visual assessment or through functional evaluation (data shown only for PKC α , **Fig. 2-8 B-C**). The majority of tested viruses resulted in significant changes in total expression of the target protein as well as altered protein activity; the effect of infection with adenovirus coding for wild-type PKC α adenovirus was particularly notable due to the marked and reproducible effect of overexpression (**Fig. 2-8 A**, bottom panel) on insulin signaling (**Fig. 2-8 A**, upper and mid panels) and insulin suppression of forskolin-induced GNG (**Fig. 2-8 B-C**). Agents that induce insulin resistance (i.e. certain species of free fatty acids, TNF α , and phorbol esters) have been shown to activate PKC α (Wrede et al., 2003; Rosenzweig et al., 2002), and this may lead to insulin resistance via serine phosphorylation of IRS-1 (Nawaratne et al., 2006; Cipok et al., 2006) as well as inhibition of insulin-stimulated tyrosine (auto)phosphorylation of the insulin receptor (Rosenzweig et al., 2002).

Primary mouse hepatocytes isolated using the modified method of Klauing et al. (1981a) were able to function in a manner consistent with whole liver. Cells synthesized glycogen, produced glucose and lipid *de novo*, oxidized long-chain fatty acids, upregulated first-phase xenobiotic-metabolizing enzymes in response to inducers, and were readily infected by

adenoviruses. Metabolic and drug-metabolizing functions responded to substrate in a time and concentration-dependent manner, and the absolute rate and/or quantity of output was similar to published values. Furthermore, all metabolic functions were responsive to hormones and/or pharmacological agents. Unfortunately, limited useful culture time, the main restriction of primary hepatocytes, was also apparent in the current system. While hepatocytes did not die or detach from the plate with prolonged culture time, phenotype degraded rapidly after the first 24 h; a falling-off in functional capacity, including glycogen synthesis and gluconeogenesis, closely paralleled the loss of phenotype (data not shown). However, despite the time constraints associated with primary hepatocytes, researchers have utilized these cells for decades to perform targeted, mechanistic studies. The high yield and batch-to-batch consistency of properly isolated primary mouse hepatocytes facilitates experimental throughput, while the range of assays and manipulations that may be performed provides for multiple readouts at the genomic, signaling, and metabolic level. Application of the current system in the context of an experimental system will be described in detail in the following chapter.

CHAPTER III

PCB 126 and other dioxin-like PCBs specifically suppress hepatic PEPCK expression by

AhR-dependent and-independent mechanisms

3. A. Introduction

Polychlorinated biphenyls are a group of bicyclic chlorinated hydrocarbons that are lipophilic and highly resistant to physical, chemical, and enzymatic breakdown (WHO, 2003). PCBs saw widespread industrial use in the United States from the 1930s until their production was banned in 1979 under the Toxic Substances Control Act; internationally, PCB production was terminated under the Stockholm Convention on Persistent Organic Pollutants in 2001. However, due to seepage into the environment, accidental spills, and improper disposal, combined with their persistence and propensity for bioaccumulation, PCBs are still found at measurable levels in soil (Turrio-Baldassarri et al., 2007), fresh water (Ward et al., 2010), aquatic wildlife (Perez-Fuentetaja et al., 2010), and mammals (Bruns-Weller et al., 2010; Huwe et al., 2009), including humans (Patterson, Jr. et al., 2008). Exposure to PCBs and other dioxin and dioxin-like compounds has long been documented to incite a variety of adverse neurological, reproductive, developmental, immunological, and metabolic effects in both wildlife and humans depending on dose, timing, and length of exposure (White and Birnbaum, 2009).

PCBs are roughly grouped into two categories: dioxin-like and non-dioxin-like, according to their structural and chemical properties as well as their physiological effects. The term dioxin-like refers to structural and physiological similarities to the prototypical dioxin 2,3,7,8-tetrachlorodibenzo-p-dioxin (TCDD), a highly toxic byproduct of certain industrial processes (2006b). TCDD and its congeners, including dioxin-like PCBs, are thought to exert

their toxic effects through binding to the aryl hydrocarbon receptor (AhR), a widely expressed nuclear transcription factor that binds a broad range of xenobiotics (Carlson et al., 2009; Hestermann et al., 2000; Ramadoss et al., 2005; Hankinson, 2005). The unliganded AhR resides in the cytosol, and upon binding of ligand, translocates into the nucleus, heterodimerizes with the aryl hydrocarbon receptor nuclear translocator, and binds to xenobiotic response elements of its target genes. The actual downstream targets of activated AhR remain largely unknown, but include several members of the cytochrome P450 family of first-phase drug metabolizing enzymes (Ramadoss et al., 2005). The putative mechanism of dioxin-induced toxicity is thought to be a combination of high specificity for AhR binding and persistent AhR activation secondary to poor metabolism by the CYPs, leading to a range of organ and species-dependent maladaptive responses (Okey et al., 1994).

Aryl hydrocarbon receptor binding is one of the criteria required for a compound to be assigned a toxic equivalency factor, an index developed in the 1980s to compare the relative toxicity of dioxins and their congeners; the TEF index uses TCDD as its reference standard (TEF = 1). To be assigned a TEF, the World Health Organization has stipulated that a compound must be structurally similar to TCDD, bind to and activate the AhR, and persist and bioaccumulate in the food chain (WHO, 2003). PCB 126 is a dioxin-like PCB with the highest TEF amongst the PCBs (TEF = 0.1); the next most potent PCB congener, PCB 169, has a 3-fold lower TEF (van den Berg et al., 2006). Despite its relatively minor contribution as a constituent of PCB mixtures by weight, the potency of PCB 126 underlies its toxicological significance as the major contributor to the toxicity equivalency, which has been reported to be as high as 90% (Bhavsar et al., 2008). It has also been shown that in humans, a wide range of DLCs can be detected, but the

majority of toxicity is attributed to only seven species, one of which is PCB 126 (Patterson, Jr. et al., 2008).

Previous studies evaluating the impact of dioxins and dioxin-like compounds on animal metabolism have mostly utilized TCDD. A common finding in TCDD feeding studies is a general wasting syndrome characterized by reduced body weight/stunted growth, hypoglycemia, refusal to eat, and with prolonged treatment, death (Unkila et al., 1995; Viluksela et al., 1999; Weber et al., 1991a; Fan and Rozman, 1994). Investigations into the mechanism of TCDD's pathogenic effects have identified suppression of liver glycogen and decreased hepatic gluconeogenesis as contributing factors to TCDD-induced wasting (Viluksela et al., 1999; Stahl et al., 1993; Viluksela et al., 1995). Given the potentially more widespread environmental contamination of PCBs relative to TCDD, the relatively similar TEFs of PCB 126 and TCDD, and the significant contribution of PCB 126 to general PCB toxicity, the effects of PCB 126 on hepatic glucose metabolism are potentially very important. To date, only a few studies have characterized the effect of PCB 126 feeding on metabolism in mammals (Fisher et al., 2006; Boll et al., 1998), and no detailed *in vitro* study has evaluated the direct effect of PCB 126 on hepatic glycogen stores or GNG. The current study was thus designed to investigate the metabolic impact of PCB 126 in primary mouse hepatocytes, as well as to evaluate the role of the AhR in mediating the effects of PCB 126 and other dioxin-like PCBs.

3.B. Materials and Methods

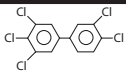
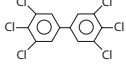
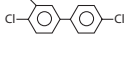
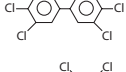
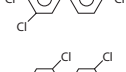
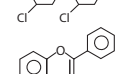
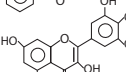

Materials - All PCBs were from Accustandard. Unless mentioned otherwise, reagents were from Sigma.

Isolation and culture of primary mouse hepatocytes – Hepatocytes were isolated from 8 – 12 week-old male C57BL/6 mice as described in Chapter 2. All cells were used within 30 h of isolation.

Treatment of cells - Cells were treated at the time and in the media as described in Chapter 2. For inhibitor studies, cells were pre-incubated as indicated for 1 h prior to addition of PCBs or beta-naphthoflavone; all PCB and/or beta-naphthoflavone incubations were 16 h in length. Forskolin stimulation for gene expression studies was performed by direct addition to cells at h 13 and was always 3 h in length. All forskolin treatments were performed at a final concentration of 25 μ M. Forskolin and all compounds and inhibitors were prepared in DMSO; final DMSO concentration for treatments and vehicle controls were identical and ranged from 0.35 - 0.75%. A summary of the compounds used in this paper may be found in **Fig. 3-1 A**.

Total glycogen – Total cellular glycogen was measured following lysis of cells and ethanol precipitation of glycogen as described in Chapter 2. Quantitation of liberated glucose was assayed via the glucose oxidase-peroxidase method by measuring the oxidation of 2,2'-azino-bis(3-ethylbenzthiazoline-6-sulphonic acid) at 405 nm (Thermo Multiskan MCC).

Gluconeogenesis (GNG) - Gluconeogenesis was performed in cells after 16 h of treatment as described in Chapter 2 with minor modifications. Briefly, cells were washed twice with glucose-free, phenol red-free DMEM. The assay was performed in glucose-free, phenol red-free media supplemented with 44 mM NaHCO₃ 2 mM L-glutamine, Pen/Strep, 10 mM HEPES (pH 7.4), 10 nM dexamethasone, and 10 mM of the specified substrate; 25 μ M forskolin was also added to the appropriate media stocks. At 1 h intervals, an aliquot of media was removed for analysis of glucose by the glucose oxidase-peroxidase assay. The remainder of the media was then removed

Compound	CAS #	Common name	Class	TEF (WHO 2005)
PCB 126	 57465-28-8	3,3',4,4',5-pentachlorobiphenyl	Non-ortho-substituted coplanar	0.1
PCB 169	 32774-16-6	3,3',4,4',5,5'-hexachlorobiphenyl	Non-ortho-substituted coplanar	0.03
PCB 81	 70362-50-4	3,4,4',5-tetrachlorobiphenyl	Non-ortho-substituted coplanar	0.0003
PCB 77	 32598-13-3	3,3',4,4'-tetrachlorobiphenyl	Non-ortho-substituted coplanar	0.00010
PCB 105	 32598-14-4	2,3,3',4,4'-pentachlorobiphenyl	Mono-ortho-substituted coplanar	0.00003
PCB 153	 35065-27-1	2,2',4,4',5,5'-hexachlorobiphenyl	Di-ortho-substituted non-coplanar	N/A
BNF	 6051-87-2	5,6- benzoflavone	Polycyclic aryl hydrocarbon	N/A
Myricetin	 529-44-2	3,3',4',5,5',7'-hexahydroxyflavone	Flavonol	N/A

Gene	RefSeq	Direction	Primer sequence; 5' → 3'	Amplicon size
18S	NR_003278.1	Forward Reverse	CGGCTACCACATCCAAGGA GCTGGAATTACCGCGGCT	187 bp
CYP1A1	NM_009992.3	Forward Reverse	TATCTCGTCAGCAAACCTTCAG ATATGGCACAGATGACATTGG	100 bp
CYP1A2	NM_009993.3	Forward Reverse	ACCGATACACATCCTTTGTC CTTCTCATCATGGTTGACCT	131 bp
Fbp1	NM_019395.2	Forward Reverse	TCGCACAGCTCTATGGTATCG AGAACACAGGTAGCGTAGGAC	124 bp
G6pc	NM_008061.3	Forward Reverse	TGCAAGGGAGAACTCAGCAA TTGCGCTCTTGCAAGAAAGAC	145 bp
PEPCK	NM_011044.2	Forward Reverse	TGGTGGGAACTCACTACTCGG ATGCCAGGATCAGCATATGC	105 bp
Pcx	NM_001162946.1	Forward Reverse	TGCCAAGCAGGTAGGCTATGA GCGGGAATTGACCTCGATGAA	91 bp

Figure 3-1: Summary tables. A) Summary of compounds used on primary mouse hepatocytes
B) Primer sequences used for qRT-PCR.

and fresh media added for the next time point. At the termination of the assay, cells were lysed in 0.75% SDS for measurement of protein.

Lactate dehydrogenase (LDH) activity - LDH activity in the supernatant was measured using a kit (Cayman Chemical) according to the manufacturer's instructions. Intracellular LDH activity was measured after removal of all media, washing cells twice with cold PBS, and releasing intracellular LDH by hypotonic lysis (60 min with shaking at 4 °C in the dark in H₂O buffered with 5 mM HEPES). Absorbance of the reduced tetrazolium salt, INT, was measured at 490 nm on a spectrophotometer (Molecular Devices Versamax). Total LDH activity was calculated as the sum of released (media) and intracellular LDH.

Ethoxyresorufin-O-deethylase (EROD) – EROD activity was measured as described in Chapter 2.

Quantitative real-time PCR (qRT-PCR) – Design and validation of primers, isolation of RNA, synthesis of cDNA, and qRT-PCR were performed as described in Chapter 2. As mentioned in Chapter 2, both 18S and beta-actin were confirmed to be suitable reference genes, and 18S was selected for all experiments. A list of primer sequences may be found in **Fig. 3-1 B**.

Beta oxidation – Beta-oxidation of palmitic acid was performed as described in Chapter 2 using a 3:1 molar ratio of palmitate to BSA.

Immunoblotting - Lysates were prepared and differential ultracentrifugation to pellet glycogen was performed as outlined in Danos et al. (2009). An aliquot of the supernatant and resuspended glycogen pellet was removed for protein assessment, samples were sonicated, and 2x Laemmli sample buffer was added to the remainder. Samples were boiled and separated by SDS-PAGE using 10% acrylamide gels. Proteins were transferred to PVDF membranes (Immulon), blocked

with 5% skim milk in TBST, and probed with phospho- and total glycogen phosphorylase (Gasa et al., 2000) as well as phospho- and total glycogen synthase (Cell Signaling). Incubations were performed overnight at 4 °C in 5% milk-TBST (1:1000 - 1:3000 antibody concentration), after which membranes were washed with TBST and probed with an HRP-linked secondary antibody (GE Healthcare; 1:5000) for 1 h. Membranes were washed with TBST and TBS, developed with ECL (GE Healthcare), and bands detected by exposing membranes on film (Kodak Biomax). Films were scanned (Canon 8800F) and quantitation performed using ImageJ software.

Statistical analysis - Comparisons between two treatments or conditions were performed with two-tailed Student's *t*-tests. Comparisons between > 2 treatments or conditions were made using 1-way ANOVA with post-hoc Tukey-Kramer analysis. JMP 7.0 was used for all analysis, and significance was set at $p < 0.05$.

3.C. Results

PCB 126 reduces basal glycogen content - The majority of studies evaluating the effect of dioxin-like PCBs on total glycogen content have consisted of feeding and/or exposure studies performed mainly in non-mammalian aquatic animals (Encomio and Chu, 2000; Hugla and Thome, 1999; Vijayan et al., 2006) and only rarely in mammals (Deml and Oesterle, 1986). To determine the ability of PCBs to directly impact hepatic glycogen levels, primary mouse hepatocytes were incubated for 16 h with 100 nM PCB 126, 77, or 153 (**Fig. 3-2 A**). PCB 126 was selected as the reference PCB for this study because it is the most potent PCB congener with respect to its TEF (van den Berg et al., 2006; Jensen et al., 2010), and a dose of 100 nM was chosen as a standard PCB concentration based upon data showing it to be sufficient to maximally activate the AhR across a wide range of species, conditions, and PCB congeners (Petruelis and

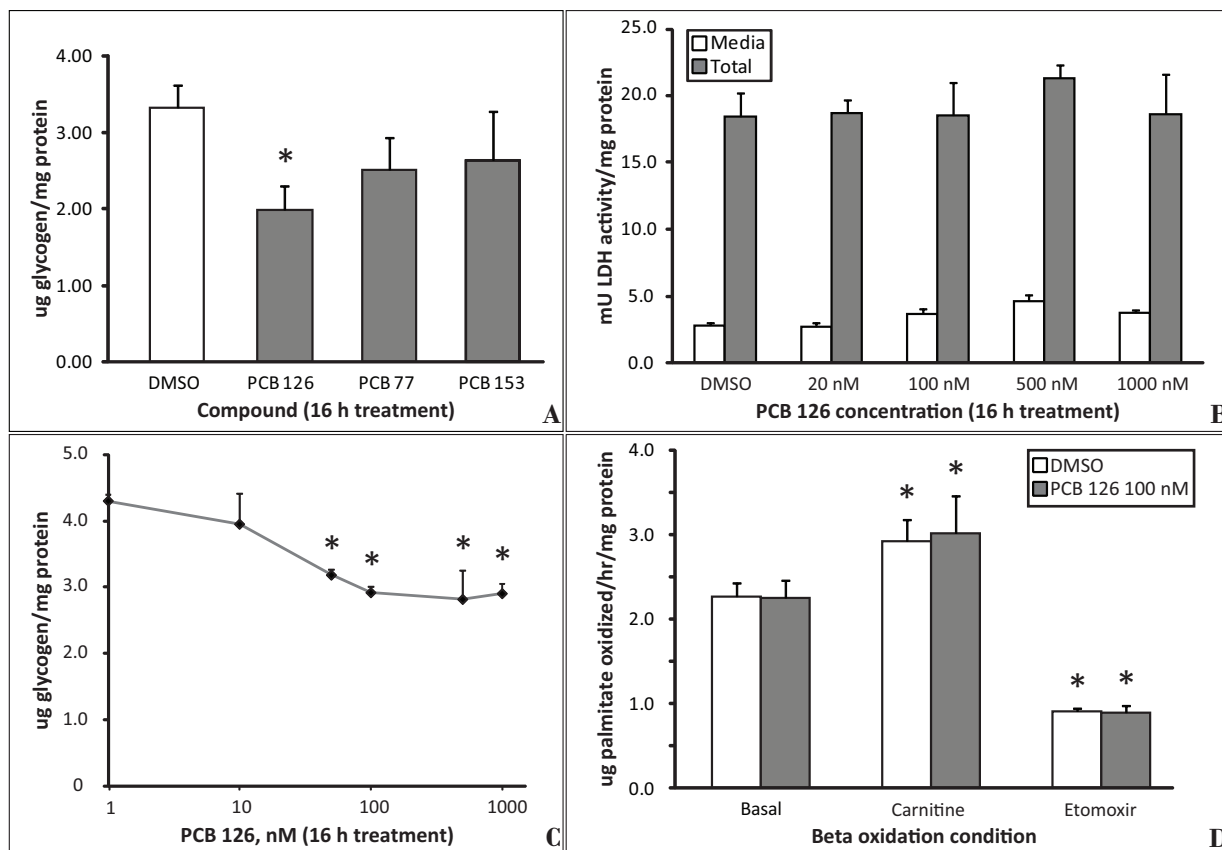


Figure 3-2: PCB 126 suppresses glycogen storage in primary murine hepatocytes independent of effects on toxicity or lipid metabolism. A) Comparison of PCB 126, 77, or 153 on basal glycogen levels. Cells were treated with the listed PCB at 100 nM or vehicle (DMSO) for 16 h in 5 mM glucose, lysed, and total glycogen and protein determined. * = $p < 0.05$ for PCB 126 vs. DMSO, $n = 3$ experiments performed in triplicate. B) Evaluation of LDH leakage (Media) relative to released and intracellular (Total) LDH activity in PCB 126 treated cells. Cells were treated as in (A); $n = 3$ experiments performed in triplicate. C) Glycogen suppression with increasing doses of PCB 126. Cells were treated and processed as described in (A). * = $p < 0.05$ for PCB 126 vs. DMSO, $n = 2$ experiments performed in triplicate. D) Effect of PCB 126 on beta oxidation of palmitate. Cells were treated as described in (A). Total palmitate concentration was 200 μ M. Carnitine (1 mM) was added at the start of the assay, and etomoxir (10 μ M) was added 30 min prior to the start of the assay, and was also present during the assay. Total length of beta oxidation was 1 h. * = $p < 0.05$ for carnitine or etomoxir vs. basal, $n = 2$ experiments performed in triplicate. All error bars represent means \pm SD.

Bunce, 1999; Silkworth et al., 2005; Jonsson et al., 2007). For comparison, PCB 77, a structurally similar dioxin-like PCB with a TEF several orders of magnitude lower than that of PCB 126, as well as PCB 153, a non dioxin-like PCB with no documented TEF (van den Berg et al., 2006; Haws et al., 2006), were tested. PCB 153 was without effect on hepatic glycogen content and PCB 77 tended to lower glycogen by approximately 20% ($p < 0.10$); however, PCB 126 significantly and consistently suppressed total glycogen content by $> 30\%$.

Glycogen content in primary mouse hepatocytes could be nonspecifically impacted by cellular stress; therefore, to confirm that the PCB 126 effect on glycogen was not secondary to acute toxicity, lactate dehydrogenase release into the media relative to total intracellular LDH activity was measured (**Fig. 3-2 B**). PCB 126 had no effect on total or released LDH at concentrations up to 10x higher than the maximally effective dose (as determined by effect on basal glycogen) of 100 nM (**Fig. 3-2 B - C**). Glycogen levels also tend to change inversely with respect to beta oxidation and lipogenesis (unpublished observations), and others have reported that dioxin-like PCBs and TCDD augment hepatic lipogenesis (Boll et al., 1998; Gorski et al., 1988). However, in the current system, PCB 126 had no effect on beta oxidation of palmitate (**Fig. 3-2 D**) or basal or insulin-stimulated lipogenesis from glucose (data not shown).

Effect of PCB 126 on basal glycogen content is independent of glucose concentration, glycogen metabolizing enzymes, or glycogenolysis - The liver takes up glucose primarily through the high K_m , insulin-insensitive GLUT2 transporter, and the experiments performed in the previous section were conducted in basal (5 mM) glucose concentrations. To determine the contribution of glucose uptake to total glycogen content in the presence of PCB 126, hepatocytes were incubated in 5 mM versus 25 mM glucose overnight. The 5x increase in glucose resulted in a

proportionately higher level of total glycogen in both the vehicle-treated control and PCB 126 condition, with a consistent percent inhibition of total glycogen by PCB 126 (**Fig. 3-3 A**).

The effect of PCB 126 on the primary glycogen metabolizing enzymes, glycogen synthase (GS) and glycogen phosphorylase (GP) was then examined. These two enzymes are reciprocally regulated by their phosphorylation state, with GS being inactivated by progressive phosphorylation while GP is activated by phosphorylation on a single N-terminal serine residue. These enzymes are also regulated allosterically by metabolites, and their subcellular localization is modulated by alterations in extracellular glucose levels (Ferrer et al., 2003). By virtue of inducing dramatically higher total glycogen levels, 25 mM glucose caused proportionately more total GP and GS to be detected in the glycogen pellet, with corresponding increases in the respective phosphorylated enzyme pools. Under all conditions, PCB 126 had no effect on total or phospho-GP or -GS levels or subcellular localization (**Fig. 3-3 B-C**). Finally, the rate of glycogenolysis in glucose-free media was unaltered by PCB 126 (**Fig. 3-3 D**). These findings cumulatively indicated that PCB 126 was likely modulating hepatic glycogen stores in an indirect manner.

PCB 126 selectively suppresses forskolin-stimulated gluconeogenesis from lactate but not glycerol - In the liver, 50% or more of total glycogen arises from the indirect pathway, where non-glucose precursors provide the carbon backbone for glycogen via GNG (Satake et al., 2002). Because the suppression of glycogen by PCB 126 was not due to changes in glucose uptake/immediate glucose metabolism, glycogen metabolizing enzymes, or glycogenolysis, the impact of PCB 126 on GNG was evaluated by monitoring the conversion of lactate to glucose. PCB 126 did not affect the basal (unstimulated) rate of GNG, but significantly reduced forskolin-stimulated glucose output from lactate (**Fig. 3-4 A**). The suppression was evident during the first

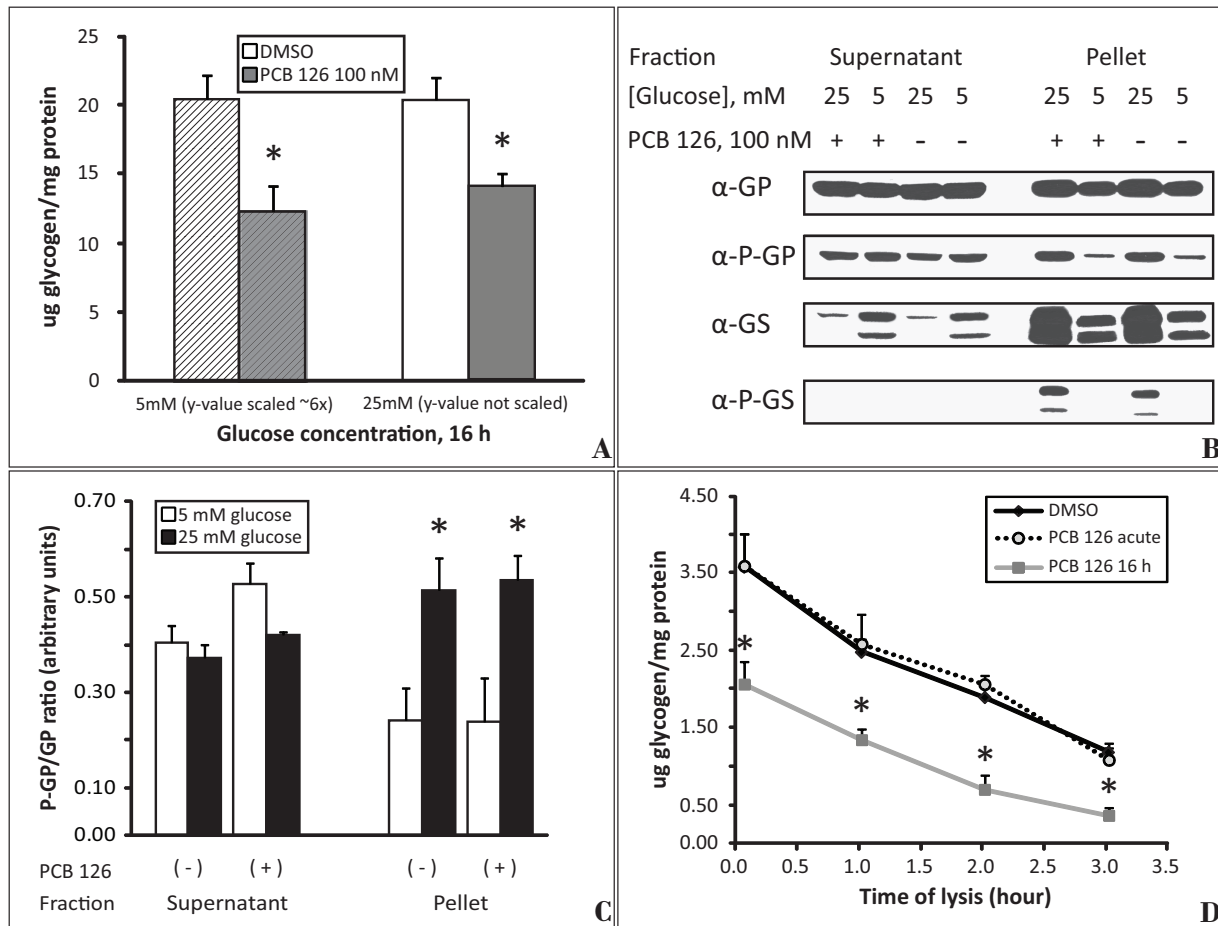


Figure 3-3: PCB 126 treatment does not modulate glucose incorporation into glycogen, glycogen metabolizing enzymes, or glycogenolysis in primary hepatocytes. A) Effect of extracellular glucose on PCB 126-mediated suppression of glycogen. Cells were incubated with 100 nM PCB 126 or vehicle (DMSO) for 16 h in 5 mM (hatched bars) or 25 mM glucose. * = $p < 0.05$ for PCB 126 vs. DMSO within each glucose condition, $n = 3$ experiments performed in triplicate. B) Effect of PCB 126 on glycogen metabolizing enzymes. Cells were treated as described in (A), cytosolic (Supernatant) and glycogen-enriched (Pellet) fractions were prepared by centrifugation and analyzed by immunoblotting against total or phosphorylated (P) glycogen phosphorylase (GP) or glycogen synthase (GS). Blot is representative of two separate experiments performed in duplicate. C) ImageJ quantitation of (B); * = $p < 0.05$ for PCB 126 vs. DMSO within each glucose condition. D) Glycogenolysis in glucose free media following PCB 126 treatment. Cells were treated with 100 nM PCB 126 for 16 h, 100 nM PCB 126 only during glycogenolysis (PCB 126 acute), or vehicle both overnight and during glycogenolysis (DMSO). Cells were lysed at the specified time points and total glycogen and protein measured. * = $p < 0.05$ for PCB 126 16 h vs. DMSO, $n = 2$ experiments performed in quadruplicate. All error bars represent means \pm SD.

hour of forskolin stimulation, and was persistent during the entire four-hour time course used for the assay. The contribution of glycogen to total glucose output in the basal or forskolin-stimulated condition was negligible, based on the fact that (a) glycogen stores account for <10% of total (basal) glucose output at the first time point and significantly less in following time points (**Fig. 3-3 D**), and (b) 25 μ M forskolin induces near-complete glycogenolysis within 30 minutes under the 5 mM overnight glucose condition used in these experiments (data not shown). The presence or absence of 100 nM PCB 126 during the 4 h GNG time course had no impact on any results, indicating that PCB 126 was not allosterically inhibiting GNG enzymes (data not shown). Interestingly, when glycerol was used as a carbon source in place of lactate, glycerol was not only a more efficient gluconeogenic fuel, resulting in higher basal and forskolin-stimulated GNG, but also completely prevented PCB 126 from suppressing GNG, whether basal or forskolin-stimulated (**Fig. 3-4 B**); the reason for the enhanced efficiency of glycerol as a fuel for GNG is unknown, but may be related to the lower energetic cost and fewer enzymatic regulatory steps required for its conversion to glucose compared to lactate (**Fig. 3-4 C**). Thus, the impact of acute PCB 126 exposure appeared to specifically suppress hepatic GNG in a substrate-dependent manner.

PCB 126 selectively suppresses forskolin induction of PEPCK, but not G6pc - GNG is controlled by the increased expression of several rate-limiting enzymes such as phosphoenolpyruvate carboxykinase (PEPCK) and glucose-6-phosphatase (G6pc). Several previous studies have shown that TCDD suppresses the activity and/or expression of PEPCK (Viluksela et al., 1999; Stahl et al., 1993; Viluksela et al., 1995; Diani-Moore et al., 2010; Hsia and Kreamer, 1985; Stahl et al., 1992), and when measured, the activity of G6pc was decreased more modestly and subsequent to the effects of TCDD on PEPCK (Stahl et al., 1992; Hsia and

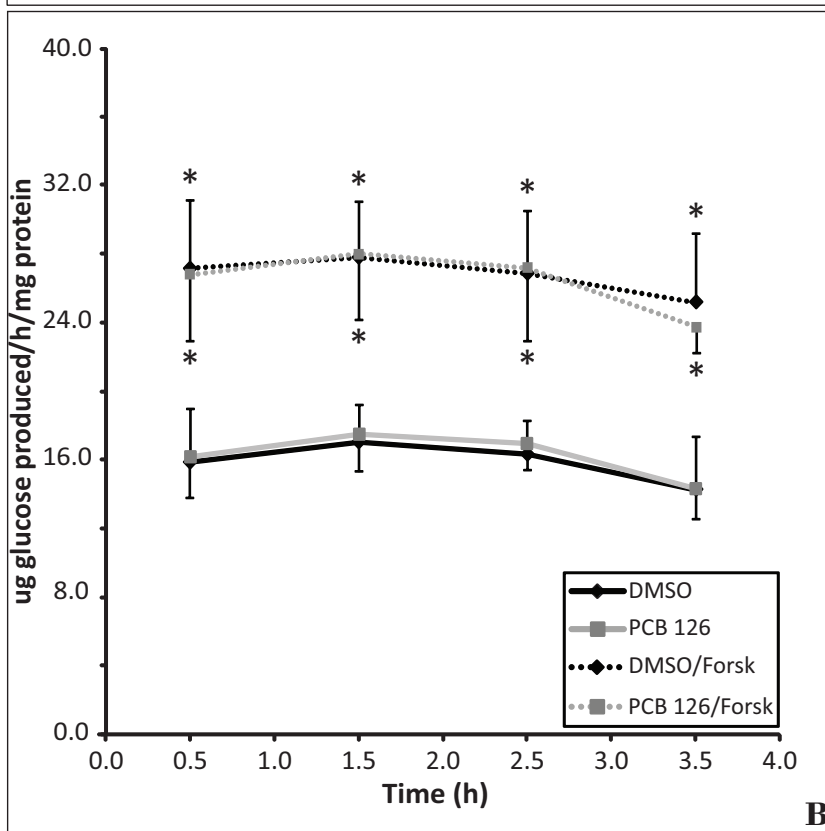
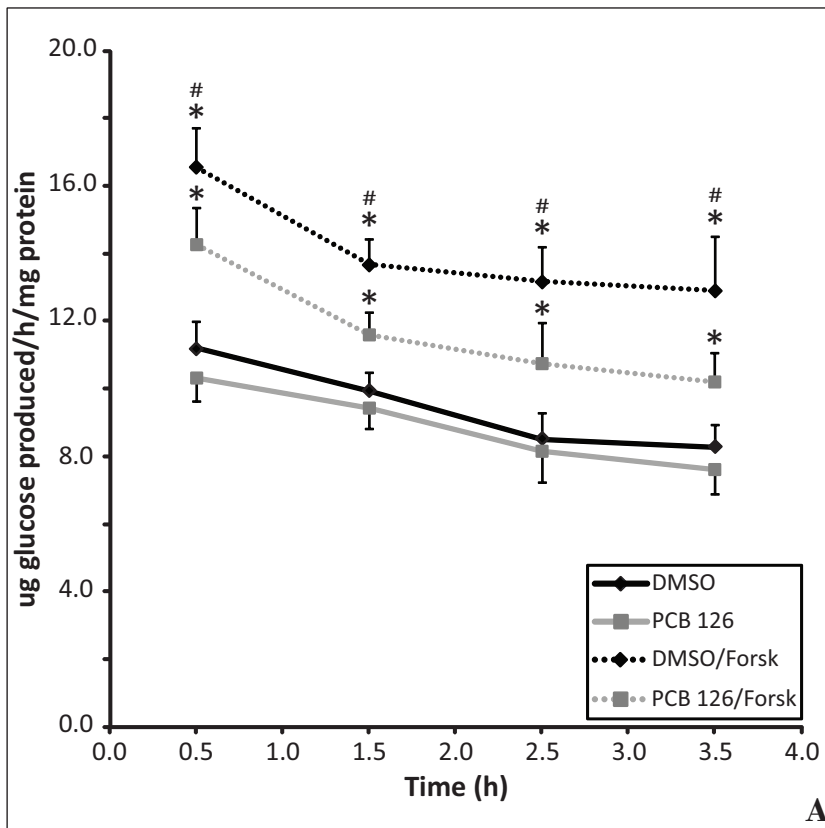


Figure 3-4: Suppression of forskolin-induced GNG from lactate but not glycerol following PCB 126 treatment. A) PCB 126 effect on basal and forskolin-stimulated GNG over 4 h with lactate as a carbon source. Cells were treated with 100 nM PCB 126 or vehicle (DMSO) for 16 h in 5 mM glucose. Cells were washed and glucose-free media containing 10 mM lactate, with 25 μ M forskolin or DMSO was added. Media was removed and assayed for glucose at 1 h intervals. * = $p < 0.05$ for Forskolin vs. DMSO within each respective 16 h treatment condition; # = $p < 0.05$ for PCB 126/Forskolin vs. DMSO/Forskolin, $n = 3$ experiments performed in triplicate. B) Cells were treated and the GNG assay performed as in (A), but with 10 mM glycerol in the place of lactate. All error bars represent means \pm SD (continued on next page).

Substrate	Production	Consumption	Enzyme	Reaction	Compartment
Lactate	NADH		LDH	Lactate --> Pyruvate	Cytosol
		ATP	Pcx	Pyruvate --> OAA	Mitochondria
		GTP	PEPCK	OAA --> PEP	Cytosol*
		ATP	PGK	3PG --> 1,3BPG	Cytosol
		NADH	GAPDH	1,3BPG --> GA3P	Cytosol
Glycerol		ATP	GK	Glycerol --> Glycerol-3P	Cytosol
	FADH2		GPDH	Glycerol-3P --> DHAP	Mitochondria

* This reaction is predominantly cytosolic in the mouse and rat due to dominance of the cytosolic isoform of PEPCK in these species

C

(Figure 3-4 continued from previous page)

C) Summary of energetic cost of GNG from lactate versus glycerol. Substrate = added substrate, Production = reducing equivalent generated during GNG from respective *Substrate*, Consumption = reducing equivalent or high-energy nucleotide utilized during GNG from respective *Substrate*, Enzyme = enzyme catalyzing *Production* or *Consumption* reaction, Reaction = reaction catalyzed by *Enzyme*, Compartment = location of *Enzyme* and *Reaction*. Note that reducing equivalent and high-energy nucleotide molar quantities are all “1” to reflect the quantity needed to process one mole of 3-carbon *Substrate* into ½ mole of glucose.

Kreamer, 1985; Weber et al., 1995; Weber et al., 1991b). To our knowledge, only a single paper has reported that PCBs decrease PEPCK expression (Boll et al., 1998), but the molecular mechanism by which PEPCK mRNA was lowered and its impact on hepatic metabolism were not investigated. To determine the mechanism for the suppression of forskolin-stimulated GNG with lactate, but not glycerol, the effect of short-term forskolin stimulation on gluconeogenic gene expression in PCB 126-treated hepatocytes was evaluated using qRT-PCR. Consistent with the gluconeogenesis data, the expression of PEPCK mRNA was unchanged in the basal (non-forskolin stimulated) state by 16 h PCB 126 exposure (**Fig. 3-5 A, left half**). Three hours of 25 μ M forskolin treatment robustly augmented PEPCK transcription in the vehicle control, and PCB 126 treatment blunted this response by more than 65% (**Fig. 3-5 B, left half**). In parallel, the regulation of G6pc mRNA expression was determined. Basal levels of G6pc were unchanged by PCB 126 (**Fig. 3-5 A, right half**). G6pc gene transcription was also strongly upregulated by forskolin, but unlike the actions of TCDD, PCB 126 was unable to blunt the induction of G6pc following 3 h of 25 μ M forskolin treatment (**Fig. 3-5 B, right half**). The impact of PCB 126 and forskolin on the expression of pyruvate carboxylase (Pcx) and fructose-1,6-bisphosphatase (Fbp1) was also assessed. Neither gene was significantly induced by 3 h of 25 μ M forskolin, and PCB 126 had no effect in the absence or presence of forskolin (**Fig. 3-5 C-D**).

Insulin is the principle means by which PEPCK and G6pc are hormonally suppressed (Barthel and Schmoll, 2003). To further demonstrate the specificity of PCB 126 on PEPCK expression, 10 nM insulin was co-incubated along with forskolin, and the induction of PEPCK and G6pc was assessed by qRT-PCR. Insulin did not affect the basal level of either PEPCK or G6pc (data not shown). However, insulin suppressed forskolin-driven PEPCK gene expression by approximately 65% (**Fig 3-5 E, left section**). Unlike PCB 126, insulin potently suppressed

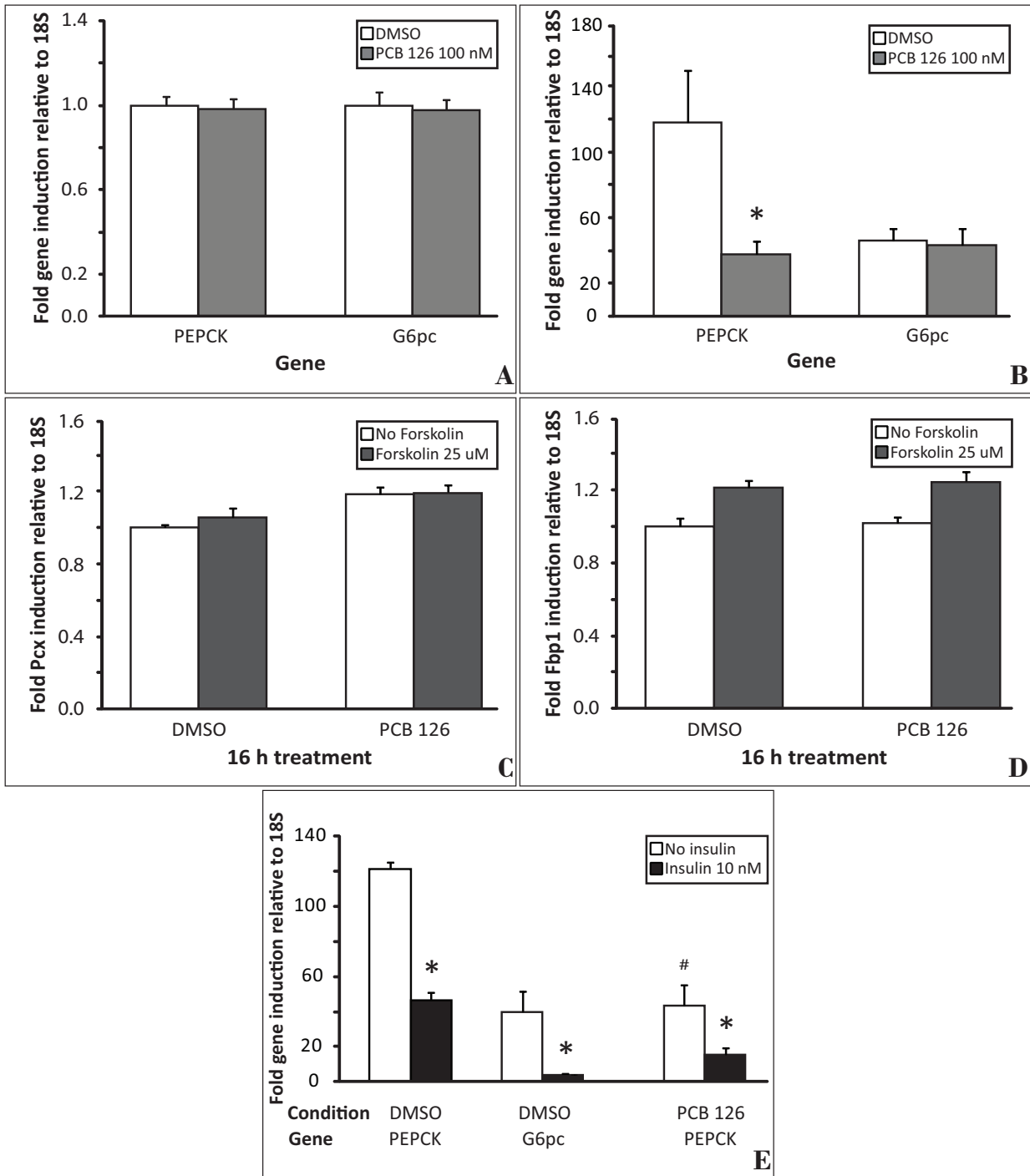


Figure 3-5: PCB 126 specifically suppresses forskolin-induced expression of PEPCK (continued on next page)

(Figure 3-5 continued from previous page)

A) Comparison of basal levels of PEPCK and G6pc mRNA in the presence or absence of PCB 126. Cells were treated with 100 nM PCB 126 for 16 h in 5 mM glucose and gene expression measured by qRT-PCR; n = 3 experiments performed in triplicate. B) Forskolin-induced levels of PEPCK and G6pc mRNA in the presence or absence of PCB 126. Cells were treated with 100 nM PCB 126 for 13 h in 5 mM glucose. 25 μ M forskolin or vehicle control (DMSO) was directly added for the final 3 h, and gene expression measured by qRT-PCR. Expression levels are relative to respective basal levels as shown in (A). * = $p < 0.05$ for forskolin-stimulated gene expression, PCB 126 vs. DMSO, n = 3 experiments performed in triplicate. C) Basal and forskolin-stimulated pyruvate carboxylase (Pcx) gene expression in the presence or absence of PCB 126. Cells were treated as in (B) and Pcx mRNA levels were determined; n = 3 experiments performed in triplicate. D) Basal and forskolin-stimulated fructose-1,6-bisphosphatase (Fbp1) gene expression in the presence or absence of PCB 126. Cells were treated as in (B) and Fbp1 mRNA levels were determined; n = 3 experiments performed in triplicate. E) Insulin suppression of PEPCK and G6pc. Cells were treated as in (B), except 10 nM insulin was co-incubated with the 3 h forskolin treatment. * = $p < 0.05$ for 10 nM insulin vs. no insulin, n = 2 experiments performed in triplicate. All error bars represent means \pm SD.

forskolin-stimulated G6pc expression as well (**Fig. 3-5 E, middle section**). Moreover, the suppressive effect of insulin was additive to that of PCB 126 with respect to PEPCK (**Fig. 3-5 E, right section**), resulting in an additional 65% suppression of PEPCK induction by forskolin, providing additional support for a non insulin-related mechanism for PCB 126 suppression of forskolin-stimulated PEPCK mRNA.

AhR does not appear to directly mediate PCB 126 suppression of forskolin-stimulated PEPCK gene expression - It has been postulated by several other studies that the effect of TCDD on PEPCK is not mediated by the AhR (Stahl et al., 1993; Weber et al., 1991a; Weber et al., 1995). To evaluate this hypothesis in the current system, the effect of PCB 126 on classical downstream AhR targets was examined. CYP1A1 and CYP1A2 gene induction, as well as activation of EROD activity, were used as readouts for AhR agonism. Consistent with AhR activation, PCB 126 strongly increased transcription of both CYP1A1 and CYP1A2 (**Fig. 3-6 A**) and augmented EROD activity as well (**Fig. 3-6 B**).

Next, AhR inhibitors were screened to test the impact of AhR inhibition on PCB 126 suppression of forskolin-induced PEPCK. Out of over a dozen compounds, only a single compound, myricetin, a flavonol (Zhang et al., 2003), was able to antagonize AhR according to screening parameters - that is, at the effective dose, the compound must (a) not be toxic (data not shown), (b) antagonize AhR as assessed by CYP1A1 (**Fig. 3-6 C**) and CYP1A2 (**Fig. 3-6 D**) expression, and (c) not independently impact basal or forskolin-stimulated PEPCK and G6pc (**Fig. 3-6 E**). Although myricetin was able to significantly suppress activation of AhR by PCB 126, co-incubation of cells with myricetin and PCB 126 did not alter the PCB effect on PEPCK gene transcription following forskolin stimulation (**Fig. 3-6 E**). While supportive of a non-AhR mechanism, incomplete suppression of AhR by myricetin prevented AhR agonism from being

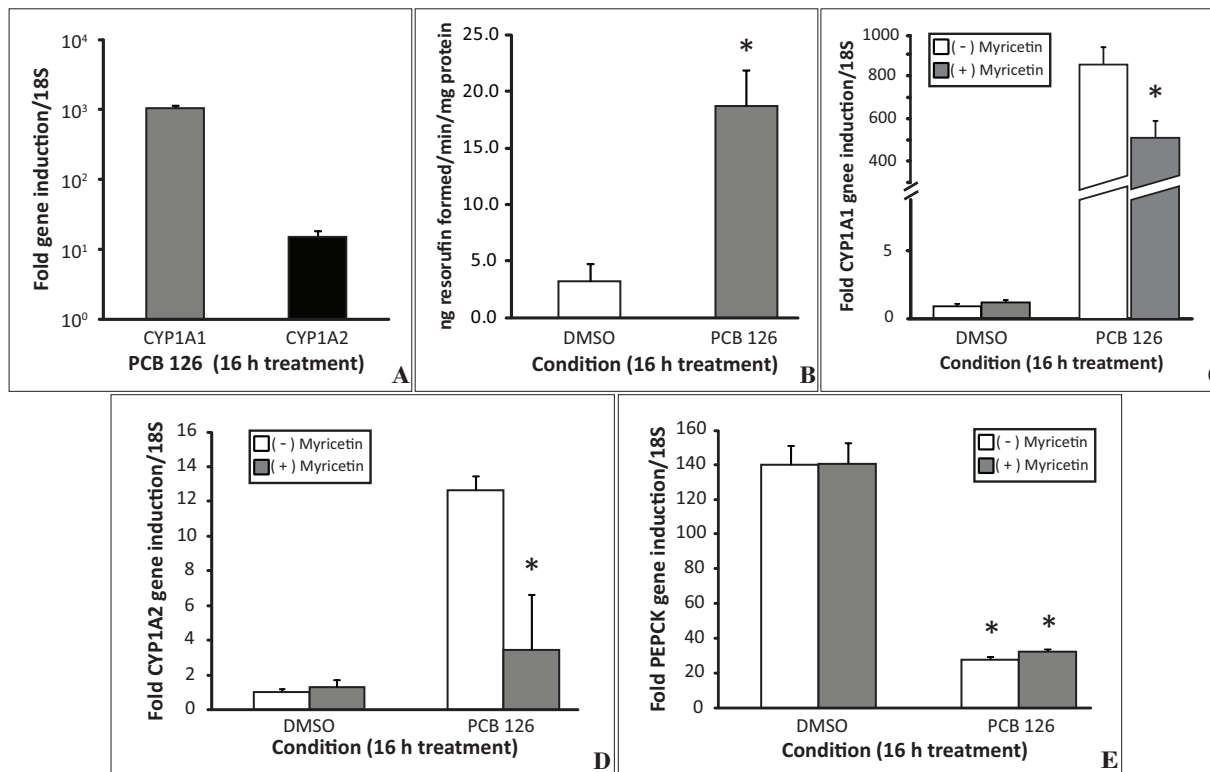


Figure 3-6: A partial AhR antagonist does not affect the suppression of forskolin-stimulated PEPCK gene expression by PCB 126. A) Gene-based confirmation of activation of AhR by PCB 126. Cells were treated with 100 nM PCB 126 for 16 h in 5 mM glucose and gene expression of CYP1A1 and CYP1A2 measured by qRT-PCR; n = 3 experiments performed in triplicate. B) Activity-based confirmation of activation of AhR by PCB 126. Cells were treated as in (A). All media was removed, cells were lysed by freeze/thaw, and EROD activity was measured. * = $p < 0.05$ for PCB 126 vs. DMSO, n = 3 experiments performed in triplicate. C) Confirmation of partial AhR antagonism by myricetin. Cells were pretreated with 25 μ M myricetin for 1 h prior to the addition of 100 nM PCB 126 for 16 h in 5 mM glucose. Myricetin and PCB 126 were co-incubated for the duration of the treatment, and CYP1A1 gene expression determined by qRT-PCR. * = $p < 0.05$ for PCB 126 (+) myricetin vs. PCB 126 (-) myricetin, n = 2 experiments performed in triplicate. D) Cells were treated as in (C), except CYP1A2 gene expression was measured; * = $p < 0.05$ for PCB 126 (+) myricetin vs. PCB 126 (-) myricetin, n = 2 experiments performed in triplicate. E) Effect of myricetin on basal and PCB 126 suppression of forskolin-induced PEPCK mRNA. Cells were treated as described in (C), except 25 μ M forskolin was added at h 13 of treatment for the final 3 h. Expression of PEPCK was determined by qRT-PCR. * = $p < 0.05$ for PCB 126 vs. DMSO within each respective (-) or (+) myricetin condition, n = 2 experiments performed in triplicate. All error bars represent means \pm SD.

ruled out as a mechanism of action due to potential residual effects of PCB 126 on AhR in the presence of myricetin.

Other non ortho-substituted dioxin-like PCBs, but not all non-AhR agonists, have similar effects as PCB 126 on PEPCK - Due to the limitations of a pharmacological inhibitor, i.e. partial inhibition and potential off-target effects, the effect of other PCBs at various doses was examined to test the hypothesis that the ability of PCB 126 to suppress forskolin-induced PEPCK was independent of its possibly coincidental ability to activate AhR. In addition to PCB 126, three other non-ortho-substituted coplanar dioxin-like PCBs were selected for testing: PCB 169, PCB 81, and PCB 77 (**Fig. 3-1 B**). PCB 105 was included to represent a mono-ortho-substituted coplanar dioxin-like PCB with a significantly lower TEF relative to the other dioxin-like PCBs (van den Berg et al., 2006; Haws et al., 2006; Jensen et al., 2010). Finally, PCB 153 served as a negative PCB control, as it is both non-coplanar and non-dioxin-like, and as such, has no assigned TEF (van den Berg et al., 2006; Haws et al., 2006). Beta- naphthoflavone (BNF), a polycyclic aryl hydrocarbon commonly utilized as an AhR agonist, was included as a non-PCB AhR agonist control (Bohonowych and Denison, 2007; Jaruchotikamol et al., 2007). The aforementioned PCBs and BNF were tested at three concentrations; PCBs were tested at 5x lower and higher doses (20 nM and 500 nM, respectively) compared to the standard 100 nM, while BNF was tested at commonly used micromolar concentrations. The treatment protocol was identical to the standard regimen used throughout this paper (16 h).

The ability of the compounds to activate AhR was first determined by assessing EROD activity (**Fig 3-7 A**) and CYP1A1 (**Fig 3-7 B**) and CYP1A2 (**Fig 3-7 C**) gene transcription. With the exception of PCB 105, all of the dioxin-like PCBs were potent inducers of AhR, while as expected, PCB 153 was ineffective as an AhR agonist. At the lowest tested dose for the PCBs

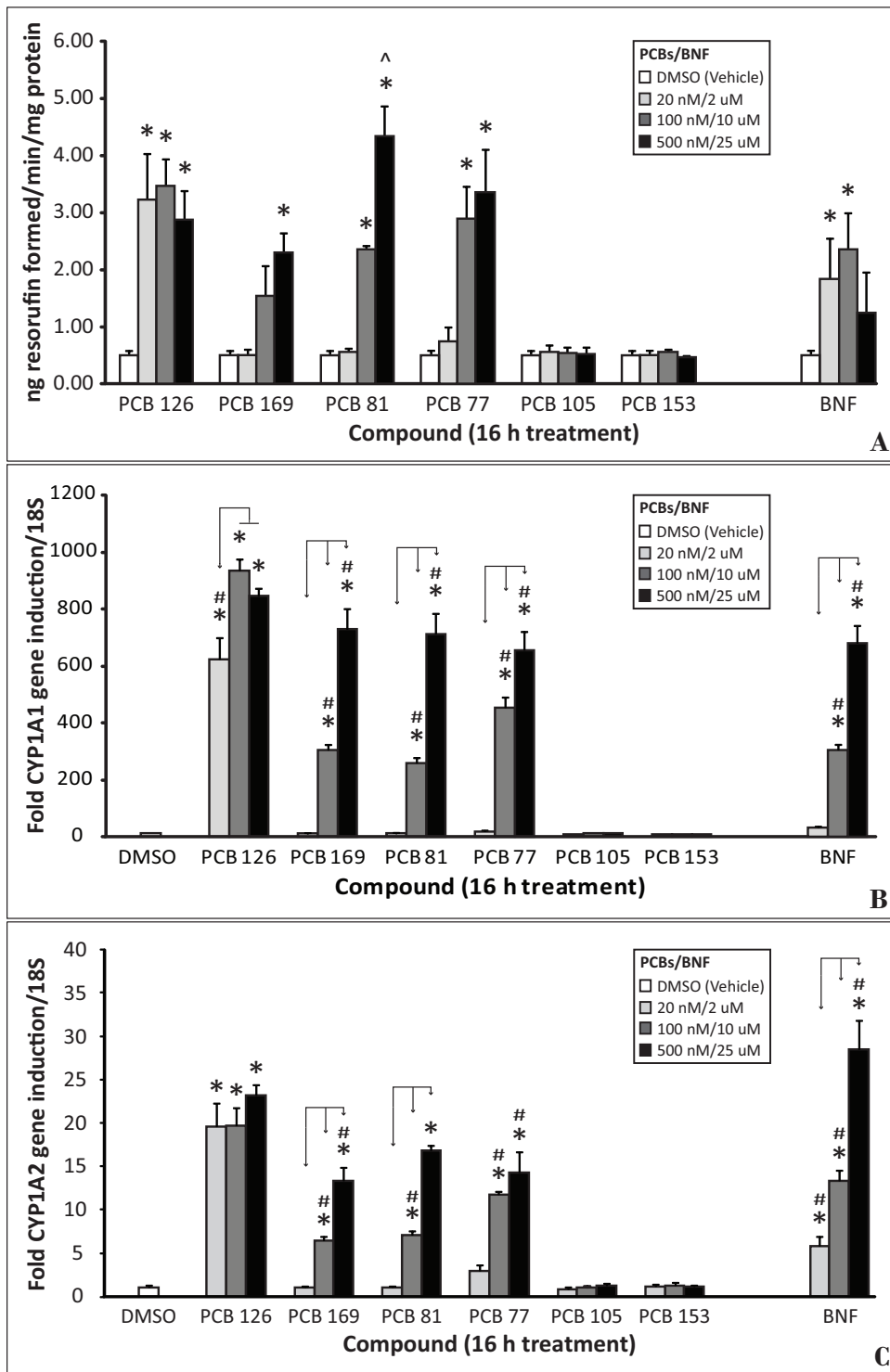
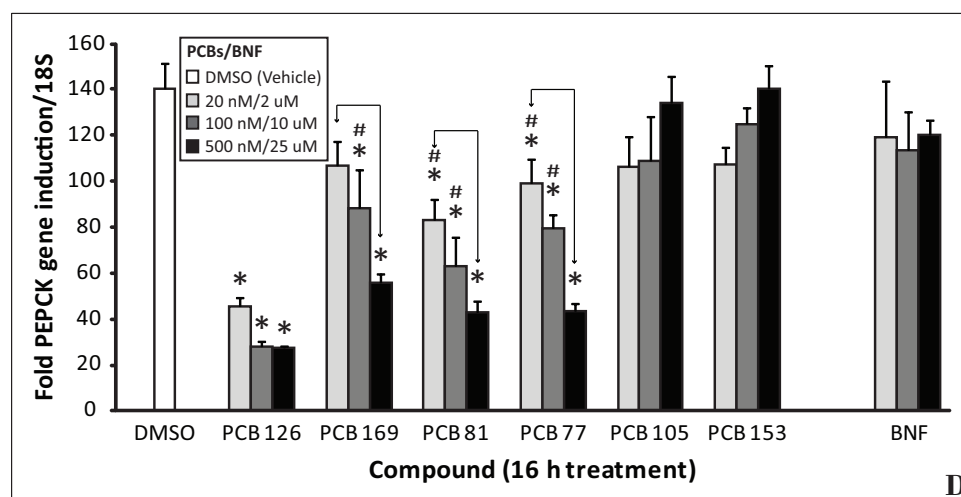


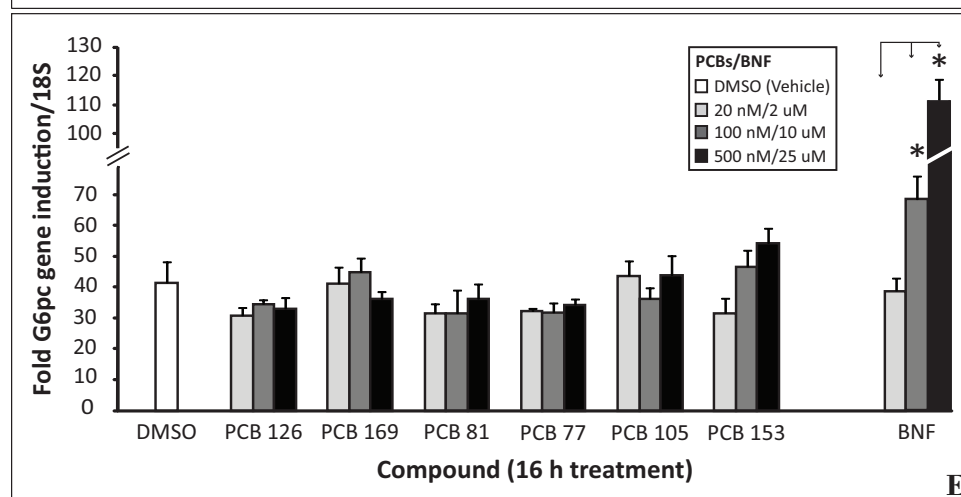
Figure 3-7: Other non ortho-substituted dioxin-like PCBs, but not all AhR agonists, are able to suppress forskolin-stimulated PEPCK (continued on next page)

(Figure 3-7 continued from previous page)

A) Induction of EROD activity to assess AhR activation by PCBs and BNF. Cells were treated with the specified concentrations of the listed compounds for 16 h in 5 mM glucose, all media was removed, cells were lysed by freeze/thaw, and EROD activity was measured; * = $p < 0.05$ for effect of compound vs. DMSO, ^ = $p < 0.05$ for effect of compound vs. all other treatments, $n = 3$ experiments performed in triplicate. B) Induction of CYP1A1 gene to assess AhR activation by PCBs and BNF. Cells were treated as in (A), and CYP1A1 expression was determined by qRT-PCR. * = $p < 0.05$ for effect of compound vs. DMSO, # = $p < 0.05$ for effect of compound vs. both DMSO and PCB 126 100 nM, $n = 3$ experiments performed in triplicate. C) Induction of CYP1A2 gene to assess AhR activation by PCBs and BNF. Cells were treated as in (A), and CYP1A2 expression was determined by qRT-PCR. * = $p < 0.05$ for effect of compound vs. DMSO, # = $p < 0.05$ for compound effect vs. both DMSO and PCB 126 100 nM, $n = 3$ experiments performed in triplicate.



D) Suppression of forskolin-induced PEPCK gene expression by PCBs and BNF. Cells were treated as in (A), except 25 μ M forskolin was added at h 13 of treatment for 3 h and PEPCK expression was determined by qRT-PCR. * = $p < 0.05$ for compound effect vs. DMSO, # = $p < 0.05$ for compound effect vs. both DMSO and PCB 126 100 nM, $n = 3$ experiments performed in triplicate.



E) Effect of forskolin-stimulated G6Pc gene expression by PCBs and BNF. Cells were treated as in (A), except 25 μ M forskolin was added at h 13 of treatment for 3 h and G6Pc gene expression was determined by qRT-PCR. * = $p < 0.05$ for compound effect vs. DMSO, $n = 3$ experiments performed in triplicate.

(20 nM), only PCB 126 induced CYP1A activity and gene transcription in a statistically significant manner (**Fig. 3-7 A-C**). PCB 126 maximally induced CYP1A1 and CYP1A2 at 100 nM, with no further increase at 500 nM; the other dioxin-like PCBs and BNF clustered together with respect to their potency towards CYP1A1 induction, with statistically significant dose-dependence, (**Fig. 3-7 B**). At each respective low, middle, and high dose, PCB 169, PCB 81, PCB 77, and BNF induced CYP1A1 to levels that were not significantly different between compounds (**Fig. 3-7 B**). Similar trends were observed for CYP1A2 (**Fig. 3-7 C**).

The pattern of EROD activity closely paralleled that of CYP1A1 gene transcription, with a few notable differences. First, the greatest overall induction of EROD was observed with 500 nM PCB 81 as opposed to any dose of PCB 126. Second, BNF (and to a lesser extent, PCB 126) appeared to demonstrate the classical inverted U-shaped dose-response curve often observed in the EROD assay, where at sufficiently high concentrations, an AhR agonist competitively inhibits CYP1A activity (Petrulis and Bunce, 1999; Petrulis and Bunce, 2000). Finally, EROD activation by PCB 169 was notably weaker than that of the other dioxin-like PCBs, despite it having the second highest TEF of the PCBs screened and a relative AhR binding potency equivalent to that of PCB 81 (Jensen et al., 2010).

The effect of the various PCBs and BNF on forskolin-stimulated PEPCCK (**Fig. 3-7 D**) and G6pc (**Fig. 3-7 E**) gene transcription was then evaluated. Even at the lowest 20 nM dose, PCB 126 was maximally effective at suppressing forskolin-induced PEPCCK; there was no statistically significant further decrease at 100 nM or 500 nM. For all of the other dioxin-like PCBs, there was a dose-response with respect to PCB concentration and PEPCCK gene suppression. In terms of PEPCCK suppression, there were statistically significant differences both within and between compounds at the two lower doses of each dioxin-like PCB (excluding PCB

126). However, at 500 nM, all of the dioxin-like PCBs reduced PEPCCK to a level that was not significantly different from that observed with any dose of PCB 126. Interestingly, BNF, while able to potently induce CYP1A1, CYP1A2, and EROD, was completely without effect on forskolin-stimulated PEPCCK gene transcription. Consistent with observations made using 100 nM of PCB 126, no PCB at any concentration affected forskolin-stimulated G6pc gene expression (**Fig. 3-7 E**). Inexplicably, BNF significantly, and in a dose-dependent manner, augmented G6pc expression beyond that attained with forskolin alone.

Relationship between AhR activation and PEPCCK suppression -When the data from **Fig. 3-7 B** and **Fig. 3-7 D** were compared on an X-Y plot, there was a statistically significant interaction between AhR activation (as determined by CYP1A1 induction) and PEPCCK gene suppression (**Fig. 3-8**); when CYP1A2 or EROD was substituted for CYP1A1, a similar, statistically significant interaction was seen (data not shown). Despite being statistically significant, the inverse relationship between AhR and PEPCCK was not without notable exceptions; at 20 nM, both PCB 81 and PCB 77 significantly suppressed PEPCCK by approximately 35%, while at the same dose, PCB 169 demonstrated no statistically significant effect (**Fig. 3-7 C**). To stress a previous point, none of the dioxin-like PCBs, with the exception of PCB 126, induced CYP1A1 (**Fig. 3-7 B**), CYP1A2 (**Fig. 3-7 C**) or EROD (**Fig. 3-7 A**) at 20 nM, implying that PEPCCK suppression was occurring in the absence of detectable AhR activation. There was also no significant increase in PEPCCK suppression going from 20 nM to 100 nM of PCB 81 or 77 (**Fig. 3-7 D**) despite a several fold-increase in EROD and CYP1A2 and a several order of magnitude increase in CYP1A1 gene expression. In fact, for PEPCCK, a significant effect of dose within PCB 169, 81, and 77 was only observed when comparing the lowest dose (20 nM) with the highest dose (500 nM); these doses span a CYP1A1 induction range of approximately 700-fold.

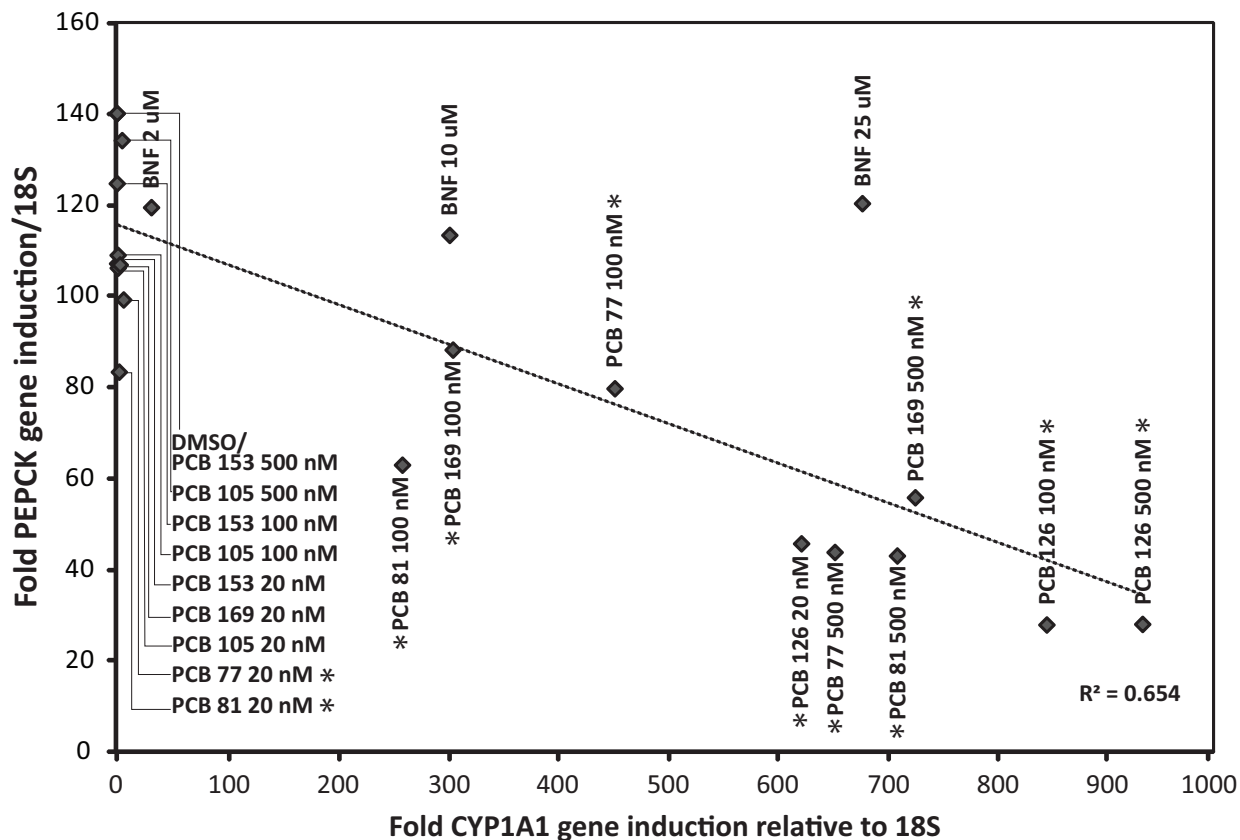


Figure 3-8: Standard least squares analysis of CYP1A1 gene induction by compounds vs. fold PEPCK gene induction by forskolin in the presence of respective compounds. Individual points represent fold induction of CYP1A1 gene following 16 h of treatment (X-axis) relative to PEPCK gene induction after 3 h of 25 μ M forskolin treatment. Data is derived from figures 3-7 A and 3-7 D. * = $p < 0.05$ for PCB effect on forskolin-stimulated PEPCK vs. DMSO. Error bars not shown for clarity.

Finally, BNF behaved similarly with respect to EROD, CYP1A1, and CYP1A2 gene expression compared to PCB 169, 81, and 77, but did not suppress PEPCK to any extent.

3.D. Discussion

The impact of *in vivo* exposure to dioxins has focused on TCDD due to its extreme toxicity with respect to all other dioxins and dioxin-like compounds. While TCDD is the most toxic member of the dioxin family, PCB 126 is the most toxic congener among the PCBs. Although the TEF of PCB 126 is an order of magnitude lower than that of TCDD, the widespread production of PCBs over sixty years implies that the distribution and concentration of PCB 126, as well as other dioxin-like PCBs, may be more penetrant than that of TCDD. The classical molecular mechanism of TCDD-induced toxicity is potent, persistent, and ultimately pathological induction of AhR-mediated genes, while the physiological impact of TCDD poisoning varies according to species but generally includes hypoglycemia and wasting that often leads to death. In the only currently known *in vivo* metabolic study using PCB 126, a similar hypoglycemic effect was reported in PCB 126-treated rats. However, while *in vivo* studies afford insight into whole-body effects, *in vitro* studies allow for resolution of the direct versus indirect impact of a compound. The findings of this paper support the ability of PCB 126 and other non-ortho-substituted dioxin-like PCB congeners to directly suppress hepatic glycogen and hepatic gluconeogenesis, the latter effect mediated through specific suppression of PEPCK gene transcription through a mechanism that involves AhR, although AhR activation does not appear to be the sole determinant of the ability of a compound to antagonize forskolin stimulation of PEPCK mRNA.

Glycogen stores contribute significantly (approximately 50%) to the maintenance of short-term glycemia, with *de novo* glucose synthesis providing the remainder of circulating

glucose during an overnight fast (Nascimento et al., 2008; Petersen et al., 1996). Depression of total hepatic glycogen has been reported following TCDD exposure in rats (Unkila et al., 1995; Viluksela et al., 1999), mice (Dunlap et al., 2002), fish (Volz et al., 2005), and more recently in embryonic chick liver (Diani-Moore et al., 2010); studies of PCB 126 effects on liver glycogen in mammals, however, are lacking. Furthermore, the majority of studies using TCDD or PCB mixtures have observed decreased glycogen following a several-day treatment period (Unkila et al., 1995; Viluksela et al., 1999), or have used doses that induced frank toxicity (Thome et al., 1995). The fact that short-term treatment with PCB 126 was able to directly suppress hepatic glycogen (**Fig. 3-2 A**) independent of cytotoxicity (**Fig. 3-2 B**), implies that impaired glycogen metabolism may play an early and primary role in dioxin-induced hypoglycemia, as opposed to being a later, secondary phenomenon associated with decreased food intake and general toxicity.

Under prolonged fasting conditions, the contribution of gluconeogenesis to maintenance of glycemia overshadows that of glycogen (Thome et al., 1995; Corssmit et al., 2001). The two principle, hormonally regulated gluconeogenic genes, PEPCK and G6pc, have both been reported to be suppressed by TCDD and PCB 126 treatment *in vivo* and *in vitro*. However, the majority of mammalian studies support the finding that the suppression of PEPCK occurs at an earlier time point, is dose-responsive, and decreases to a more drastic extent than that of G6pc, implying that PEPCK suppression may be specific, and G6pc suppression a secondary effect—at least in mammalian liver. To study the direct impact of PCB 126 on hepatic GNG and the expression of PEPCK and G6pc, the effects of forskolin as well as two differentially regulated gluconeogenic fuels were tested. Both TCDD and a PCB mixture are known to suppress the upregulation of PEPCK induced by fasting or cAMP analogs (Boll et al., 1998; Viluksela et al., 1999), making the induced condition (forskolin-stimulated in this study) potentially more

physiologically relevant. As gluconeogenic substrates, lactate and glycerol were selected based on their differential points of entry in the GNG pathway. The synthesis of glucose from lactate is under the control of several critical gluconeogenic enzymes, including Pcx, cytosolic PEPCK, Fbp1, and G6pc. In contrast, glycerol enters the gluconeogenic pathway at a more proximal point, and, enzymatically, is subject to regulation by Fbp1 and G6pc (**Fig. 3-9**) (Burgess et al., 2004). The use of these two differentially regulated substrates under both unstimulated and stimulated conditions led to the novel finding that PCB 126 was able to suppress forskolin-stimulated GNG selectively from lactate (**Fig. 3-4 A**) but not glycerol (**Fig. 3-4 B**) and combined with qRT-PCR data, also confirmed that PCB 126 only affected the forskolin-stimulated expression of PEPCK, and not G6pc (**Fig. 3-5 B**). The absence of any effect of PCB 126 on either Pcx or Fbp1 (**Fig. 3-5 C-D**) lends additional support to the specificity of PCB 126 with respect to gluconeogenesis.

The differential efficiency by which lactate and glycerol were utilized for *de novo* glucose synthesis in the current system may be due to several factors, some of which may be artifacts of the culture conditions. There are several key discrepancies in the metabolism of lactate versus glycerol during GNG. Key enzymatic differences have been described above, although an additional consideration is the requirement of acetyl-CoA for maximal Pcx activity; under the conditions utilized for GNG -i.e. glucose free media with no free fatty acids or acetylcarnitine- it is possible that GNG from precursors under the control of Pcx may be submaximal. However, the fact that GNG from lactate or pyruvate is robustly responsive to forskolin argues against flux through Pcx being rate-limiting; in further support, studies with oleate, linoleate, or palmitate incubation overnight have not yielded higher values compared to BSA controls (unpublished observations). Whether provision of additional sources of acetyl-

CoA might further augment the forskolin responsiveness of GNG from lactate or pyruvate remains to be determined. In rat liver studies, glycerol is generally inferior (Rajasekar and Anuradha, 2007; Sumida et al., 2002) or equivalent to lactate (Sugano et al., 1980) as a gluconeogenic fuel, although increased efficacy has also been reported (Carmona and Freedland, 1989; Veneziale and Lohmar, 1973). Glycerol, as a reduced fuel, is capable of potentially elevating the NADH:NAD⁺ ratio in the cytosol; indirectly, this occurs through reduction of mitochondrial of FAD to FADH₂, and directly, during glycolysis following conversion of glycerol→glycerol 3-P→DHAP→GA3P→1,3-BPG. The ramifications of glycerol-induced increases in the cytosolic redox state under the current conditions are unknown, though, as the absence of glucose would be expected to at least partially mitigate any negative impact of excessive reducing equivalent synthesis, and it has been previously demonstrated that glycerol may a more efficient gluconeogenic fuel than lactate despite (glycerol) inducing a 7x increase in the lactate/pyruvate ratio (Carmona and Freedland, 1989). Lactate is also a reduced fuel, but the process of GNG with lactate as a substrate is more energetically demanding compared to glycerol (**Fig. 3-4 C**); whether differences in cellular energy state are responsible for the observed substrate efficiencies with respect to GNG in the current study will require direct measurement of ATP/ADP and NADH/NAD⁺ levels.

Although previous studies do not support the direct involvement of the AhR in dioxin-mediated PEPCK suppression, AhR is the classical mechanism of action for TCDD and the dioxin-like PCBs, and therefore its role in the current study was investigated. The current data, as well as that from other studies, implies that activation of AhR is likely to be involved, but its activation is not the sole determinant of this effect, nor is AhR likely to directly antagonize PEPCK. First, there is no identifiable core dioxin (xenobiotic) response element (GCGTG; (Sun

et al., 2004)) in the region up to 5 KB upstream of the start site in the mouse cytosolic PEPCK gene. Second, BNF, a potent AhR agonist, was without effect on PEPCK (**Fig. 3-8**). The reason for the marked difference in effect with the non-ortho-substituted PCBs (PCB 126, 169, 81, and 77) and BNF is unknown at this point, but may be due to differences in the efficacy by which these compounds are metabolized by the CYP genes induced by AhR agonism (Schlezing et al., 2006). Third, further support comes from the recent finding that in chicken embryo hepatocytes, TCDD suppression of gluconeogenesis and gluconeogenic genes was mediated by AhR, but through an indirect mechanism involving the TCDD-inducible PARP (TiPARP) (Diani-Moore et al., 2010). The findings of this study differ from ours in that both PEPCK and G6pc were suppressed by TCDD, but differences in the compound used (TCDD vs. PCB 126) as well as the species from which hepatocytes were isolated may account for these discrepancies. For example, in avian species, up to 90% of total PEPCK is mitochondrial, while in mouse and rat, 90% of PEPCK is cytosolic (reviewed in (Hanson and Garber, 1972)). However, the fact that TCDD, PCB 126, PCB 169, PCB 81, and PCB 77 are all capable of suppressing PEPCK argues in favor of involvement of AhR; the finding that a partial inhibitor of AhR (**Fig. 3-6 C-D**) was unable to reverse PCB 126 suppression of forskolin-induced PEPCK (**Fig. 3-6 E**) does not preclude the involvement of AhR, as a 40-50% suppression of the effect of 100 nM PCB 126 on AhR activation still leaves sufficient residual activity to maximally suppress PEPCK (**Fig. 3-8**). However, the sum of the inhibitor data, the ability of certain dioxin-like PCBs to suppress PEPCK without frank activation of AhR, the inability for BNF to suppress PEPCK despite its potent stimulation of AhR, and the recent and past literature support the hypothesis that AhR activation alone is not sufficient to mediate this effect.

The involvement of AhR in PEPCK suppression could be better investigated with a more specific, potent inhibitor of AhR. Currently, there is no widely available pharmacological inhibitor for AhR. However, despite many reports of plant-derived flavones, flavonols, and related compounds being capable of inhibiting AhR, our inhibitor screen of over a dozen candidates found minimal efficacy with several relatively well-characterized compounds even at high micromolar concentrations (i.e. alpha-naphthoflavone, resveratrol, and quercetin), while other putative inhibitors (i.e. curcumin) had highly variable mouse-to-mouse efficacy, and also strongly inhibited forskolin-stimulated GNG gene expression. Finally, the observation that certain inhibitors (i.e. alpha-naphthoflavone) were able to suppress EROD activity induction by PCB 126 but by themselves augmented CYP1A1 and CYP1A2 gene transcription underlines the importance of evaluating both EROD and an AhR target gene (or genes) during inhibitor screens.

In conclusion, this study has shown the following novel findings: (a) PCB 126 suppresses hepatic glycogen metabolism by a glucose and glycogen synthase and phosphorylase-independent mechanism, (b) PCB 126 selectively and potently suppresses forskolin-stimulated, but not basal gluconeogenesis from lactate, but not glycerol (**Fig. 3-9**), (c) PCB 126 selectively and directly suppresses forskolin-stimulated, but not basal PEPCK mRNA, and has no effect on the other key gluconeogenic genes, and (d) other dioxin-like PCBs capable of productive AhR binding mimic the effect of PCB 126 with respect to forskolin-stimulated PEPCK gene expression, yet not all AhR ligands are capable of PEPCK suppression (e.g. BNF). Furthermore, current and past data suggests that the mechanism by which this effect occurs is not through direct AhR modulation, but may rather be via a downstream target of an AhR target gene. The finding, however, that PCBs which were unable to productively bind to the AhR (i.e. PCB 105 and PCB 153) at concentrations tested in this study had no effect on PEPCK induction, while all

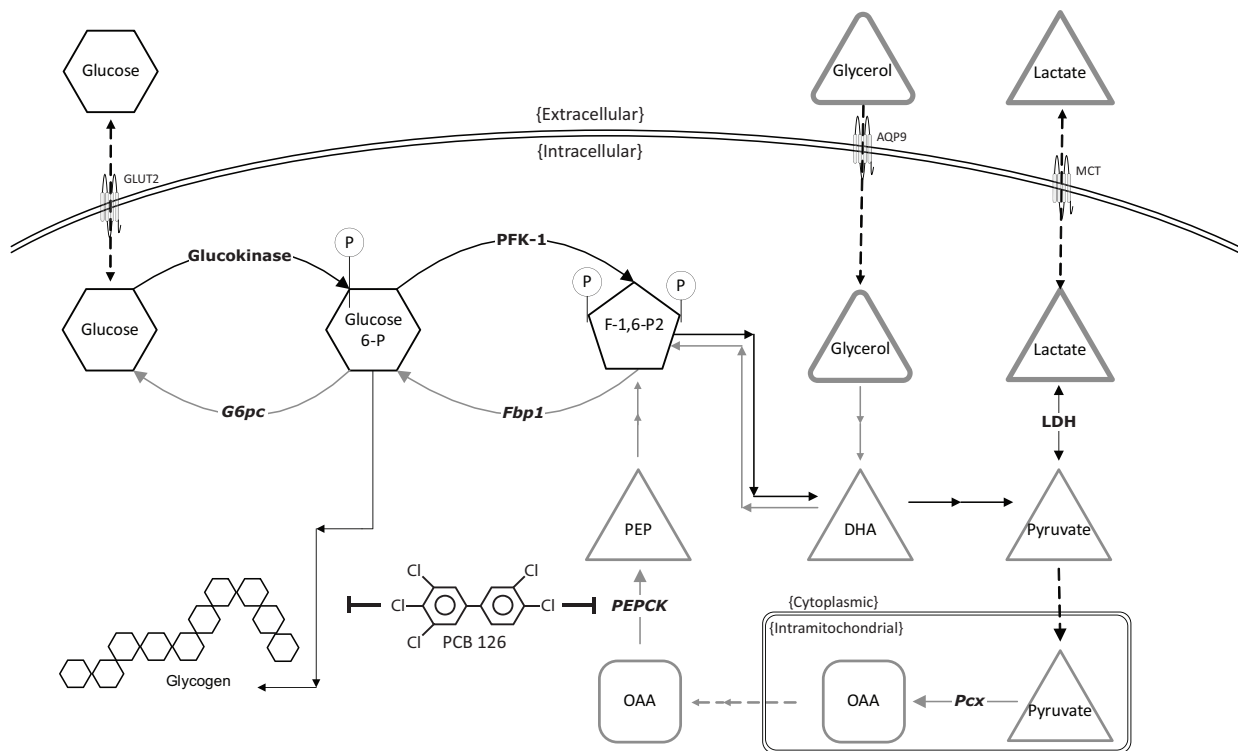


Figure 3-9: Overview of PCB 126 effects on hepatic glucose metabolism. A simplified model of glycolysis, glycogen synthesis, and gluconeogenesis in a mouse hepatocyte is presented. Forward metabolism of glucose (glycolysis and glycogen synthesis) is depicted by black arrows, while reverse metabolism of glucose (GNG) is denoted by gray arrows. Enzymes of forward glucose metabolism are in standard bold text, while enzymes of reverse glucose metabolism are in italicized bold text. In this model, PCB 126 inhibits GNG from lactate by suppression of PEPCK gene transcription, and also inhibits glycogen by an unknown mechanism. GNG from glycerol is not affected by PCB 126 because glycerol is under the control of Fbp1 and G6pc under conditions which promote GNG, and thus bypasses PEPCK. Note that important pathways, including the glycerol phosphate shuttle and malate-aspartate shuttle, are omitted for clarity; refer to Figure 4-3 for greater detail.

four PCBs that were capable of productive AhR binding were able to suppress forskolin augmentation of PEPCK strongly suggests that productive AhR binding is required, but not solely sufficient for suppressing forskolin-induced PEPCK mRNA. Further studies utilizing liver-specific AhR knockout mice, comparison of poorly vs. readily metabolizable ligands on PEPCK, and expanding the database of dioxins and dioxin-like compounds with respect to their effect on hepatic GNG and GNG genes may offer additional mechanistic insight.

CHAPTER IV

Additional studies and future directions for application of primary mouse hepatocytes in mechanistic studies of DLCs

4.A. Introduction

Animal models are used in favor of *in vitro* systems in DLC studies, due to the physiological relevance of *in vivo* work as well as the limited readouts available with most cell culture systems. Elucidation of molecular mechanisms, though, requires extensive control of experimental parameters and minimization of variables – qualities inherent to *in vitro* systems. Since the liver is the central target of DLCs, the majority of research has focused on this organ, and for mechanistic investigations, primary hepatocytes are the preferred –and arguably (given the poor overall performance of available liver cell lines) - the only tool. Most work involving primary hepatocytes in the field of DLC toxicology has evaluated the impact of DLCs on phase-I xenobiotic metabolizing enzymes, taking advantage of the reproducibility of induction of CYP1A1 and CYP1A2 in whole liver versus isolated hepatocytes. However, while the majority of DLC toxicity is related to the potency of AhR activation, CYP enzyme induction may not have direct/independent adverse effects, and thus may be considered to be a simple readout of AhR activation. Few studies have made use of the fact that several of the pathologies observed following DLC exposure *in vivo*, including steatosis and hypoglycemia, may be reproduced in primary hepatocytes. Furthermore, as demonstrated in the current system, these effects may be observed in physiologically relevant metabolic assays, and not simply at the level of transcription or enzyme activity. Data presented in chapters 2 and 3 demonstrate the utility of primary mouse hepatocytes isolated and cultured in a manner that closely maintains their integrity and functional

capacity in the context of studying the mechanism of DLC-induced hypoglycemia. Despite the promising findings outlined in those chapters, much work remains to be performed with respect to optimization of the culture conditions for prolonged maintenance of primary mouse hepatocytes, and many questions must still be addressed concerning the involvement of the AhR in suppression of PEPCK by dioxin-like PCBs.

4.B. Long-term maintenance of hepatocyte phenotype and function

There is no consensus as to how long hepatocytes may be maintained in culture and still be considered *hepatocytes*, and the range of functions that freshly isolated hepatocytes perform would make routine validation of longer-term cultures a significant undertaking. Assuming proper isolation and handling techniques are employed, plating conditions appear to be the determining factor in long-term sustainability. The importance of media supplementation is unclear, although serum is known to accelerate the de-differentiation process (Tuschl and Mueller, 2006). Whether a factor or factors could slow down this process without adversely affecting other functions is unknown, as phenotype preservation through manipulation of media composition has not been well-investigated. Most research has centered on the type of substrate hepatocytes are grown upon, and growth surface research appears to hold the most promise for prolonging the useful lifespan of primary hepatocytes. Growth surface manipulation has the additional advantage of only altering the physical attachment platform without introducing potentially interfering biological or chemical variables.

Standard coatings for 2-D culture include type I collagen and gelatin. While hepatocytes are known to secrete factors that may promote attachment, and serum has been reported to aid in attachment (Klaunig et al., 1981b), plating cells in 10% FBS on uncoated, standard tissue

culture-treated plastic results in a drastically compromised phenotype (unpublished observations). Freshly isolated hepatocytes attach to thin-layer type I or IV collagen within 30 min, but require over 2 h to attach to uncoated plastic; additionally, the appearance of well-defined nuclei, a granulated cytoplasm devoid of vacuoles, and clear cell-cell junctions is substantially attenuated in hepatocytes plated on uncoated versus collagen-coated plates. The type of substrate used clearly has a marked effect on re-establishment of a hepatocyte phenotype *in vitro*, and it is therefore reasonable to assume that alternative growth strata may notably impact long-term phenotype.

Three-dimensional (3-D) and sandwich-type cell culture involving collagen, gelatin, or other gel-forming compounds are common techniques utilized in tissue engineering to increase long-term viability and provide a growth environment that better mimics *in vivo* conditions (Wen et al., 2009; Mathijs et al., 2009). Cell-cell contact is required for optimal maintenance of a cuboidal hepatocyte phenotype in 2-D culture; however, even under optimal 2-D culture density, cell contact is limited to a single plane. Therefore, it was unsurprising that pilot experiments using thin-layer (2-D) coatings of GelTrex (1 mg/mL) yielded similar findings to thin-layer (2-D) collagen in terms of phenotype and function. Interestingly, embedding hepatocytes in a high concentration of GelTrex (15 mg/mL; 3-D) enhanced insulin-stimulated glycogen synthesis compared to thin-layer GelTrex or collagen (**Fig. 4-1**). Unfortunately, light microscopy was not ideal for visualizing cells embedded in a gel, preventing clear observation of cell appearance within the gel. Cells which could be seen appeared small and rounded, which may correspond with superior maintenance of function over time compared to the typical (in 2-D culture) flattened epithelial shape (Li et al., 2005). In a separate experiment using a concentration of GelTrex sufficient to form a thin gel (10 mg/mL), cells were generally smaller and less spread-

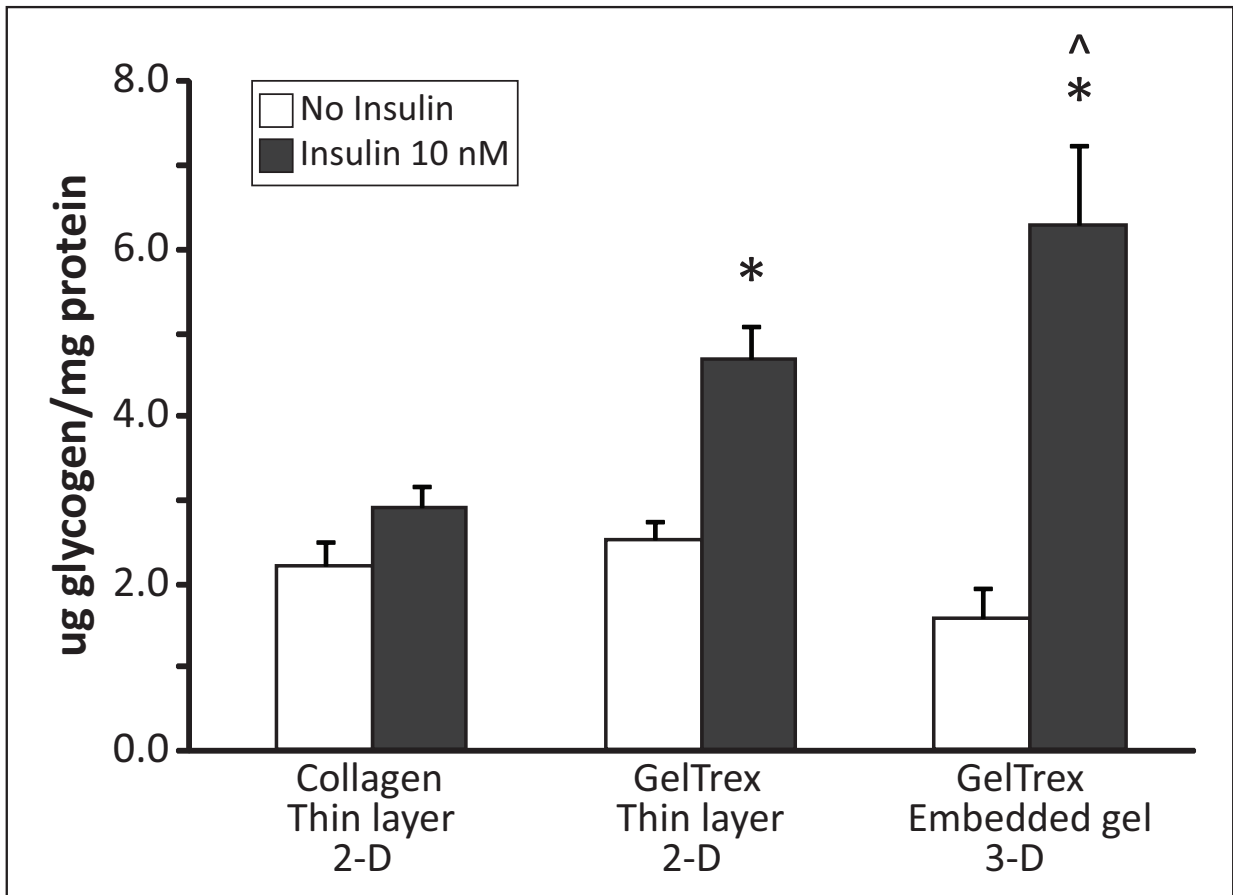
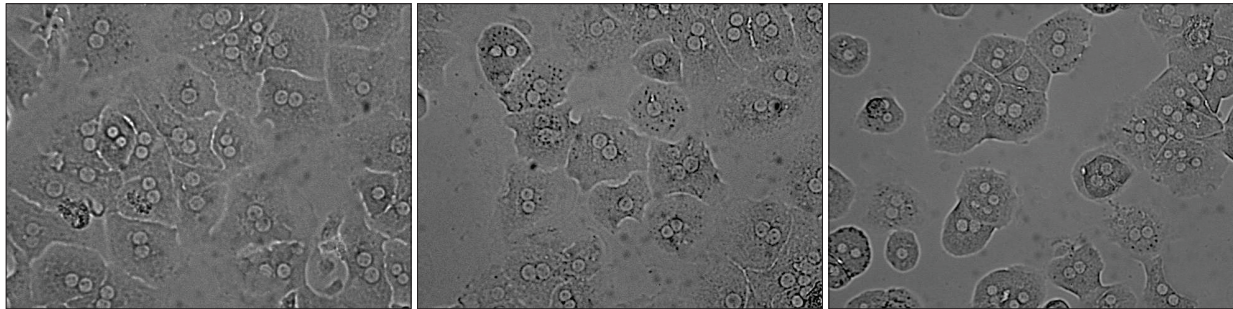


Figure 4-1: Effect of various plating strata on primary mouse hepatocyte glycogen synthesis. Cells were cultured overnight on the specified strata in 5 mM glucose. Cells were then treated with 25 mM glucose +/- 10 nM insulin for 4 h. * = $p < 0.05$ for insulin effect within respective strata condition, ^ = $p < 0.05$ for total glycogen versus all other conditions, n = single experiment performed in triplicate.

out compared to thin-layer GelTrex or collagen, although long-term phenotype and function were not evaluated (**Fig. 4-2**). Additional experiments should be performed for longer-term culture of hepatocytes embedded in collagen or GelTrex/MatriGel-type gels, as the added cost and labor associated with such techniques would be greatly counterbalanced by the ability to perform long-term treatments. Microscopy techniques better suited for depth-of-field visualization (i.e. confocal) should be employed for phenotype determination, as this clearly has a strong relationship to function, but the *ideal* phenotype may vary depending on the culture substratum. Visualization will also be critical to rapidly evaluate optimal plating density, as adding the variable of height/thickness will require adjustment of values used for 2-D culture. Finally, functions other than the industry-standard assessment assays- that is, EROD/ECOD or measurement of albumin release- should be used to validate performance; metabolic readouts such as glycogen synthesis or GNG may be more sensitive indicators of hepatocyte health, and it would be useful to better establish their suitability as indicators of long-term hepatocyte function.

4.C. Addressing the physiological significance of dioxin-like PCB suppression of cytosolic PEPCK

DLC-induced hypoglycemia has been attributed to suppression of hepatic PEPCK (Stahl et al., 1992; Viluksela et al., 1999). This hypothesis is largely based on observations that liver PEPCK activity and/or mRNA levels are suppressed in a time and dose-dependent manner following TCDD or PCB 126 treatment, in conjunction with the classical view that PEPCK is a critical control point for hepatic GNG. While PEPCK is a key gluconeogenic enzyme and is required for the *de novo* synthesis of glucose from substrates that must first be converted to PEP (i.e. lactate, pyruvate, alanine), its designation as a control point for overall GNG flux has recently been called into question. In mice, liver-specific cytosolic PEPCK knockout results in partial, but not



Collagen, thin layer (5 $\mu\text{g}/\text{cm}^2$)
Thin layer coating, 2-D

GelTrex, 1 mg protein/mL
Thin layer coating, 2-D

GelTrex, 10 mg protein/mL
Thin layer gel, 2-D

Figure 4-2: Visualization of hepatocyte phenotype after 24 h of culture on various 2-D strata. Images taken at 400x magnification after culture in standard media conditions at 5 mM glucose.

total suppression of GNG, due to intact GNG from glycerol (Burgess et al., 2004; Burgess et al., 2007); if DLCs specifically suppress PEPCK and are capable of inducing wasting at doses that incite no, or only mild hepatotoxicity (i.e. inflammation and minor hepatomegaly without fibrosis or necrosis), then lethal hypoglycemia should not ensue due to PEPCK suppression alone, evidenced by the ability of liver-specific PEPCK knockout mice to survive an overnight fast. Decreased expression of cytosolic PEPCK clearly plays a role in hypoglycemia secondary to DLC exposure, but may not be the determining factor in lethal hypoglycemia. It is unknown if mitochondrial PEPCK is affected by DLCs, but its role, if any, is likely to be minimal in mice and rats. While the liver of some mammals, including humans, cows, and guinea pigs, contains roughly equal proportions of cytosolic and mitochondrial PEPCK, in rats and mice, almost all PEPCK is cytosolic (in birds, the reverse is true) (Hanson and Garber, 1972). The fact that mice lacking cytosolic PEPCK in the liver are unable to synthesize glucose from lactate implies that mitochondrial PEPCK is unable to compensate even when cytosolic PEPCK is entirely absent.

Recent evidence has underlined the importance of PEPCK as a key regulatory point for TCA flux (Yang et al., 2009; Burgess et al., 2004). During GNG from lactate, NADH is generated in the cytosol; an additional molecule of NADH is synthesized during the glyceraldehyde-3-phosphate dehydrogenase (GAPDH) step. However, only a single molecule of NADH is consumed during GNG, at the malate dehydrogenase (MDH)-catalyzed reduction of malate to OAA. Excess NADH may be recycled to the mitochondria by the malate-aspartate shuttle, essentially a reversal of the aforementioned reaction. Alternatively, mitochondrial PEPCK may assist in maintaining the NADH/NAD⁺ ratio by exporting PEP directly into the cytosol, bypassing the NADH-generating MDH reaction (**Fig. 4-3**). Ablation or suppression of cytosolic PEPCK would therefore be predicted to elevate the mitochondrial NADH/NAD⁺ ratio

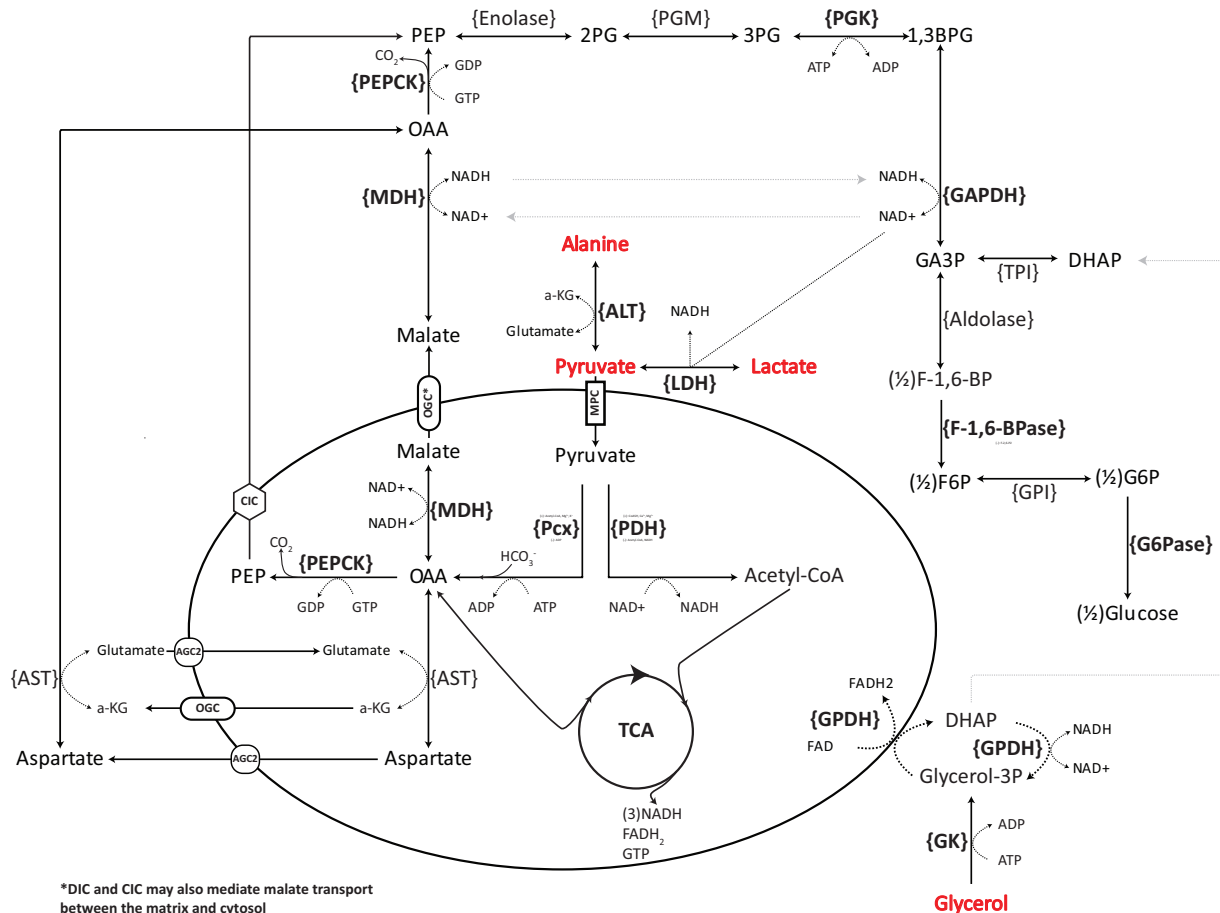


Figure 4-3: Overview of hepatic GNG and integration with NADH production and the TCA cycle. Enzymes are enclosed within brackets, with key enzymes in bold font. Oval represents mitochondrial matrix and all other space represents cytoplasm. Key GNG substrates are in thick bold (red) font. Black lines represent reactions or transport steps, while light gray lines are used for organizational purposes only. AGC2 = aspartate/glutamate carrier isoform 2, CIC = citrate carrier, MPC = mitochondrial pyruvate carrier, OGC = oxoglutarate carrier.

by decreasing the rate of oxidation of $\text{NADH} \rightarrow \text{NAD}^+$ by virtue of reduced flux through GAPDH in addition to abrogating the consumption of GTP during the conversion of $\text{OAA} \rightarrow \text{PEP}$. This appears to be the case in the liver-specific PEPCCK knockout mouse, which exhibits accumulation of TCA intermediates, which in turn allosterically inhibit TCA flux; furthermore, an elevated NADH/NAD^+ ratio suppresses beta oxidation, resulting in steatosis after an overnight fast (Burgess et al., 2004). A similar situation may exist when PEPCCK is suppressed by other means, including DLC exposure. Since steatosis following AhR agonist treatment induces microvesicular steatosis, which tends to be pro-inflammatory, increased cellular energy charge secondary to suppression of PEPCCK may play a catalytic role in DLC-induced hepatic injury (Kawano et al., 2010). The failure to see effects of overnight PCB 126 on hepatocyte lipid accumulation (i.e. beta oxidation or lipogenesis) in the current study may be the result of culture conditions, which will be discussed below.

Optimally, determination of dioxin-like PCB effects on cellular NADH/NAD^+ ratios and the associated metabolic pathways likely to be affected would be performed in the presence of physiologically relevant fasting concentrations of glucose, as glucose-free media may artificially reduce the intracellular energy charge and partially antagonize the generation of a highly reduced state. Beta oxidation and lipogenesis should be approached similarly; beta oxidation in particular is performed in a nutrient-poor buffered salt solution which is designed to minimize interference from exogenous factors. In the context of NADH/NAD^+ ratios, a physiologically relevant medium (i.e. glucose plus 3-carbon precursors) may be more appropriate to allow for maintenance of any established shifts in the ratio secondary to overnight PCB incubation. Overnight incubation in low concentrations of radiolabeled free fatty acids (i.e. oleate and palmitate) followed by measurement of beta oxidation and Oil Red O staining may assist in

resolving changes in beta oxidation due to PCB exposure; previous experience with free fatty acids has shown that detectable lipid accumulation occurs even after a few hours of exposure to low (100-200 μM) concentrations of long-chain fatty acids (unpublished observations). Recently, it has been shown that AhR activation may directly stimulate uptake and transport of fatty acids by the liver (Kawano et al., 2010; Lee et al., 2010). It will therefore be important to resolve changes in lipid accumulation due to direct uptake/esterification versus suppressed oxidation/increased lipogenesis secondary to alterations in the NADH/NAD⁺ ratio.

Finally, more detailed and longer-term time courses should be performed using both dioxin-like PCBs and forskolin to elucidate the impact of prolonged exposure on hepatic PEPCK, GNG, and lipid metabolism. Studies in this paper utilized a static 16 h PCB exposure time combined with short-term (3 h) forskolin incubation. These decisions were based on the fact that hepatocyte phenotype begins to rapidly degrade after 24 h of culture, combined with the observation that overnight treatment with forskolin (5 μM or 25 μM) completely ablated the induction of PEPCK mRNA, with absolute expression levels returning to baseline (data not shown). Furthermore, the 3 h forskolin treatment time closely coincided with the length of the GNG assay (4 h). However, hepatocytes continue to demonstrate a robust forskolin response with respect to GNG even after 24 h of forskolin exposure. Whether upregulated PEPCK protein levels account for sustained increases in GNG even when PEPCK gene expression is at basal levels, or the upregulation of other GNG genes compensates, is unknown. Since the suppressive effect of dioxin-like PCBs on PEPCK mRNA was only detectable in the forskolin-stimulated (3-4 h) condition, it would be informative to determine if suppression of GNG (by dioxin-like PCB) could still be detected under conditions where mRNA levels had returned to baseline but function was still upregulated. It is possible that Pcx and FBP1, the other key GNG enzymes

that did not demonstrate a forskolin response after 3 h of exposure, might do so with longer exposure times (Thonpho et al., 2010). It is also unknown whether dioxin-like PCBs exert stronger effects with incubation times > 16 h, and whether prolonged co-incubation of dioxin-like PCBs with cAMP agonists might affect other GNG genes.

Prolonged DLC exposure may also assist in elucidating their impact on lipogenic genes, which TCDD and other DLCs have been reported to affect. Treatment of cells with PCB 126 for 16 h had no effect on key genes involved in lipogenesis, including acetyl-coA carboxylase, fatty acid synthase, and hexokinase (data not shown). However, these genes are known to be regulated by substrate and hormones; treatment of rat hepatocytes with a PCB mixture elevated lipogenic enzyme activity, but this effect required several days of incubation and the presence of insulin (Boll et al., 1998). Given the long half-life of DLCs, chronic (i.e. >2 d) exposure to DLCs would more closely represent physiological exposure. However, assessing metabolic function in the context of prolonged treatment times *in vitro* would require a well-validated hepatocyte system that is functionally stable for several days, reaffirming the need for a means to prolong the phenotype of cultured mouse hepatocytes.

4.D. Confirmation of AhR involvement in dioxin-like PCB suppression of hepatocyte PEPCK through isolation of hepatocytes from the hepatocyte-specific AhR and ARNT knockout mice

The mechanism of dioxin-like PCB suppression of forskolin-induced PEPCK in primary mouse hepatocytes is unknown, but is likely to involve the AhR. Due to the extensive number of transcription factors and co-activators that regulate PEPCK expression, it would be useful to first determine the necessity of AhR in mediating this effect. While silencing of the AhR could be

used to answer this question, it would require transfection and a lag/incubation period, introducing a 16-24 hour shift in the time course of all experiments; it has been well established that in mouse and rat primary hepatocytes, gene expression and activity, particularly of the P450 enzymes, changes drastically during the first few hours and days of culture (Boess et al., 2003; Clayton and Darnell, Jr., 1983; Michalopoulos et al., 1976; Guzelian et al., 1979). A more feasible alternative would be to take advantage of the fact that hepatocyte-specific AhR and ARNT-null mice have already been generated- yet isolated hepatocyte work has not been published on these strains (Walisser et al., 2005; Nukaya et al., 2010b). These mice have normal liver phenotypes and no evidence of structural duct abnormalities or fibrosis seen in the global AhR knockout, which might interfere with perfusion efficiency. Furthermore, these mice have been bred on a C57 background, meaning the majority of data already generated in this paper could be applicable with minimal validation using wild-type littermates.

Comparison of gluconeogenic gene expression in AhR knockout versus ARNT knockout mice would be particularly interesting due to the recent observation that disruption of ARNT in the liver may alter glucose and lipid metabolism. The hepatocyte-specific ARNT knockout appears to have a normal liver phenotype, but the liver-specific conditional ARNT knockout mouse demonstrates mild hyperglycemia and reduced glucose tolerance combined with increased hepatic glucose production secondary to increased expression of PEPCK, Fbp1, and G6Pc; importantly, the latter effects may be a result of increased C/EBP α expression (Wang et al., 2009). This may be particularly relevant in the case of DLC exposure, as TCDD treatment suppressed C/EBP α expression in a hepatoma cell line (Liu et al., 1998), implying a possible link between AhR/ARNT, C/EBP α , and gluconeogenic genes. It is not immediately clear how loss of ARNT could result in augmented gluconeogenesis, while heterodimerization of ARNT with

active AhR- which could be viewed as a *loss* of available ARNT- could result in the opposite effect (i.e. reduction of C/EBP α and lower PEPCK expression). Nonetheless, the potential for ARNT to bridge the gap between AhR and C/EBP α justifies further investigation.

4.E. Conclusion

Hepatocytes are challenging to isolate, difficult to culture, and have very limited useful life spans. Nonetheless, they are irreplaceable as tools for mechanistic investigations, not only in the field of DLC toxicology, but also in a myriad of aspects of hepatic metabolism. Few cell types, primary or immortalized, are able to perform the wide array of functions that hepatocytes can. However, most investigations focus on very specific aspects of hepatocyte function, such as xenobiotic metabolism or glucose output, and rarely integrate multiple key functions. In this paper, a complete set of metabolic, biochemical, and molecular assays performed in primary mouse hepatocytes has been presented, along with practical application of said assays to study the *in vitro* toxicology of DLCs from a metabolic perspective. The value of this approach may be best appreciated by the ability to link findings at the transcriptional level to physiologically relevant readouts in a rapid and reproducible manner. Severe systematic limitations still exist, though, primarily due to the short time with which hepatocyte phenotype and function can be maintained in culture. Extensive work continues to be performed in this field, and it is quite likely that functionally competent hepatocyte cultures may be sustainable for days or even weeks with minimal alterations in culture substrate, paving the way for higher-throughput, longer-term investigations.

Reference List

- (2006a). NTP Toxicology and Carcinogenesis Studies of a Binary Mixture of 3,3',4,4',5-Pentachlorobiphenyl (PCB 126) (CAS No. 57465-28-8) and 2,3',4,4',5-Pentachlorobiphenyl (PCB 118) (CAS No. 31508-00-6) in Female Harlan Sprague-Dawley Rats (Gavage Studies). *Natl. Toxicol. Program. Tech. Rep. Ser.* 1-218.
- (2006b). NTP Toxicology and Carcinogenesis Studies of a Mixture of 2,3,7,8-Tetrachlorodibenzo-p-Dioxin (TCDD) (CAS No. 1746-01-6), 2,3,4,7,8-Pentachlorodibenzofuran (PeCDF) (CAS No. 57117-31-4), and 3,3',4,4',5-Pentachlorobiphenyl (PCB 126) (CAS No. 57465-28-8) in Female Harlan Sprague-Dawley Rats (Gavage Studies). *Natl. Toxicol. Program. Tech. Rep. Ser.* 1-180.
- Agius,L., Peak,M., and Alberti,K.G. (1990). Regulation of glycogen synthesis from glucose and gluconeogenic precursors by insulin in periportal and perivenous rat hepatocytes. *Biochem. J.* 266, 91-102.
- Androutsopoulos,V.P., Tsatsakis,A.M., and Spandidos,D.A. (2009). Cytochrome P450 CYP1A1: wider roles in cancer progression and prevention. *BMC. Cancer* 9, 187.
- Barthel,A. and Schmoll,D. (2003). Novel concepts in insulin regulation of hepatic gluconeogenesis. *Am. J. Physiol Endocrinol. Metab* 285, E685-E692.
- Beebe,S.J., Redmon,J.B., Blackmore,P.F., and Corbin,J.D. (1985). Discriminative insulin antagonism of stimulatory effects of various cAMP analogs on adipocyte lipolysis and hepatocyte glycogenolysis. *J. Biol. Chem.* 260, 15781-15788.
- Berry,M.N. (1974). High-yield preparation of morphologically intact isolated parenchymal cells from rat liver. *Methods Enzymol.* 32, 625-632.
- Bhavsar,S.P., Reiner,E.J., Hayton,A., Fletcher,R., and MacPherson,K. (2008). Converting Toxic Equivalents (TEQ) of dioxins and dioxin-like compounds in fish from one Toxic Equivalency Factor (TEF) scheme to another. *Environ. Int.* 34, 915-921.
- Birnbaum,L.S. and Tuomisto,J. (2000). Non-carcinogenic effects of TCDD in animals. *Food Addit. Contam* 17, 275-288.
- Blankenship,A. and Matsumura,F. (1997). 2,3,7,8-Tetrachlorodibenzo-p-dioxin-induced activation of a protein tyrosine kinase, pp60src, in murine hepatic cytosol using a cell-free system. *Mol. Pharmacol.* 52, 667-675.
- Bock,K.W. and Kohle,C. (2009). The mammalian aryl hydrocarbon (Ah) receptor: from mediator of dioxin toxicity toward physiological functions in skin and liver. *Biol. Chem.* 390, 1225-1235.

- Boess,F., Kamber,M., Romer,S., Gasser,R., Muller,D., Albertini,S., and Suter,L. (2003). Gene expression in two hepatic cell lines, cultured primary hepatocytes, and liver slices compared to the in vivo liver gene expression in rats: possible implications for toxicogenomics use of in vitro systems. *Toxicol. Sci.* 73, 386-402.
- Bohonowych,J.E. and Denison,M.S. (2007). Persistent binding of ligands to the aryl hydrocarbon receptor. *Toxicol. Sci.* 98, 99-109.
- Boll,M., Weber,L.W., Messner,B., and Stampfl,A. (1998). Polychlorinated biphenyls affect the activities of gluconeogenic and lipogenic enzymes in rat liver: is there an interference with regulatory hormone actions? *Xenobiotica* 28, 479-492.
- Bruns-Weller,E., Knoll,A., and Heberer,T. (2010). High levels of polychlorinated dibenzodioxins/furans and dioxin like-PCBs found in monitoring investigations of sheep liver samples from Lower Saxony, Germany. *Chemosphere* 78, 653-658.
- Burgess,S.C., Hausler,N., Merritt,M., Jeffrey,F.M., Storey,C., Milde,A., Koshy,S., Lindner,J., Magnuson,M.A., Malloy,C.R., and Sherry,A.D. (2004). Impaired tricarboxylic acid cycle activity in mouse livers lacking cytosolic phosphoenolpyruvate carboxykinase. *J. Biol. Chem.* 279, 48941-48949.
- Burgess,S.C., He,T., Yan,Z., Lindner,J., Sherry,A.D., Malloy,C.R., Browning,J.D., and Magnuson,M.A. (2007). Cytosolic phosphoenolpyruvate carboxykinase does not solely control the rate of hepatic gluconeogenesis in the intact mouse liver. *Cell Metab* 5, 313-320.
- Burgess,S.C., Leone,T.C., Wende,A.R., Croce,M.A., Chen,Z., Sherry,A.D., Malloy,C.R., and Finck,B.N. (2006). Diminished hepatic gluconeogenesis via defects in tricarboxylic acid cycle flux in peroxisome proliferator-activated receptor gamma coactivator-1alpha (PGC-1alpha)-deficient mice. *J. Biol. Chem.* 281, 19000-19008.
- Buters,J.T., Sakai,S., Richter,T., Pineau,T., Alexander,D.L., Savas,U., Doehmer,J., Ward,J.M., Jefcoate,C.R., and Gonzalez,F.J. (1999). Cytochrome P450 CYP1B1 determines susceptibility to 7, 12-dimethylbenz[a]anthracene-induced lymphomas. *Proc. Natl. Acad. Sci. U. S. A* 96, 1977-1982.
- Carlson,E.A., McCulloch,C., Koganti,A., Goodwin,S.B., Sutter,T.R., and Silkworth,J.B. (2009). Divergent transcriptomic responses to aryl hydrocarbon receptor agonists between rat and human primary hepatocytes. *Toxicol. Sci.* 112, 257-272.
- Carmona,A. and Freedland,R.A. (1989). Effect of glycerol and dihydroxyacetone on hepatic lipogenesis. *Arch. Biochem. Biophys.* 271, 130-138.
- Chen,K.S. and Lardy,H.A. (1985). Multiple requirements for glycogen synthesis by hepatocytes isolated from fasted rats. *J. Biol. Chem.* 260, 14683-14688.
- Cipok,M., Aga-Mizrachi,S., Bak,A., Feurstein,T., Steinhart,R., Brodie,C., and Sampson,S.R. (2006). Protein kinase Calpha regulates insulin receptor signaling in skeletal muscle. *Biochem. Biophys. Res. Commun.* 345, 817-824.

- Clayton,D.F. and Darnell,J.E., Jr. (1983). Changes in liver-specific compared to common gene transcription during primary culture of mouse hepatocytes. *Mol. Cell Biol.* 3, 1552-1561.
- Corssmit,E.P., Romijn,J.A., and Sauerwein,H.P. (2001). Review article: Regulation of glucose production with special attention to nonclassical regulatory mechanisms: a review. *Metabolism* 50, 742-755.
- Craft,E.S., Devito,M.J., and Crofton,K.M. (2002). Comparative responsiveness of hypothyroxinemia and hepatic enzyme induction in Long-Evans rats versus C57BL/6J mice exposed to TCDD-like and phenobarbital-like polychlorinated biphenyl congeners. *Toxicol. Sci.* 68, 372-380.
- Danos,A.M., Osmanovic,S., and Brady,M.J. (2009). Differential regulation of glycogenolysis by mutant protein phosphatase-1 glycogen-targeting subunits. *J. Biol. Chem.* 284, 19544-19553.
- Deml,E. and Oesterle,D. (1986). Enhancing effect of co-administration of polychlorinated biphenyls and diethylnitrosamine on enzyme-altered islands induced by diethylnitrosamine in rat liver. *Carcinogenesis* 7, 1697-1700.
- Dentin,R., Pegorier,J.P., Benhamed,F., Fougelle,F., Ferre,P., Fauveau,V., Magnuson,M.A., Girard,J., and Postic,C. (2004). Hepatic glucokinase is required for the synergistic action of ChREBP and SREBP-1c on glycolytic and lipogenic gene expression. *J. Biol. Chem.* 279, 20314-20326.
- Devito,M.J., Ross,D.G., Dupuy,A.E., Jr., Ferrario,J., McDaniel,D., and Birnbaum,L.S. (1998). Dose-response relationships for disposition and hepatic sequestration of polyhalogenated dibenzo-p-dioxins, dibenzofurans, and biphenyls following subchronic treatment in mice. *Toxicol. Sci.* 46, 223-234.
- Diani-Moore,S., Ram,P., Li,X., Mondal,P., Youn,D.Y., Sauve,A.A., and Rifkind,A.B. (2010). Identification of the Aryl Hydrocarbon Receptor Target Gene TiPARP as a Mediator of Suppression of Hepatic Gluconeogenesis by 2,3,7,8-Tetrachlorodibenzo-p-dioxin and of Nicotinamide as a Corrective Agent for This Effect. *J. Biol. Chem.* 285, 38801-38810.
- Dickson,L.M., Lingohr,M.K., McCuaig,J., Hugl,S.R., Snow,L., Kahn,B.B., Myers,M.G., Jr., and Rhodes,C.J. (2001). Differential activation of protein kinase B and p70(S6)K by glucose and insulin-like growth factor 1 in pancreatic beta-cells (INS-1). *J. Biol. Chem.* 276, 21110-21120.
- Diliberto,J.J., Burgin,D., and Birnbaum,L.S. (1997). Role of CYP1A2 in hepatic sequestration of dioxin: studies using CYP1A2 knock-out mice. *Biochem. Biophys. Res. Commun.* 236, 431-433.
- Dunlap,D.Y., Ikeda,I., Nagashima,H., Vogel,C.F., and Matsumura,F. (2002). Effects of src-deficiency on the expression of in vivo toxicity of TCDD in a strain of c-src knockout mice procured through six generations of backcrossings to C57BL/6 mice. *Toxicology* 172, 125-141.
- Encomio,V. and Chu,F.L. (2000). The effect of PCBs on glycogen reserves in the eastern oyster *Crassostrea virginica*. *Mar. Environ. Res.* 50, 45-49.

- Fan, F. and Rozman, K.K. (1994). Relationship between acute toxicity of 2,3,7,8-tetrachlorodibenzo-p-dioxin (TCDD) and disturbance of intermediary metabolism in the Long-Evans rat. *Arch. Toxicol.* *69*, 73-78.
- Fernandez-Salguero, P., Pineau, T., Hilbert, D.M., McPhail, T., Lee, S.S., Kimura, S., Nebert, D.W., Rudikoff, S., Ward, J.M., and Gonzalez, F.J. (1995). Immune system impairment and hepatic fibrosis in mice lacking the dioxin-binding Ah receptor. *Science* *268*, 722-726.
- Fernandez-Salguero, P.M., Hilbert, D.M., Rudikoff, S., Ward, J.M., and Gonzalez, F.J. (1996). Aryl-hydrocarbon receptor-deficient mice are resistant to 2,3,7,8-tetrachlorodibenzo-p-dioxin-induced toxicity. *Toxicol. Appl. Pharmacol.* *140*, 173-179.
- Ferrer, J.C., Favre, C., Gomis, R.R., Fernandez-Novell, J.M., Garcia-Rocha, M., de, I., I, Cid, E., and Guinovart, J.J. (2003). Control of glycogen deposition. *FEBS Lett.* *546*, 127-132.
- Fisher, J.W., Campbell, J., Muralidhara, S., Bruckner, J.V., Ferguson, D., Mumtaz, M., Harmon, B., Hedge, J.M., Crofton, K.M., Kim, H., and Almekinder, T.L. (2006). Effect of PCB 126 on hepatic metabolism of thyroxine and perturbations in the hypothalamic-pituitary-thyroid axis in the rat. *Toxicol. Sci.* *90*, 87-95.
- Flaveny, C., Perdew, G.H., and Miller, C.A., III (2009). The Aryl-hydrocarbon receptor does not require the p23 co-chaperone for ligand binding and target gene expression in vivo. *Toxicol. Lett.* *189*, 57-62.
- Fleig, W.E., Enderle, D., Steudter, S., Nother-Fleig, G., and Ditschuneit, H. (1987). Regulation of basal and insulin-stimulated glycogen synthesis in cultured hepatocytes. Inverse relationship to glycogen content. *J. Biol. Chem.* *262*, 1155-1160.
- Foretz, M., Hebrard, S., Leclerc, J., Zarrinpashneh, E., Soty, M., Mithieux, G., Sakamoto, K., Andreelli, F., and Viollet, B. (2010). Metformin inhibits hepatic gluconeogenesis in mice independently of the LKB1/AMPK pathway via a decrease in hepatic energy state. *J. Clin. Invest.* *120*, 2355-2369.
- Franc, M.A., Moffat, I.D., Boutros, P.C., Tuomisto, J.T., Tuomisto, J., Pohjanvirta, R., and Okey, A.B. (2008). Patterns of dioxin-altered mRNA expression in livers of dioxin-sensitive versus dioxin-resistant rats. *Arch. Toxicol.* *82*, 809-830.
- French, C.T., Hanneman, W.H., Chubb, L.S., Billings, R.E., and Andersen, M.E. (2004). Induction of CYP1A1 in primary rat hepatocytes by 3,3',4,4',5-pentachlorobiphenyl: evidence for a switch circuit element. *Toxicol. Sci.* *78*, 276-286.
- Gabbay, R.A. and Lardy, H.A. (1984). Site of insulin inhibition of cAMP-stimulated glycogenolysis. *J. Biol. Chem.* *259*, 6052-6055.
- Gallin, W.J. (1997). Development and maintenance of bile canaliculi in vitro and in vivo. *Microsc. Res. Tech.* *39*, 406-412.

- Garrison, J.C. and Haynes, R.C., Jr. (1973). Hormonal control of glycogenolysis and gluconeogenesis in isolated rat liver cells. *J. Biol. Chem.* 248, 5333-5343.
- Gasa, R., Jensen, P.B., Berman, H.K., Brady, M.J., DePaoli-Roach, A.A., and Newgard, C.B. (2000). Distinctive regulatory and metabolic properties of glycogen-targeting subunits of protein phosphatase-1 (PTG, GL, GM/RG1) expressed in hepatocytes. *J. Biol. Chem.* 275, 26396-26403.
- Gerondaes, P., Alberti, K.G., and Agius, L. (1988). Fatty acid metabolism in hepatocytes cultured with hypolipidaemic drugs. Role of carnitine. *Biochem. J.* 253, 161-167.
- Geusau, A., Abraham, K., Geissler, K., Sator, M.O., Stingl, G., and Tschachler, E. (2001). Severe 2,3,7,8-tetrachlorodibenzo-p-dioxin (TCDD) intoxication: clinical and laboratory effects. *Environ. Health Perspect.* 109, 865-869.
- Giesy, J.P. and Kannan, K. (1998). Dioxin-like and non-dioxin-like toxic effects of polychlorinated biphenyls (PCBs): implications for risk assessment. *Crit Rev. Toxicol.* 28, 511-569.
- Gomez-Lechon, M.J., Lahoz, A., Jimenez, N., Vicente, C.J., and Donato, M.T. (2006). Cryopreservation of rat, dog and human hepatocytes: influence of preculture and cryoprotectants on recovery, cytochrome P450 activities and induction upon thawing. *Xenobiotica* 36, 457-472.
- Gonzalez-Manchon, C., Ayuso, M.S., and Parrilla, R. (1989). Control of hepatic gluconeogenesis: role of fatty acid oxidation. *Arch. Biochem. Biophys.* 271, 1-9.
- Gonzalez-Manchon, C., Martin-Requero, A., Ayuso, M.S., and Parrilla, R. (1992). Role of endogenous fatty acids in the control of hepatic gluconeogenesis. *Arch. Biochem. Biophys.* 292, 95-101.
- Gorski, J.R., Weber, L.W., and Rozman, K. (1988). Tissue-specific alterations of de novo fatty acid synthesis in 2,3,7,8-tetrachlorodibenzo-p-dioxin (TCDD)-treated rats. *Arch. Toxicol.* 62, 146-151.
- Grefhorst, A., Hoekstra, J., Derks, T.G., Ouwens, D.M., Baller, J.F., Havinga, R., Havekes, L.M., Romijn, J.A., and Kuipers, F. (2005). Acute hepatic steatosis in mice by blocking beta-oxidation does not reduce insulin sensitivity of very-low-density lipoprotein production. *Am. J. Physiol Gastrointest. Liver Physiol* 289, G592-G598.
- Gu, Y.Z., Hogenesch, J.B., and Bradfield, C.A. (2000). The PAS superfamily: sensors of environmental and developmental signals. *Annu. Rev. Pharmacol. Toxicol.* 40, 519-561.
- Guo, Y.L., Lambert, G.H., Hsu, C.C., and Hsu, M.M. (2004). Yucheng: health effects of prenatal exposure to polychlorinated biphenyls and dibenzofurans. *Int. Arch. Occup. Environ. Health* 77, 153-158.
- Guzelian, P.S., Diegelmann, R.F., Lamb, R.G., and Fallon, H.J. (1979). Effects of hormones on changes in cytochrome P-450, prolyl hydroxylase, and glycerol phosphate acyltransferase in

- primary monolayer cultures of parenchymal cells from adult rat liver. *Yale J. Biol. Med.* 52, 5-12.
- Guzman,M. and Castro,J. (1989). Zonation of fatty acid metabolism in rat liver. *Biochem. J.* 264, 107-113.
- Hankinson,O. (2005). Role of coactivators in transcriptional activation by the aryl hydrocarbon receptor. *Arch. Biochem. Biophys.* 433, 379-386.
- Hanson,R.W. and Garber,A.J. (1972). Phosphoenolpyruvate carboxykinase. I. Its role in gluconeogenesis. *Am. J. Clin. Nutr.* 25, 1010-1021.
- Hanson,R.W. and Reshef,L. (1997). Regulation of phosphoenolpyruvate carboxykinase (GTP) gene expression. *Annu. Rev. Biochem.* 66, 581-611.
- Hansson,P.K., Asztely,A.K., Clapham,J.C., and Schreyer,S.A. (2004). Glucose and fatty acid metabolism in McA-RH7777 hepatoma cells vs. rat primary hepatocytes: responsiveness to nutrient availability. *Biochim. Biophys. Acta* 1684, 54-62.
- Hartmann,H., Probst,I., Jungermann,K., and Creutzfeldt,W. (1987). Inhibition of glycogenolysis and glycogen phosphorylase by insulin and proinsulin in rat hepatocyte cultures. *Diabetes* 36, 551-555.
- Haws,L.C., Su,S.H., Harris,M., Devito,M.J., Walker,N.J., Farland,W.H., Finley,B., and Birnbaum,L.S. (2006). Development of a refined database of mammalian relative potency estimates for dioxin-like compounds. *Toxicol. Sci.* 89, 4-30.
- Heres,L., Hoogenboom,R., Herbes,R., Traag,W., and Urlings,B. (2010). Tracing and analytical results of the dioxin contamination incident in 2008 originating from the Republic of Ireland. *Food Addit. Contam Part A Chem. Anal. Control Expo. Risk Assess.* 27, 1733-1744.
- Hestermann,E.V., Stegeman,J.J., and Hahn,M.E. (2000). Relative contributions of affinity and intrinsic efficacy to aryl hydrocarbon receptor ligand potency. *Toxicol. Appl. Pharmacol.* 168, 160-172.
- Howard,R.B., Christensen,A.K., Gibbs,F.A., and Pesch,L.A. (1967). The enzymatic preparation of isolated intact parenchymal cells from rat liver. *J. Cell Biol.* 35, 675-684.
- Hsia,M.T. and Kreamer,B.L. (1985). Delayed wasting syndrome and alterations of liver gluconeogenic enzymes in rats exposed to the TCDD congener 3,3', 4,4'-tetrachloroazoxybenzene. *Toxicol. Lett.* 25, 247-258.
- Hugla,J.L. and Thome,J.P. (1999). Effects of polychlorinated biphenyls on liver ultrastructure, hepatic monooxygenases, and reproductive success in the barbel. *Ecotoxicol. Environ. Saf* 42, 265-273.
- Huwe,J., Pagan-Rodriguez,D., Abdelmajid,N., Clinch,N., Gordon,D., Holterman,J., Zaki,E., Lorentzsen,M., and Dearfield,K. (2009). Survey of polychlorinated dibenzo-p-dioxins,

polychlorinated dibenzofurans, and non-ortho-polychlorinated biphenyls in U.S. meat and poultry, 2007-2008: effect of new toxic equivalency factors on toxic equivalency levels, patterns, and temporal trends. *J. Agric. Food Chem.* *57*, 11194-11200.

Ishii,S., Iizuka,K., Miller,B.C., and Uyeda,K. (2004). Carbohydrate response element binding protein directly promotes lipogenic enzyme gene transcription. *Proc. Natl. Acad. Sci. U. S. A* *101*, 15597-15602.

Jaffe,H.A., Danel,C., Longenecker,G., Metzger,M., Setoguchi,Y., Rosenfeld,M.A., Gant,T.W., Thorgeirsson,S.S., Stratford-Perricaudet,L.D., Perricaudet,M., and . (1992). Adenovirus-mediated in vivo gene transfer and expression in normal rat liver. *Nat. Genet.* *1*, 372-378.

Jaruchotikamol,A., Jarukamjorn,K., Sirisangtrakul,W., Sakuma,T., Kawasaki,Y., and Nemoto,N. (2007). Strong synergistic induction of CYP1A1 expression by andrographolide plus typical CYP1A inducers in mouse hepatocytes. *Toxicol. Appl. Pharmacol.* *224*, 156-162.

Jensen,B.A., Reddy,C.M., Nelson,R.K., and Hahn,M.E. (2010). Developing tools for risk assessment in protected species: Relative potencies inferred from competitive binding of halogenated aromatic hydrocarbons to aryl hydrocarbon receptors from beluga (*Delphinapterus leucas*) and mouse. *Aquat. Toxicol.* *100*, 238-245.

Jonsson,M.E., Orrego,R., Woodin,B.R., Goldstone,J.V., and Stegeman,J.J. (2007). Basal and 3,3',4,4',5-pentachlorobiphenyl-induced expression of cytochrome P450 1A, 1B and 1C genes in zebrafish. *Toxicol. Appl. Pharmacol.* *221*, 29-41.

Kawano,Y., Nishiumi,S., Tanaka,S., Nobutani,K., Miki,A., Yano,Y., Seo,Y., Kutsumi,H., Ashida,H., Azuma,T., and Yoshida,M. (2010). Activation of the aryl hydrocarbon receptor induces hepatic steatosis via the upregulation of fatty acid transport. *Arch. Biochem. Biophys.* *504*, 221-227.

Kennedy,S.W., Lorenzen,A., James,C.A., and Collins,B.T. (1993). Ethoxyresorufin-O-deethylase and porphyrin analysis in chicken embryo hepatocyte cultures with a fluorescence multiwell plate reader. *Anal. Biochem.* *211*, 102-112.

Kinlaw,W.B., Church,J.L., Harmon,J., and Mariash,C.N. (1995). Direct evidence for a role of the "spot 14" protein in the regulation of lipid synthesis. *J. Biol. Chem.* *270*, 16615-16618.

Klaunig,J.E., Goldblatt,P.J., Hinton,D.E., Lipsky,M.M., Chacko,J., and Trump,B.F. (1981a). Mouse liver cell culture. I. Hepatocyte isolation. *In Vitro* *17*, 913-925.

Klaunig,J.E., Goldblatt,P.J., Hinton,D.E., Lipsky,M.M., and Trump,B.F. (1981b). Mouse liver cell culture. II. Primary culture. *In Vitro* *17*, 926-934.

Lahtela,J.T., Wals,P.A., and Katz,J. (1990). Glucose metabolism and recycling by hepatocytes of OB/OB and ob/ob mice. *Am. J. Physiol* *259*, E389-E396.

- Landau,B.R., Wahren,J., Chandramouli,V., Schumann,W.C., Ekberg,K., and Kalhan,S.C. (1996). Contributions of gluconeogenesis to glucose production in the fasted state. *J. Clin. Invest* 98, 378-385.
- Lee,J.H., Wada,T., Febbraio,M., He,J., Matsubara,T., Lee,M.J., Gonzalez,F.J., and Xie,W. (2010). A novel role for the dioxin receptor in fatty acid metabolism and hepatic steatosis. *Gastroenterology* 139, 653-663.
- Li,K., Qu,X., Wang,Y., Tang,Y., Qin,D., Wang,Y., and Feng,M. (2005). Improved performance of primary rat hepatocytes on blended natural polymers. *J. Biomed. Mater. Res. A* 75, 268-274.
- Liem,A.K., Furst,P., and Rappe,C. (2000). Exposure of populations to dioxins and related compounds. *Food Addit. Contam* 17, 241-259.
- Lingohr,M.K., Bull,R.J., Kato-Weinstein,J., and Thrall,B.D. (2002). Dichloroacetate stimulates glycogen accumulation in primary hepatocytes through an insulin-independent mechanism. *Toxicol. Sci.* 68, 508-515.
- Liu,P.C., Dunlap,D.Y., and Matsumura,F. (1998). Suppression of C/EBPalpha and induction of C/EBPbeta by 2,3,7,8-tetrachlorodibenzo-p-dioxin in mouse adipose tissue and liver. *Biochem. Pharmacol.* 55, 1647-1655.
- M'Zali,H., Guichard,C., Lavau,M., and Plas,C. (1997). Time-dependent effects of insulin on lipid synthesis in cultured fetal rat hepatocytes: a comparison between lipogenesis and glycogenesis. *Metabolism* 46, 345-354.
- Malewiak,M.I., Griglio,S., Kalopissis,A.D., and Le,L., X (1983). Oleate metabolism in isolated hepatocytes from lean and obese Zucker rats. Influence of a high fat diet and in vitro response to glucagon. *Metabolism* 32, 661-668.
- Mathijs,K., Kienhuis,A.S., Brauers,K.J., Jennen,D.G., Lahoz,A., Kleinjans,J.C., and van Delft,J.H. (2009). Assessing the metabolic competence of sandwich-cultured mouse primary hepatocytes. *Drug Metab Dispos.* 37, 1305-1311.
- Matsumura,F. (2009). The significance of the nongenomic pathway in mediating inflammatory signaling of the dioxin-activated Ah receptor to cause toxic effects. *Biochem. Pharmacol.* 77, 608-626.
- Matsumura,F., Enan,E., Dunlap,D.Y., Pinkerton,K.E., and Peake,J. (1997). Altered in vivo toxicity of 2,3,7,8-tetrachlorodibenzo-p-dioxin (TCDD) in C-SRC deficient mice. *Biochem. Pharmacol.* 53, 1397-1404.
- McHale,C.M., Zhang,L., Hubbard,A.E., Zhao,X., Baccarelli,A., Pesatori,A.C., Smith,M.T., and Landi,M.T. (2007). Microarray analysis of gene expression in peripheral blood mononuclear cells from dioxin-exposed human subjects. *Toxicology* 229, 101-113.
- Menuelle,P. and Plas,C. (1991). Variations in the antagonistic effects of insulin and glucagon on glycogen metabolism in cultured foetal hepatocytes. *Biochem. J.* 277 (Pt 1), 111-117.

- Michalopoulos,G., Sattler,C.A., Sattler,G.L., and Pitot,H.C. (1976). Cytochrome P-450 induction by phenobarbital and 3-methylcholanthrene in primary cultures of hepatocytes. *Science* 193, 907-909.
- Miller,T.B., Jr., Garnache,A., and Cruz,J. (1984). Insulin regulation of glycogen synthase phosphatase in primary cultures of hepatocytes. *J. Biol. Chem.* 259, 12470-12474.
- Moon,A. and Rhead,W.J. (1987). Complementation analysis of fatty acid oxidation disorders. *J. Clin. Invest* 79, 59-64.
- Moore,M.C., Cherrington,A.D., Cline,G., Pagliassotti,M.J., Jones,E.M., Neal,D.W., Badet,C., and Shulman,G.I. (1991). Sources of carbon for hepatic glycogen synthesis in the conscious dog. *J. Clin. Invest* 88, 578-587.
- Morck,A., Larsen,G., and Wehler,E.K. (2002). Covalent binding of PCB metabolites to lipids: route of formation and characterization. *Xenobiotica* 32, 625-640.
- Morral,N., Edenberg,H.J., Witting,S.R., Altomonte,J., Chu,T., and Brown,M. (2007). Effects of glucose metabolism on the regulation of genes of fatty acid synthesis and triglyceride secretion in the liver. *J. Lipid Res.* 48, 1499-1510.
- Nakajima,T., Horiuchi,M., Yamanaka,H., Kizaki,Z., Inoue,F., Kodo,N., Kinugasa,A., Saheki,T., and Sawada,T. (1997). The effect of carnitine on ketogenesis in perfused livers from juvenile visceral steatosis mice with systemic carnitine deficiency. *Pediatr. Res.* 42, 108-113.
- Nascimento,K.F., Garcia,R.F., Gazola,V.A., de Souza,H.M., Obici,S., and Bazotte,R.B. (2008). Contribution of hepatic glycogenolysis and gluconeogenesis in the defense against short-term insulin induced hypoglycemia in rats. *Life Sci.* 82, 1018-1022.
- Nawaratne,R., Gray,A., Jorgensen,C.H., Downes,C.P., Siddle,K., and Sethi,J.K. (2006). Regulation of insulin receptor substrate 1 pleckstrin homology domain by protein kinase C: role of serine 24 phosphorylation. *Mol. Endocrinol.* 20, 1838-1852.
- Nebert,D.W., Dalton,T.P., Okey,A.B., and Gonzalez,F.J. (2004). Role of aryl hydrocarbon receptor-mediated induction of the CYP1 enzymes in environmental toxicity and cancer. *J. Biol. Chem.* 279, 23847-23850.
- Newgard,C.B., Moore,S.V., Foster,D.W., and McGarry,J.D. (1984). Efficient hepatic glycogen synthesis in refeeding rats requires continued carbon flow through the gluconeogenic pathway. *J. Biol. Chem.* 259, 6958-6963.
- Nguyen,T.H. and Ferry,N. (2004). Liver gene therapy: advances and hurdles. *Gene Ther.* 11 *Suppl 1*, S76-S84.
- Nukaya,M., Lin,B.C., Glover,E., Moran,S.M., Kennedy,G.D., and Bradfield,C.A. (2010a). The aryl hydrocarbon receptor-interacting protein (AIP) is required for dioxin-induced hepatotoxicity but not for the induction of the Cyp1a1 and Cyp1a2 genes. *J. Biol. Chem.* 285, 35599-35605.

- Nukaya,M., Moran,S., and Bradfield,C.A. (2009). The role of the dioxin-responsive element cluster between the Cyp1a1 and Cyp1a2 loci in aryl hydrocarbon receptor biology. *Proc. Natl. Acad. Sci. U. S. A* 106, 4923-4928.
- Nukaya,M., Walisser,J.A., Moran,S.M., Kennedy,G.D., and Bradfield,C.A. (2010b). Aryl hydrocarbon receptor nuclear translocator in hepatocytes is required for aryl hydrocarbon receptor-mediated adaptive and toxic responses in liver. *Toxicol. Sci.* 118, 554-563.
- Okamoto,T., Kanemoto,N., Ban,T., Sudo,T., Nagano,K., and Niki,I. (2009). Establishment and characterization of a novel method for evaluating gluconeogenesis using hepatic cell lines, H4IIE and HepG2. *Arch. Biochem. Biophys.* 491, 46-52.
- Okey,A.B., Riddick,D.S., and Harper,P.A. (1994). The Ah receptor: mediator of the toxicity of 2,3,7,8-tetrachlorodibenzo-p-dioxin (TCDD) and related compounds. *Toxicol. Lett.* 70, 1-22.
- Ontko,J.A. (1972). Metabolism of free fatty acids in isolated liver cells. Factors affecting the partition between esterification and oxidation. *J. Biol. Chem.* 247, 1788-1800.
- Ozeki,J., Uno,S., Ogura,M., Choi,M., Maeda,T., Sakurai,K., Matsuo,S., Amano,S., Nebert,D.W., and Makishima,M. (2011). Aryl hydrocarbon receptor ligand 2,3,7,8-tetrachlorodibenzo-p-dioxin enhances liver damage in bile duct-ligated mice. *Toxicology* 280, 10-17.
- Park,J.Y., Shigenaga,M.K., and Ames,B.N. (1996). Induction of cytochrome P4501A1 by 2,3,7,8-tetrachlorodibenzo-p-dioxin or indolo(3,2-b)carbazole is associated with oxidative DNA damage. *Proc. Natl. Acad. Sci. U. S. A* 93, 2322-2327.
- Patterson,D.G., Jr., Turner,W.E., Caudill,S.P., and Needham,L.L. (2008). Total TEQ reference range (PCDDs, PCDFs, cPCBs, mono-PCBs) for the US population 2001-2002. *Chemosphere* 73, S261-S277.
- Peak,M., al-Habori,M., and Agius,L. (1992). Regulation of glycogen synthesis and glycolysis by insulin, pH and cell volume. Interactions between swelling and alkalinization in mediating the effects of insulin. *Biochem. J.* 282 (Pt 3), 797-805.
- Perez-Fuentetaja,A., Lupton,S., Clapsadl,M., Samara,F., Gatto,L., Biniakewitz,R., and Aga,D.S. (2010). PCB and PBDE levels in wild common carp (*Cyprinus carpio*) from eastern Lake Erie. *Chemosphere* 81, 541-547.
- Petersen,K.F., Price,T., Cline,G.W., Rothman,D.L., and Shulman,G.I. (1996). Contribution of net hepatic glycogenolysis to glucose production during the early postprandial period. *Am. J. Physiol* 270, E186-E191.
- Petrulis,J.R. and Bunce,N.J. (1999). Competitive inhibition by inducer as a confounding factor in the use of the ethoxyresorufin-O-deethylase (EROD) assay to estimate exposure to dioxin-like compounds. *Toxicol. Lett.* 105, 251-260.
- Petrulis,J.R. and Bunce,N.J. (2000). Competitive behavior in the interactive toxicology of halogenated aromatic compounds. *J. Biochem. Mol. Toxicol.* 14, 73-81.

- Petrulis, J.R. and Perdew, G.H. (2002). The role of chaperone proteins in the aryl hydrocarbon receptor core complex. *Chem. Biol. Interact.* *141*, 25-40.
- Poland, A. and Knutson, J.C. (1982). 2,3,7,8-tetrachlorodibenzo-p-dioxin and related halogenated aromatic hydrocarbons: examination of the mechanism of toxicity. *Annu. Rev. Pharmacol. Toxicol.* *22*, 517-554.
- Rajasekar, P. and Anuradha, C.V. (2007). Fructose-induced hepatic gluconeogenesis: effect of L-carnitine. *Life Sci.* *80*, 1176-1183.
- Ramadoss, P., Marcus, C., and Perdew, G.H. (2005). Role of the aryl hydrocarbon receptor in drug metabolism. *Expert. Opin. Drug Metab Toxicol.* *1*, 9-21.
- Ramnanan, C.J., Edgerton, D.S., Rivera, N., Irimia-Dominguez, J., Farmer, B., Neal, D.W., Lautz, M., Donahue, E.P., Meyer, C.M., Roach, P.J., and Cherrington, A.D. (2010). Molecular characterization of insulin-mediated suppression of hepatic glucose production in vivo. *Diabetes* *59*, 1302-1311.
- Richieri, G.V. and Kleinfeld, A.M. (1995). Unbound free fatty acid levels in human serum. *J. Lipid Res.* *36*, 229-240.
- Rifkind, A.B. (2006). CYP1A in TCDD toxicity and in physiology-with particular reference to CYP dependent arachidonic acid metabolism and other endogenous substrates. *Drug Metab Rev.* *38*, 291-335.
- Roe, J.H. and Dailey, R.E. (1966). Determination of glycogen with the anthrone reagent. *Anal. Biochem.* *15*, 245-250.
- Rosenzweig, T., Braiman, L., Bak, A., Alt, A., Kuroki, T., and Sampson, S.R. (2002). Differential effects of tumor necrosis factor-alpha on protein kinase C isoforms alpha and delta mediate inhibition of insulin receptor signaling. *Diabetes* *51*, 1921-1930.
- Safe, S.H. (1998). Development validation and problems with the toxic equivalency factor approach for risk assessment of dioxins and related compounds. *J. Anim Sci.* *76*, 134-141.
- Salhanick, A.I., Chang, C.L., and Amatruda, J.M. (1989). Hormone and substrate regulation of glycogen accumulation in primary cultures of rat hepatocytes. *Biochem. J.* *261*, 985-992.
- Satake, S., Moore, M.C., Igawa, K., Converse, M., Farmer, B., Neal, D.W., and Cherrington, A.D. (2002). Direct and indirect effects of insulin on glucose uptake and storage by the liver. *Diabetes* *51*, 1663-1671.
- Schleizinger, J.J., Struntz, W.D., Goldstone, J.V., and Stegeman, J.J. (2006). Uncoupling of cytochrome P450 1A and stimulation of reactive oxygen species production by co-planar polychlorinated biphenyl congeners. *Aquat. Toxicol.* *77*, 422-432.

- Schmidt, J.V., Su, G.H., Reddy, J.K., Simon, M.C., and Bradfield, C.A. (1996). Characterization of a murine Ahr null allele: involvement of the Ah receptor in hepatic growth and development. *Proc. Natl. Acad. Sci. U. S. A* *93*, 6731-6736.
- Schulze, H.P., Huhn, W., and Dargel, R. (1986). Effect of catecholamines on the metabolic fate of nonesterified fatty acids in isolated hepatocytes from newborn rats. *Metabolism* *35*, 787-791.
- Selzner, M. and Clavien, P.A. (2001). Fatty liver in liver transplantation and surgery. *Semin. Liver Dis.* *21*, 105-113.
- Shinkyo, R., Sakaki, T., Ohta, M., and Inouye, K. (2003). Metabolic pathways of dioxin by CYP1A1: species difference between rat and human CYP1A subfamily in the metabolism of dioxins. *Arch. Biochem. Biophys.* *409*, 180-187.
- Silkworth, J.B., Koganti, A., Illouz, K., Possolo, A., Zhao, M., and Hamilton, S.B. (2005). Comparison of TCDD and PCB CYP1A induction sensitivities in fresh hepatocytes from human donors, sprague-dawley rats, and rhesus monkeys and HepG2 cells. *Toxicol. Sci.* *87*, 508-519.
- Sorg, O., Zennegg, M., Schmid, P., Fedosyuk, R., Valikhnovskyi, R., Gaide, O., Kniazevych, V., and Saurat, J.H. (2009). 2,3,7,8-tetrachlorodibenzo-p-dioxin (TCDD) poisoning in Victor Yushchenko: identification and measurement of TCDD metabolites. *Lancet* *374*, 1179-1185.
- Spector, A.A. (1975). Fatty acid binding to plasma albumin. *J. Lipid Res.* *16*, 165-179.
- Spurway, T.D., Sherratt, H.A., Pogson, C.I., and Agius, L. (1997). The flux control coefficient of carnitine palmitoyltransferase I on palmitate beta-oxidation in rat hepatocyte cultures. *Biochem. J.* *323 (Pt 1)*, 119-122.
- Stahl, B.U. (1995). 2,3,7,8-Tetrachlorodibenzo-p-dioxin blocks the physiological regulation of hepatic phosphoenolpyruvate carboxykinase activity in primary rat hepatocytes. *Toxicology* *103*, 45-52.
- Stahl, B.U., Beer, D.G., Weber, L.W., Lebofsky, M., and Rozman, K. (1992). Decreased hepatic phosphoenolpyruvate carboxykinase gene expression after 2,3,7,8-tetrachlorodibenzo-p-dioxin treatment: implications for the acute toxicity of chlorinated dibenzo-p-dioxins in the rat. *Arch. Toxicol. Suppl* *15*, 151-155.
- Stahl, B.U., Beer, D.G., Weber, L.W., and Rozman, K. (1993). Reduction of hepatic phosphoenolpyruvate carboxykinase (PEPCK) activity by 2,3,7,8-tetrachlorodibenzo-p-dioxin (TCDD) is due to decreased mRNA levels. *Toxicology* *79*, 81-95.
- Sugano, T., Shiota, M., Tanaka, T., Miyamae, Y., Shimada, M., and Oshino, N. (1980). Intracellular redox state and stimulation of gluconeogenesis by glucagon and norepinephrine in the perfused rat liver. *J. Biochem.* *87*, 153-166.
- Sumida, K.D., Crandall, S.C., Chadha, P.L., and Qureshi, T. (2002). Hepatic gluconeogenic capacity from various precursors in young versus old rats. *Metabolism* *51*, 876-880.

- Sun, Y.V., Boverhof, D.R., Burgoon, L.D., Fielden, M.R., and Zacharewski, T.R. (2004). Comparative analysis of dioxin response elements in human, mouse and rat genomic sequences. *Nucleic Acids Res.* 32, 4512-4523.
- Tanno, K. and Aoki, Y. (1996). Phosphorylation of c-Jun stimulated in primary cultured rat liver parenchymal cells by a coplanar polychlorinated biphenyl. *Biochem. J.* 313 (Pt 3), 863-866.
- Thome, J.P., Roelandt, L., Goffinet, G., Stouvenakers, N., and Kremers, P. (1995). Cytotoxic effects of Aroclor 1254 on ultrastructure and biochemical parameters in cultured foetal rat hepatocytes. *Toxicology* 98, 83-94.
- Thonpho, A., Sereeruk, C., Rojvirat, P., and Jitrapakdee, S. (2010). Identification of the cyclic AMP responsive element (CRE) that mediates transcriptional regulation of the pyruvate carboxylase gene in HepG2 cells. *Biochem. Biophys. Res. Commun.* 393, 714-719.
- Tosh, D., Alberti, G.M., and Agius, L. (1988). Glucagon regulation of gluconeogenesis and ketogenesis in periportal and perivenous rat hepatocytes. Heterogeneity of hormone action and of the mitochondrial redox state. *Biochem. J.* 256, 197-204.
- Tosh, D., Beresford, G., and Agius, L. (1994). Glycogen synthesis from glucose by direct and indirect pathways in hepatocyte cultures from different nutritional states. *Biochim. Biophys. Acta* 1224, 205-212.
- Tuomisto, J.T., Viluksela, M., Pohjanvirta, R., and Tuomisto, J. (1999). The AH receptor and a novel gene determine acute toxic responses to TCDD: segregation of the resistant alleles to different rat lines. *Toxicol. Appl. Pharmacol.* 155, 71-81.
- Turner, S.M., Linfoot, P.A., Neese, R.A., and Hellerstein, M.K. (2005). Sources of plasma glucose and liver glycogen in fasted ob/ob mice. *Acta Diabetol.* 42, 187-193.
- Turrio-Baldassarri, L., Abate, V., Alivernini, S., Battistelli, C.L., Carasi, S., Casella, M., Iacovella, N., Iamiceli, A.L., Indelicato, A., Scarcella, C., and La, R.C. (2007). A study on PCB, PCDD/PCDF industrial contamination in a mixed urban-agricultural area significantly affecting the food chain and the human exposure. Part I: soil and feed. *Chemosphere* 67, 1822-1830.
- Tuschl, G. and Mueller, S.O. (2006). Effects of cell culture conditions on primary rat hepatocytes-cell morphology and differential gene expression. *Toxicology* 218, 205-215.
- Unkila, M., Ruotsalainen, M., Pohjanvirta, R., Viluksela, M., MacDonald, E., Tuomisto, J.T., Rozman, K., and Tuomisto, J. (1995). Effect of 2,3,7,8-tetrachlorodibenzo-p-dioxin (TCDD) on tryptophan and glucose homeostasis in the most TCDD-susceptible and the most TCDD-resistant species, guinea pigs and hamsters. *Arch. Toxicol.* 69, 677-683.
- Uno, S., Dalton, T.P., Sinclair, P.R., Gorman, N., Wang, B., Smith, A.G., Miller, M.L., Shertzer, H.G., and Nebert, D.W. (2004). Cyp1a1(-/-) male mice: protection against high-dose TCDD-induced lethality and wasting syndrome, and resistance to intrahepatocyte lipid accumulation and uroporphyrin. *Toxicol. Appl. Pharmacol.* 196, 410-421.

- Uyeda, K. and Repa, J.J. (2006). Carbohydrate response element binding protein, ChREBP, a transcription factor coupling hepatic glucose utilization and lipid synthesis. *Cell Metab* 4, 107-110.
- van de Werve, G., Assimakopoulos-Jeannot, F., and Jeanrenaud, B. (1983). Altered liver glycogen metabolism in fed genetically obese mice. *Biochem. J.* 216, 273-280.
- van den Berg, M., Birnbaum, L., Bosveld, A.T., Brunstrom, B., Cook, P., Feeley, M., Giesy, J.P., Hanberg, A., Hasegawa, R., Kennedy, S.W., Kubiak, T., Larsen, J.C., van Leeuwen, F.X., Liem, A.K., Nolt, C., Peterson, R.E., Poellinger, L., Safe, S., Schrenk, D., Tillitt, D., Tysklind, M., Younes, M., Waern, F., and Zacharewski, T. (1998). Toxic equivalency factors (TEFs) for PCBs, PCDDs, PCDFs for humans and wildlife. *Environ. Health Perspect.* 106, 775-792.
- van den Berg, M., Birnbaum, L.S., Denison, M., De, V.M., Farland, W., Feeley, M., Fiedler, H., Hakansson, H., Hanberg, A., Haws, L., Rose, M., Safe, S., Schrenk, D., Tohyama, C., Tritscher, A., Tuomisto, J., Tysklind, M., Walker, N., and Peterson, R.E. (2006). The 2005 World Health Organization reevaluation of human and Mammalian toxic equivalency factors for dioxins and dioxin-like compounds. *Toxicol. Sci.* 93, 223-241.
- Van der Burght, A.S., Tysklind, M., Andersson, P.L., Jean, H.G., and van den Berg, M. (2000). Structure dependent induction of CYP1A by polychlorinated biphenyls in hepatocytes of male castrated pigs. *Chemosphere* 41, 1697-1708.
- Veneziale, C.M. and Lohmar, P.H. (1973). Gluconeogenesis in isolated hepatic parenchymal cells. *J. Biol. Chem.* 248, 7786-7791.
- Vetelainen, R., van Vliet, A.K., and van Gulik, T.M. (2007). Severe steatosis increases hepatocellular injury and impairs liver regeneration in a rat model of partial hepatectomy. *Ann. Surg.* 245, 44-50.
- Vijayan, M.M., Aluru, N., Maule, A.G., and Jorgensen, E.H. (2006). Fasting augments PCB impact on liver metabolism in anadromous arctic char. *Toxicol. Sci.* 91, 431-439.
- Viluksela, M., Stahl, B.U., Birnbaum, L.S., and Rozman, K.K. (1998). Subchronic/chronic toxicity of a mixture of four chlorinated dibenzo-p-dioxins in rats. II. Biochemical effects. *Toxicol. Appl. Pharmacol.* 151, 70-78.
- Viluksela, M., Stahl, B.U., and Rozman, K.K. (1995). Tissue-specific effects of 2,3,7,8-Tetrachlorodibenzo-p-dioxin (TCDD) on the activity of phosphoenolpyruvate carboxykinase (PEPCK) in rats. *Toxicol. Appl. Pharmacol.* 135, 308-315.
- Viluksela, M., Unkila, M., Pohjanvirta, R., Tuomisto, J.T., Stahl, B.U., Rozman, K.K., and Tuomisto, J. (1999). Effects of 2,3,7,8-tetrachlorodibenzo-p-dioxin (TCDD) on liver phosphoenolpyruvate carboxykinase (PEPCK) activity, glucose homeostasis and plasma amino acid concentrations in the most TCDD-susceptible and the most TCDD-resistant rat strains. *Arch. Toxicol.* 73, 323-336.

- Volz,D.C., Bencic,D.C., Hinton,D.E., Law,J.M., and Kullman,S.W. (2005). 2,3,7,8-Tetrachlorodibenzo-p-dioxin (TCDD) induces organ- specific differential gene expression in male Japanese medaka (*Oryzias latipes*). *Toxicol. Sci.* *85*, 572-584.
- Walisser,J.A., Glover,E., Pande,K., Liss,A.L., and Bradfield,C.A. (2005). Aryl hydrocarbon receptor-dependent liver development and hepatotoxicity are mediated by different cell types. *Proc. Natl. Acad. Sci. U. S. A* *102*, 17858-17863.
- Wang,X.L., Suzuki,R., Lee,K., Tran,T., Gunton,J.E., Saha,A.K., Patti,M.E., Goldfine,A., Ruderman,N.B., Gonzalez,F.J., and Kahn,C.R. (2009). Ablation of ARNT/HIF1beta in liver alters gluconeogenesis, lipogenic gene expression, and serum ketones. *Cell Metab* *9*, 428-439.
- Ward,M.P., Jablonski,C., Semel,B., and Soucek,D. (2010). The biological pathway and effect of PCBs on common terns in Lake Michigan. *Ecotoxicology*. *19*, 1513-1522.
- Weber,L.W., Lebofsky,M., Greim,H., and Rozman,K. (1991a). Key enzymes of gluconeogenesis are dose-dependently reduced in 2,3,7,8-tetrachlorodibenzo-p-dioxin (TCDD)-treated rats. *Arch. Toxicol.* *65*, 119-123.
- Weber,L.W., Lebofsky,M., Stahl,B.U., Gorski,J.R., Muzi,G., and Rozman,K. (1991b). Reduced activities of key enzymes of gluconeogenesis as possible cause of acute toxicity of 2,3,7,8-tetrachlorodibenzo-p-dioxin (TCDD) in rats. *Toxicology* *66*, 133-144.
- Weber,L.W., Lebofsky,M., Stahl,B.U., Smith,S., and Rozman,K.K. (1995). Correlation between toxicity and effects on intermediary metabolism in 2,3,7,8-tetrachlorodibenzo-p-dioxin-treated male C57BL/6J and DBA/2J mice. *Toxicol. Appl. Pharmacol.* *131*, 155-162.
- Wehler,E.K., Bergman,A., Brandt,I., Darnerud,P.O., and Wachtmeister,C.A. (1989). 3,3',4,4'-Tetrachlorobiphenyl. Excretion and tissue retention of hydroxylated metabolites in the mouse. *Drug Metab Dispos.* *17*, 441-448.
- Wen,Y.A., Liu,D., Xiao,Y.Y., Luo,D., Dong,Y.F., and Zhang,L.P. (2009). Enhanced glucose synthesis in three-dimensional hepatocyte collagen matrix. *Toxicol. In Vitro* *23*, 744-747.
- White,S.S. and Birnbaum,L.S. (2009). An overview of the effects of dioxins and dioxin-like compounds on vertebrates, as documented in human and ecological epidemiology. *J. Environ. Sci. Health C. Environ. Carcinog. Ecotoxicol. Rev.* *27*, 197-211.
- WHO. Polychlorinated biphenyls: human health aspects. 1-64. 2003. Geneva, Switzerland, World Health Organization.
Ref Type: Online Source
- Wickizer,T.M., Brilliant,L.B., Copeland,R., and Tilden,R. (1981). Polychlorinated biphenyl contamination of nursing mothers' milk in Michigan. *Am. J. Public Health* *71*, 132-137.
- Williamson,J.R., Scholz,R., and Browning,E.T. (1969). Control mechanisms of gluconeogenesis and ketogenesis. II. Interactions between fatty acid oxidation and the citric acid cycle in perfused rat liver. *J. Biol. Chem.* *244*, 4617-4627.

- Wiseman,S.B. and Vijayan,M.M. (2007). Aryl hydrocarbon receptor signaling in rainbow trout hepatocytes: role of hsp90 and the proteasome. *Comp Biochem. Physiol C. Toxicol. Pharmacol.* *146*, 484-491.
- Witters,L.A. and Kemp,B.E. (1992). Insulin activation of acetyl-CoA carboxylase accompanied by inhibition of the 5'-AMP-activated protein kinase. *J. Biol. Chem.* *267*, 2864-2867.
- Witters,L.A. and Trasko,C.S. (1979). Regulation of hepatic free fatty acid metabolism by glucagon and insulin. *Am. J. Physiol* *237*, E23-E29.
- Wittsiepe,J., Furst,P., Schrey,P., Lemm,F., Kraft,M., Eberwein,G., Winneke,G., and Wilhelm,M. (2007). PCDD/F and dioxin-like PCB in human blood and milk from German mothers. *Chemosphere* *67*, S286-S294.
- Wrede,C.E., Dickson,L.M., Lingohr,M.K., Briaud,I., and Rhodes,C.J. (2002). Protein kinase B/Akt prevents fatty acid-induced apoptosis in pancreatic beta-cells (INS-1). *J. Biol. Chem.* *277*, 49676-49684.
- Wrede,C.E., Dickson,L.M., Lingohr,M.K., Briaud,I., and Rhodes,C.J. (2003). Fatty acid and phorbol ester-mediated interference of mitogenic signaling via novel protein kinase C isoforms in pancreatic beta-cells (INS-1). *J. Mol. Endocrinol.* *30*, 271-286.
- Yamatani,K., Sato,N., Wada,K., Suda,K., Wakasugi,K., Ogawa,A., Takahashi,K., Sasaki,H., and Hara,M. (1987). Two types of hormone-responsive adenylate cyclase in the rat liver. *Biochim. Biophys. Acta* *931*, 180-187.
- Yang,J., Kalhan,S.C., and Hanson,R.W. (2009). What is the metabolic role of phosphoenolpyruvate carboxykinase? *J. Biol. Chem.* *284*, 27025-27029.
- Yeh,Y.Y. (1981). Antiketogenic and antiketogenic actions of carnitine in vivo and in vitro in rats. *J. Nutr.* *111*, 831-840.
- Yin,J., Gao,Z., Liu,D., Liu,Z., and Ye,J. (2008). Berberine improves glucose metabolism through induction of glycolysis. *Am. J. Physiol Endocrinol. Metab* *294*, E148-E156.
- Yoshimura,H., Yonemoto,Y., Yamada,H., Koga,N., Oguri,K., and Saeki,S. (1987). Metabolism in vivo of 3,4,3',4'-tetrachlorobiphenyl and toxicological assessment of the metabolites in rats. *Xenobiotica* *17*, 897-910.
- Zeiger,M., Haag,R., Hockel,J., Schrenk,D., and Schmitz,H.J. (2001). Inducing effects of dioxin-like polychlorinated biphenyls on CYP1A in the human hepatoblastoma cell line HepG2, the rat hepatoma cell line H4IIE, and rat primary hepatocytes: comparison of relative potencies. *Toxicol. Sci.* *63*, 65-73.
- Zhang,S., Qin,C., and Safe,S.H. (2003). Flavonoids as aryl hydrocarbon receptor agonists/antagonists: effects of structure and cell context. *Environ. Health Perspect.* *111*, 1877-1882.